



TECHNICAL REPORT ITL-90-1

A STUDY OF THE EFFECTS OF DIFFERENTIAL LOADINGS ON COFFERDAMS

by

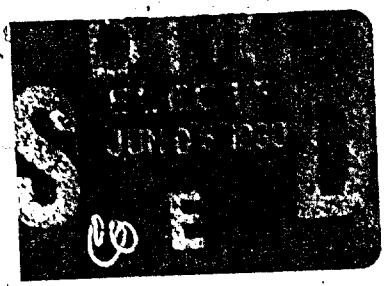
James R. Martin II, G. Wayne Clough

Virginia Polytechnic Institute
and State University

The Charles E. Via, Jr.
Department of Civil Engineering
Blacksburg, Virginia 24061



April 1990
Final Report



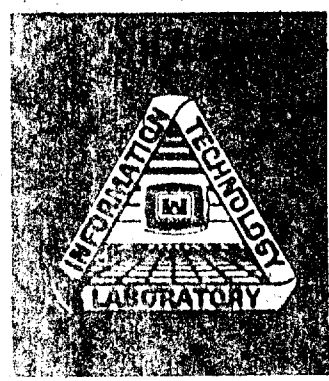
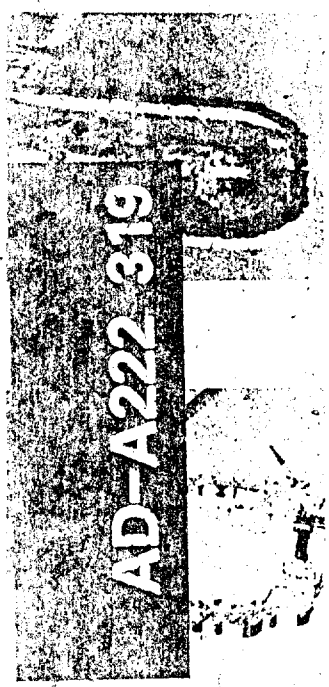
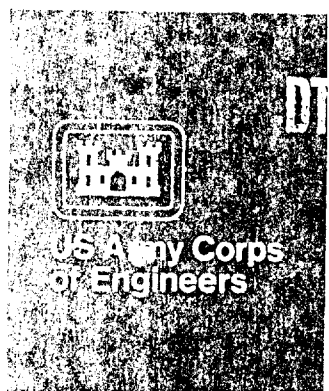
Approved For Public Release; Distribution Unlimited

Original contains color plates; All DTIC reproductions will be in black and white

Prepared for DEPARTMENT OF THE ARMY
US Army Corps of Engineers
Washington, DC 20314-1000

Under Contract No. DACW39-86-K-0007

Monitored by Information Technology Laboratory
US Army Engineer Waterways Experiment Station
3909 Halls Ferry Road, Vicksburg, Mississippi 39180-6199



Destroy this report when no longer needed. Do not return
it to the originator.

The findings in this report are not to be construed as an official
Department of the Army position unless so designated
by other authorized documents.

The contents of this report are not to be used for
advertising, publication, or promotional purposes.
Citation of trade names does not constitute an
official endorsement or approval of the use of
such commercial products.

Unclassified

SECURITY CLASSIFICATION OF THIS PAGE

REPORT DOCUMENTATION PAGE				Form Approved OMB No. 0704-0188	
1a. REPORT SECURITY CLASSIFICATION Unclassified		1b. RESTRICTIVE MARKINGS			
2a. SECURITY CLASSIFICATION AUTHORITY		3. DISTRIBUTION/AVAILABILITY OF REPORT Approved for public release; distribution unlimited.			
2b. DECLASSIFICATION/DOWNGRADING SCHEDULE					
4. PERFORMING ORGANIZATION REPORT NUMBER(S)		5. MONITORING ORGANIZATION REPORT NUMBER(S) Technical Report ITL-90-1			
6a. NAME OF PERFORMING ORGANIZATION Virginia Polytechnic Institute and State University		6b. OFFICE SYMBOL (if applicable)	7a. NAME OF MONITORING ORGANIZATION USAEWES Information Technology Laboratory		
6c. ADDRESS (City, State, and ZIP Code) Department of Civil Engineering Blacksburg, VA 24061		7b. ADDRESS (City, State, and ZIP Code) 3909 Halls Ferry Road Vicksburg, MS 39180-6199			
8a. NAME OF FUNDING/SPONSORING ORGANIZATION US Army Corps of Engineers		8b. OFFICE SYMBOL (if applicable)	9. PROCUREMENT INSTRUMENT IDENTIFICATION NUMBER Contract No. DACW39-86-K-0007		
8c. ADDRESS (City, State, and ZIP Code) Washington, DC 20314-1000		10. SOURCE OF FUNDING NUMBERS			
		PROGRAM ELEMENT NO.	PROJECT NO.	TASK NO.	WORK UNIT ACCESSION NO.
11. TITLE (Include Security Classification) A Study of the Effects of Differential Loadings on Cofferdams					
12. PERSONAL AUTHOR(S) Martin II, James R., Clough, G. Wayne					
13a. TYPE OF REPORT Final report		13b. TIME COVERED FROM _____ TO _____		14. DATE OF REPORT (Year, Month, Day) April 1990	15. PAGE COUNT 98
16. SUPPLEMENTARY NOTATION Available from National Technical Information Service, 5285 Port Royal Road, Springfield, VA 22161.					
17. COSATI CODES			18. SUBJECT TERMS (Continue on reverse if necessary and identify by block number)		
FIELD	GROUP	SUB-GROUP			
			Case histories		
			Displacements		
			Interlock stresses		
			Sheet pile cellular cofferdams		
			Soil and rock founded		
19. ABSTRACT (Continue on reverse if necessary and identify by block number) Conventional design of cellular cofferdams is largely based upon semiempirical concepts derived from classical earth pressure theories. Recent studies have suggested that most existing design methods are excessively conservative. In part, this derives from an inability to fully describe the true, relatively complex soil-structure interaction process which occurs in the flexible cellular cofferdam. In addition to the apparent conservatism in the conventional theories, they provide no means to predict movements of cofferdams. This deficiency has become more important with time, since performance and safety monitoring systems are largely oriented toward measuring deformations, and it is not possible to define reasonable levels of movements before construction. Further, finite element analysis techniques are being developed which are designed to predict cofferdam deformations, but the means for verifying the predictions are not definitive because of the lack of a broad data					
(Continued)					
20. DISTRIBUTION/AVAILABILITY OF ABSTRACT <input checked="" type="checkbox"/> UNCLASSIFIED/UNLIMITED <input type="checkbox"/> SAME AS RPT. <input type="checkbox"/> DTIC USERS			21. ABSTRACT SECURITY CLASSIFICATION Unclassified		
22a. NAME OF RESPONSIBLE INDIVIDUAL			22b. TELEPHONE (Include Area Code)		22c. OFFICE SYMBOL

DD Form 1473, JUN 86

Previous editions are obsolete.

SECURITY CLASSIFICATION OF THIS PAGE

Unclassified

Unclassified

SECURITY CLASSIFICATION OF THIS PAGE

19. ABSTRACT (Continued).

base on cofferdam performance. This investigation is directed toward providing a data base through the documentation and comparing five case histories where instrumentation was used to monitor the behavior. Primary consideration was given to the response of the cofferdams under differential loading.

In the course of the investigation, the response of each cofferdam was documented and dissected in terms of the behavior at each stage of the differential loading. A strong correlation is found to exist between the lateral cell deflection and the level of differential loading, with the exact nature of the correlation depending on certain key parameters including cell foundation, cell fill material, cell width to height ratio, presence of a stabilizing berm, and nature of loading. It is found for conservatively designed cells that the response falls into a predictable pattern which can be characterized in terms of nondimensionalized parameters for both normal and more severe levels of loading. In addition to deformations, information is provided on interlock tensions where available. The results are believed to provide a baseline for cofferdam behavior that can be useful in gaging the expected behavior of other cofferdams and for verifying the accuracy of new forms of predictive tools such as the finite element method.

Unclassified

SECURITY CLASSIFICATION OF THIS PAGE

PREFACE

The investigation described in this report was conducted by the Charles E. Via, Jr. Department of Civil Engineering, Geotechnical Engineering Group, Virginia Polytechnic Institute and State University (VPI) for the Computer-Aided Engineering Division (CAED), Information Technology Laboratory (ITL), US Army Engineer Waterways Experiment Station (WES) under the auspices of Contract No. DACW39-86-K-0007. This study is as part of the research project entitled "Structural Behavior of Sheet Pile Cellular Cofferdams" sponsored under the Civil Works Research and Development Directorate, Headquarters, US Army Corps of Engineers (HQUSACE), under the Structural Engineering Research Program. Technical Monitor for the Project is Mr. Donald Dressler, HQUSACE.

This report was prepared by Dr. G. Wayne Clough, VPI, and James R. Martin II, VPI. The work was monitored by Mr. Reed L. Mosher, CAED, under the general supervision of Dr. Edward Middleton, Chief, CAED, and Dr. N. Radhakrishnan, Chief, ITL.

COL Larry B. Fulton, EN, was Commander and Director of WES during the period of publication. Dr. Robert W. Whalin was Technical Director.

Accession For	
NTIS GRA&I	<input checked="" type="checkbox"/>
DTIC TAB	<input checked="" type="checkbox"/>
Unannounced	<input type="checkbox"/>
Justification	
By _____	
Distribution/	
Availability Codes	
Dist	Avail and/or Special
A-1	



continued on next page
 please check all information
 items will be in book
 with

CONTENTS

	<u>Page</u>
PREFACE	1
LIST OF FIGURES	3
PART I: INTRODUCTION	6
PART II: BACKGROUND	8
Cofferdam Geometries	8
Primary Design Conditions	10
Design Theories	12
External Stability	12
Internal Stability	13
Cell Interlock Force	14
Finite Element Models	16
Typical Cofferdam Performance	18
Instrumentation	19
PART III: COFFERDAMS FOUNDED ON SANDS	20
Lock and Dam 26 (R) Cofferdam--Stages 1 and 2	20
Trident Drydock Cofferdam	37
PART IV: COFFERDAMS FOUNDED ON ROCK	46
Willow Island--Second Stage Cofferdam	46
Observed Performance	49
PART V: COFFERDAMS WITH UNUSUAL CONDITIONS	57
Seagrit Marine Terminal Cofferdam	57
Williamson CBD Prototype Cells	68
PART VI: COMPARISONS OF COFFERDAM BEHAVIOR AND GENERAL TRENDS	74
Deformations of the Top of the Cells--Initial Loading	74
Deformations of the Tops of the Cells--Repeated Loading	79
Time-Dependent Movements in the Cofferdams	80
Lateral Movements of the Inboard and Outboard Sheet Piles	81
Interlock Tensions	83
PART VII: SUMMARY AND CONCLUSIONS	85
BIBLIOGRAPHY	87
TABLES 1-5	

LIST OF FIGURES

<u>No.</u>		<u>Page</u>
1	Typical cellular configurations	9
2	Typical failure modes of cellular cofferdams	11
3	Mechanism of cell distortion proposed for analysis by vertical shear method	14
4	Circumferential distribution of interlock force according to TVA analysis	15
5	Layout and instrumentation of Stage 1 Cofferdam	21
6	Typical cell schematic of Lock and Dam No. 26 (R)	21
7	Layout and instrumentation of Stage 2 Cofferdam	22
8	Detail of instrumented section, Lock and Dam No. 26 (R)	24
9	Observed interlock forces and design methods, filling complete	25
10	Movement of Cell 34 during berm placement	26
11	Movements of Cell 8 versus time	27
12	Movements of 11 typical Stage 1 cells during dewatering	28
13	Movement of Cell 33 during dewatering	28
14	Movement of Cell 34 during dewatering	29
15	Movements of Cell 81 versus time	30
16	Movements of 16 typical Stage 2 cells during dewatering	31
17	Loading response of 11 typical cells	33
18	Loading response of 16 cells	34
19	Relative displacements of inboard and outboard walls of 11 cells	35
20	Movement of Cell 34 during flood	36
21	Layout of cofferdam and instrumentation location	38
22	Schematic of typical section	38
23	Typical cell and arc	40
24	Inclinometer movements of Cell 5 during dewatering	42
25	Inboard movements of eight typical cells during dewatering	43
26	Movement of Cell 5 during dewatering	43
27	Movement of cells versus time	44
28	Layout and instrumentation of Stage 2 Cofferdam	47
29	Schematic of typical cell	47
30	Inclinometer movements of cells versus time	50
31	Inclinometer movements of Cells 24 and 27 during dewatering	50
32	Inboard wall movement of Cell 24 during dewatering	51
33	Inboard wall movement of Cell 27 during dewatering	52
34	Loading response of Cell 24	53
35	Loading response of Cell 27	53
36	Inboard wall movement of Cell 32 during dewatering	56
37	Inboard wall movements of Cell 33 during dewatering	56
38	Soil profile after initial construction, Cell 49	58
39	Profile after initial construction, Cell 58	59
40	Profile after initial construction, Cell 66	59
41	Construction of cells	61
42	Measured displacements of Cell 66 toward outboard	63
43	Movements of Cell 66 during initial construction	64
44	Measured displacements of Cell 49 toward outboard	65
45	Measured displacements of Cell 58 toward outboard	65
46	Movement at top of Cell 66 during test loading	67
47	Inclinometer movement of Cell 66 during test loading	68
48	Typical cell section	70

<u>No.</u>		<u>Page</u>
49	Geometries and instrumentation, Cells 1 and 2	70
50	Movements of cell during filling	72
51	Convention used in comparisons	75
52	Composite plot of normalized response to differential loading	75
53	Deflections versus overturning moments during dewatering	77
54	Composite plot of normalized response to differential loading	79
55	Normalized cell profiles after dewatering	82

CONVERSION FACTORS, NON-SI TO SI (METRIC)
UNITS OF MEASUREMENTS

Non-SI units of measurement can be converted to SI (metric) units as follows:

<u>Multiply</u>	<u>By</u>	<u>To Obtain</u>
degrees (angle)	0.01745329	radians
feet	0.3048	metres
inches	2.54	centimetres
kips (force) per inch	175.1268	kilonewtons per metre
pounds (force)	4.448222	newtons
pounds (force) per square foot	47.88026	pascals
pounds (mass) per cubic foot	16.01846	kilograms per cubic metre
tons (mass) per square foot	9,764.856	kilograms per square metre

A STUDY OF THE EFFECTS OF DIFFERENTIAL
LOADINGS ON COFFERDAMS

PART I: INTRODUCTION

1. Cellular cofferdams are retaining structures made up of a network of earth-filled cells which link together to provide a continuous barrier to hold back water or soil. Each cell consists of interlocking steel sheet piles which are commonly arranged in a circular configuration. Cloverleaf or diaphragm shapes are sometimes used in special cases. Ideally, the cells are filled with clean, free-draining sand and/or crushed rock. If founded on sand or clay, cells are usually installed with considerable embedment into the underlying soils to provide stability and minimize seepage.

2. For the most part, cellular cofferdams have been used as temporary water-retaining structures to allow construction inside them to proceed in the dry. With increasing frequency, however, cellular cofferdams are being installed as permanent structures serving as bulkheads, drydocks, floodwalls, and retaining walls. Cells can be connected and arranged in a straight line or curved fashion to accommodate odd-shaped working areas. This gives added versatility.

3. Design for cellular cofferdams is largely based on conventional earth pressure concepts wherein the actual process of soil-structure interaction is not considered. Recent evidence has shown that these concepts lead to conservative designs (Schroeder and Maitland 1979). Further, the conventional procedures are unable to provide any information on deformation levels to be expected during the construction and loading of the cofferdam. These are important in that they are easily measured, and they provide the key towards evaluating the stability of the cofferdam as it is built and loaded. This is particularly critical in situations which are more frequently arising where cofferdams are being used in unfavorable foundation conditions. Thus, there is a need to improve design methods which produce more economic cofferdams, and allow for assessment of cofferdam behavior under a wider variety of conditions than is now possible.

4. One method which is receiving scrutiny as a means for a more complete analysis tool for cofferdams is the finite element method (Clough and Hansen 1977; Hansen and Clough 1982; Clough and Kuppusamy 1985). It allows

one to predict stress conditions in the cell fill and foundation soils and the stresses and forces in the sheet pile system. Further, it can consider the process of soil-structure interaction within the framework of the actual loading process. Finally, it also generates information on the deformations that the cofferdam system will undergo. However, while attention has been focused on the development of the analytical aspects of the finite element technology for cofferdams, it remains to provide a well-documented field behavior base which can be used for purposes of validation in a range of conditions. The primary purpose of this study is to provide needed information toward this goal. In particular, the focus is directed toward the measured field response for the case of cofferdams subjected to differential loads. This includes the effects of berm placement, dewatering, and flooding.

5. This study examines case histories of five large cofferdams. Each cofferdam differs somewhat in cell fill material, foundation type, or loading scheme. Each is investigated individually and subsequently compared to bring out common behavioral trends. Special situations which may require added attention are pointed out and discussed as well. From these trends, norms are established from which finite element studies can be validated.

6. Part II (Background) provides background information on cellular cofferdams. Typical cofferdam geometries, conventional design methods, typical performances, and instrumentation monitoring systems are reviewed.

7. The case histories of cofferdams founded on sands are discussed in Part III (Cofferdams Founded on Sands). This part includes case studies of Lock and Dam 26 (R) - Stages 1 and 2, and Trident Drydock Cofferdam. Part IV (Cofferdams Founded on Rock) presents the Willow Island Stage 2 Cofferdam, a project involving a rock foundation.

8. Cofferdams with loading conditions, cell fill material, or foundations that are unusual are presented in Part V (Cofferdam with Unusual Conditions). Case studies from Seagirt Marine Terminal Cofferdam and Williamson (CBD) Prototype Cells are presented in this part.

9. Details of loading schemes, cell fill and foundation materials and properties, instrumentation, etc., are given with each case history in Parts III-V. Part VI (Comparisons of Cofferdam Behavior and General Trends) compares the behavior and trends of all the cases, and establishes benchmark nondimensional response curves. A summary and conclusions are given in Part VII.

PART II: BACKGROUND

10. This part provides an overview introducing the basic concepts of cofferdams and gives a brief explanation of how they work, how they are designed and modelled, and general performance criteria. The interest is to establish a context for the present design technology and provide information needed to understand the case history data.

Cofferdam Geometries

11. Various cell configurations are used in cellular cofferdam structures. Most cofferdam cells are constructed of flat web sheet piling which is linked together, driven, and arranged in a circular, diaphragm, or cloverleaf configuration. Care must be taken in the construction of the cell, especially the driving of the sheet piles. Large templates are used to maintain control during driving and to effect the desired shape of the cofferdam cell.

12. The circular cell configuration is the shape most commonly used. Adjacent circular cells are connected by smaller arc cells. Arc cells are constructed by enclosing the narrow space between adjacent cofferdam cells with a row of sheet piles arranged in a semicircular arc. This is done on the loaded and the unloaded side of the structure. The arc sections are subsequently filled with soil so that a continuous cofferdam is achieved. The arc cells share a common wall with the neighboring main cells on either side and are attached to the main cell by means of special "T" or "Y" sheet pile connectors. Each circular cell is self-supporting and not dependent upon the neighboring cell for stability. In other words, if one cell in a row of circular cells ruptures, stability of the adjacent cells is unaffected. Also, each cell is fully functional once completed. This means that construction can proceed in an orderly fashion as a newly completed cell can be used as a working platform for the construction of the next adjacent cell in the row. The cells can be constructed in any order without regard for the level of cell fill in adjacent cells.

13. Diaphragm cells can be constructed faster and less expensively than circular cells but are not independently stable and require careful control of the cell fill in adjacent cells during construction. These and other disadvantages render diaphragm cofferdams undesirable except for special circumstances.

14. Cloverleaf cells find their primary application as corner cells which connect two orthogonal rows of circular cells. The increased base width and large mass cloverleaf cells especially good for cases where stability against sliding or overturning is a problem. Cloverleaves are also used when excessive interlock tensions in circular cells limit cell radii, and will not allow the desired cell width to be achieved. However, the recent availability of high-strength sheet piles allows circular cells to be constructed with larger radii, thereby reducing the need for the more expensive cloverleaf cells. Figure 1 illustrates the cellular configurations described above.

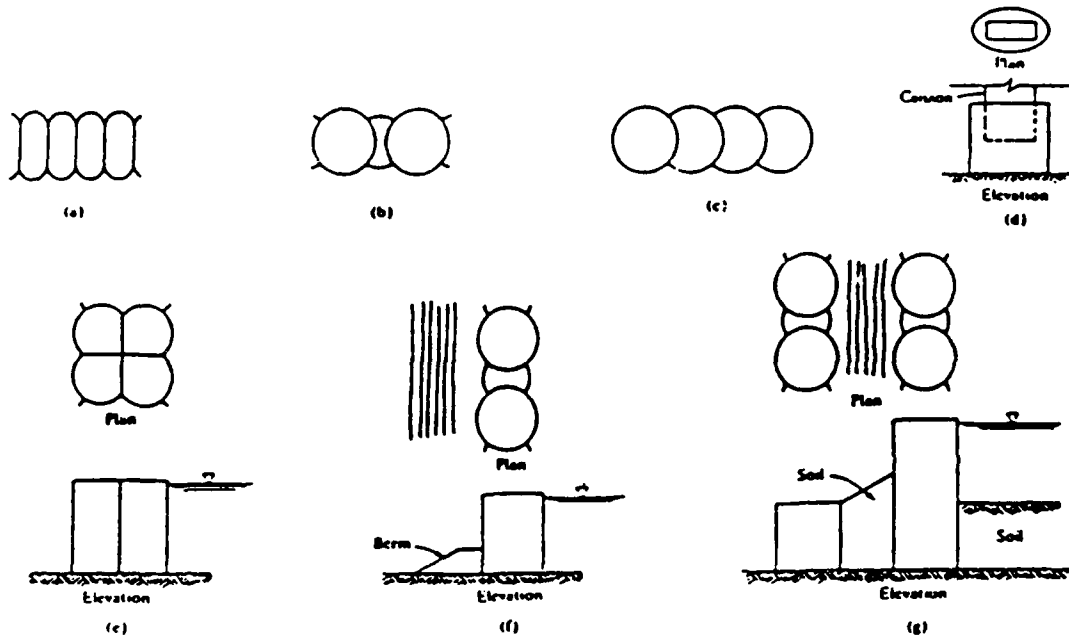


Figure 1. Typical cellular configurations

15. The size of a cellular cofferdam cell depends upon the purpose of the cofferdam. The height and width are selected to give adequate factors of safety with respect to the common modes of failure. The base width must be large enough to give adequate stability against sliding along the base and internal shear failure. The width of the cell is limited in that the sheet pile interlock tensions increase as the cell width increases. Cell height is usually limited to the height which can be achieved without exceeding the strength of the sheet pile interlocks. Sheet piles with interlock capacities of 28 kips/in.* are readily available and allow for the construction of tall cellular cofferdams. The design height is often specified according to the

* A table of factors for converting non-SI to SI (metric) units is presented on page 5.

service of the cofferdam. For permanent structures such as wharfs and drydocks, the height of the cofferdam would correspond to the working service level of the installation. For temporary, water-retaining structures, the design height of the cofferdam might be set at some distance above the high water elevation. The width to height (b/h) ratio of successfully constructed cellular cofferdams range from less than 0.6 to more than 1.0 (Dismuke 1970). The average b/h ratio falls close to 0.85. Lacroix, Esrig and Luscher (1970) suggest that experience shows that cofferdams with b/h ratios between 0.75 and 1.0 are generally stable. Stabilizing soil berms or special cell configurations become necessary as the b/h ratios decrease. Cofferdams with heights below 40 ft are generally considered small (short) cofferdams. Cofferdams with heights above 70 ft are considered large (tall) cofferdams.

Primary Design Conditions

16. Conventional cellular cofferdam design addresses three primary conditions: external stability, internal stability, and sliding along the base. These potential failure modes are illustrated in Figure 2. External stability concerns the stability of the structure with respect to externally applied loads. External stability analyses must ensure that each cell has the size, weight, and embedment necessary to resist applied loads and overturning moments without experiencing excessive translational or rotational deflections.

17. Cells founded on rock depend primarily on size and weight to provide their moment-resisting capacity. The main concern in this case is to prevent the sheet piles on the unloaded side from being uplifted. Lifting of the sheet piles can result in loss of cell fill and, ultimately, the structural integrity of the cell.

18. In addition to overturning stability, cells on sand and clay foundations must be designed to limit shear deformations and settlements at the base. In this case, the strength and compressibility of the foundation soils are important parameters and must be considered in the design of the cofferdam. The design must also consider the shear capacity of the soil-sheet pile interface below the dredge line to prevent plunging failures of the sheet piles on the unloaded side. In most applications, the driving forces that supply the lateral loads are due to differential water heads. Seepage forces and uplift pressures should be considered wherever applicable in the design phase.

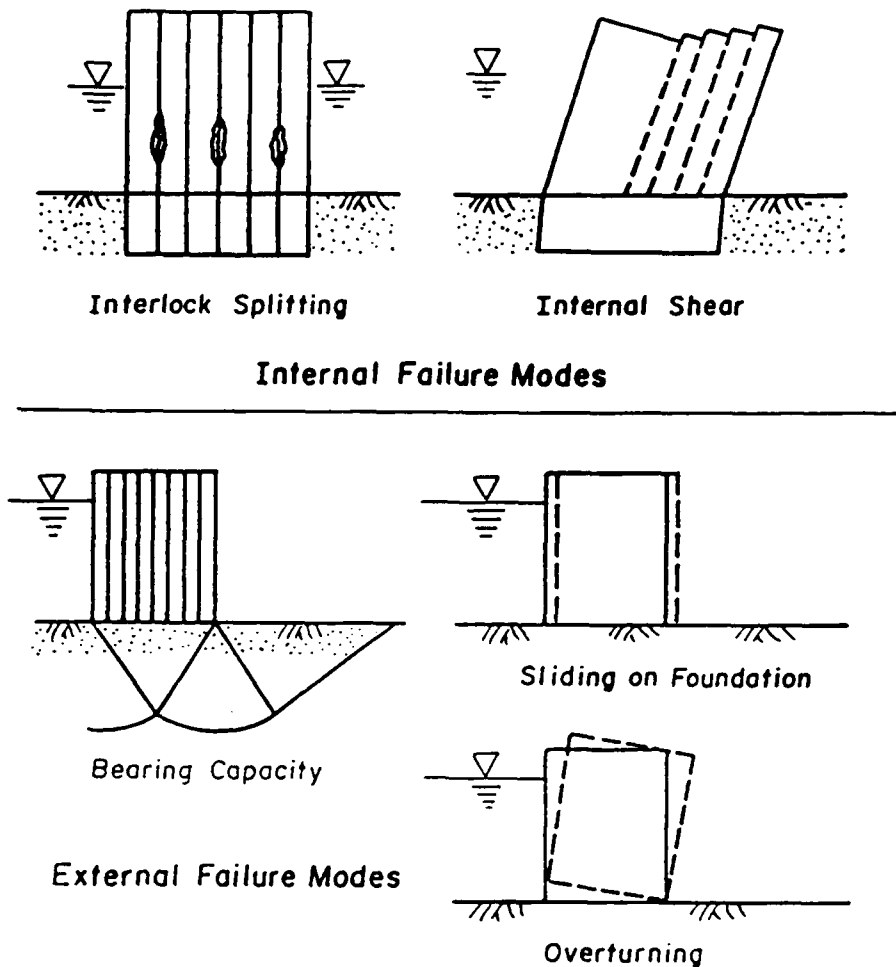


Figure 2. Typical failure modes of cellular cofferdams

19. Internal stability is generally concerned with the stability of the cells within themselves. When lateral loads are applied, the cells deflect and mobilize shear resistance along vertically oriented planes through the cell fill material. The design must ensure that the cells withstand these loads without the development of excessive shear distortions through the cell fill material. Also, the cell fill-sheet pile interface must not allow excessive slippage between the cell fill and sheet piles which would result in spillage of cell fill.

20. The cells also must be able to contain the cell fill without bursting the sheet pile interlocks. The interlocks must be designed to accommodate a combination of soil and water pressures. This condition is usually critical during cell filling when lateral earth pressures and water pressures are high.

21. Cells should additionally have the capability to resist lateral loads without the base sliding on the foundation. Cells on rock depend on base width and cell weight to provide sufficient frictional resistance along

the base. Cells on clay and sand foundations incorporate passive soil resistance on the unloaded side to help resist translational movements. This passive resistance is mobilized through embedment of the sheet piles. Stabilizing soil berms or double rows of cofferdam cells may be used in cases where stability against sliding is a problem. The design of cells on rock, sand, and clay must always consider any weak seams or zones below the pile tips which may lead to a global type of translation of the structure.

Design Theories

22. Conventional design procedures for cellular cofferdam structures are largely empirical in nature. Several design methods have been proposed, and one of the most recognized is that of Terzaghi (1945). This approach was developed for a cofferdam on a rock foundation. This is extended for cofferdams founded on sand or clay soils. Modifications to this procedure and slightly different concepts have been presented by Krynine (1945), Cummings (1957), TVA (1957), and others (Hansen 1975; Ovesen 1962, and Esrig 1970). Lacroix, Esrig, and Luscher (1970) and Dismuke (1975) presented summaries of the more accepted conventional methods. Several design examples covering the mechanics and specific applications of these methods are included in these summaries. Large-scale model studies and recently modified design procedures have been presented by Maitland and Schroeder (1979) and Schroeder and Maitland (1979). Two- and three-dimensional finite element studies have been presented by Clough and Kuppusamy (1985), Clough et al. (1987), and Mosher (1985).

External Stability

23. Traditionally, external stability analysis of gravity retaining structures includes the calculation of the stability against overturning. The cell is assumed to rotate about its toe as it is subjected to lateral loads, and the factor of safety with respect to overturning is taken as the ratio of the driving moments due to the lateral loads dividend by the resisting moment due to the weight of the cell. This assumes rigid cell behavior. However, cellular cofferdams do not behave as rigid structures and would fail by another mechanism long before failure due to overturning could occur (Lacroix, Esrig, and Luscher 1970; Dismuke 1975; Schroeder and Maitland 1979). This

mechanism would involve excessive shear distortions through the cell fill or the lifting of the sheet piles on the unloaded side. For a rigid cofferdam structure on a rock foundation, lifting of the sheet piles on the unloaded side corresponds to a soil pressure of zero at the heel and factor of safety of 3.0 against overturning. Cummings (1957) suggested that the actual factor of safety is lower than this value which prompted some designers to require a computed factor of safety against overturning greater than 3.0 (Lacroix, Esrig, and Luscher 1970). Evidence presented by Schroeder and Maitland (1979) strongly suggests that cells embedded in sands cannot fail by overturning without first experiencing failure due to the loss of internal stability. The factor of safety against overturning in this case is actually a benchmark figure used to control excessive shear distortions in the cell fill.

24. Lateral stability is analyzed through simple horizontal force equilibrium. For cells on rock, the normal effective weight of the cell is multiplied by an appropriate friction coefficient to calculate the available friction resistance across the base of the cell. The magnitude of the expected lateral loads are compared with this figure to determine the margin of safety with respect to translation. Cells on clay and sand require embedment of the sheet piles to provide passive resistance to applied lateral loads. Terzaghi (1945) recommended that cofferdams founded on sands have embedment depths equal to two-thirds of their free height. This rule of thumb was established to control underseepage and to prevent plunging failures of the sheet piles on the unloaded side. Recent model studies (Maitland and Schroeder 1979) suggest that it is not reasonable to consider the passive resistance offered by the embedded sheet piles below the plane of fixity, the point at which a plastic hinge forms in the sheet piles. (The plane of fixity concept is presented by Matlock and Reese (1969).) The factor of safety with respect to sliding is defined as the ratio of the lateral driving forces and active pressures on the loaded side of the cell to the passive pressures on the unloaded side above the plane of fixity. However, Schroeder and Maitland (1979) suggest that for cofferdams embedded in sands, a sliding failure cannot occur without the cell first experiencing loss of internal stability.

Internal Stability

25. Several approaches have been used to evaluate the margin of safety with respect to internal stability. The two most widely accepted include the

vertical shear method and the horizontal shear method.

26. The concept of sliding along vertical planes about the centerline of the cell was proposed by Terzaghi (1945) and later modified by Tennessee Valley Authority (TVA) (1957). As illustrated in Figure 3, this concept

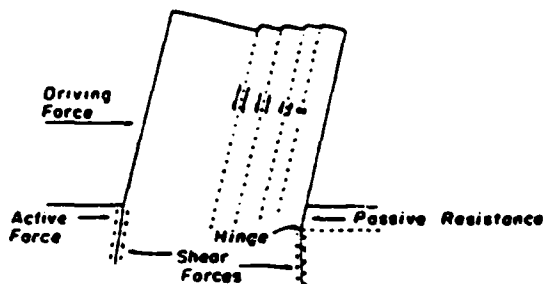


Figure 3. Mechanism of cell distortion proposed for analysis by vertical shear method

assumes that as the cell is loaded, vertical shear planes develop through the cell fill which mobilizes the shear strength of the cell fill to resist the applied loads. Failure occurs when sliding along these vertical planes produces excessive distortion of the cell fill. Terzaghi (1945) proposed that the center-line shear capacity be computed assuming that the lateral pressure acting on a vertical plane through the center line of the cell is equal to the Rankine value of active pressure. Krynine (1945), Esrig (1970), and others have disagreed with this idea, and suggest that the lateral pressure acting on a vertical plane through the center of the cell is much higher than the Rankine active value. Large-scale model tests validate the Terzaghi vertical shear mechanism but show that the lateral pressures acting on the center-line plane are at least twice as high as those proposed by Terzaghi (Schroeder and Maitland 1979).

27. The horizontal shear method was proposed by Cummings (1957). This method assumes that the cell fill resists applied lateral loads by shearing along horizontal planes throughout the fill material. This method underestimates the amount of embedment needed to resist applied lateral loads and overestimates the moment resisting capacity of embedded cells by erroneously including moment resisting forces below the dredge line (Dismuke 1975; Maitland and Schroeder 1979).

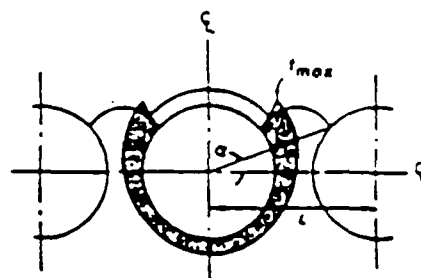
Cell Interlock Force

28. A second area of major concern with respect to the internal stability of cofferdam cells is the determination of the maximum sheet pile

interlock forces and the subsequent design of the sheet pile interlocks. Interlock forces are computed with a simple hoop stress analysis. The magnitude of the hoop forces depends on the lateral earth pressures and water pressures inside the cofferdam. The position of the phreatic surface, fill surcharges, and applied lateral loads all have an effect on the magnitude of these earth and water pressures. Upon loading, a cofferdam cell behaves somewhat like a short cantilever beam, developing a zone of compression through the cell fill on the unloaded side (Figure 10, Schroeder and Maitland 1979). As a result, lateral loads will generally decrease the hoop stress on the loaded side of the cell and increase the hoop stress on the unloaded side, especially near the dredge line. Terzaghi (1945) said that these changes were relatively small. Maitland and Schroeder (1979) agree that these changes are small but not negligible.

29. The location of the maximum interlock force generally occurs between one-fourth and one-sixth of the free height above the dredge line for cells on rock and sand foundations. Circular cells that are joined by connecting arcs develop their highest interlock forces immediately behind the "Y" or "T" section where the main cell is connected to the arc. This region of high interlock stresses constitutes the critical design case for the interlocks. Rupture of the interlocks in this location has been among the most frequent mechanisms of cellular cofferdam failure. Presently, the TVA method (1957) is perhaps the most accepted method for estimating the magnitude of the interlock forces, especially in the area close to the arc-main cell connection. The assumed distribution of interlock force according to the TVA method is shown in Figure 4. It has been suggested that the TVA method

Figure 4. Circumferential distribution of interlock force according to TVA analysis



considerably overestimates the magnitude of the interlock forces in the common wall away from the connection (Dismuke 1975). Because the arc cell is also filled with soil, pressure is provided on both sides of the common wall which reduces sheet pile tensions in this area. Further, arching tends to develop

in the arc-cell fill between the adjacent common walls. This too reduces interlock forces in the common wall.

30. Field observations and laboratory tests suggest that the interlock forces close to the arc-main cell connection are indeed higher but not greatly different from those occurring at other locations in the main cell (Schroeder, Parker, and Khuayjarernpanishk 1977; Sorota, Kinner and Haley 1981; Maitland and Schroeder 1979). Sorota, Kinner and Haley (1981) state that an allowance of a 15 percent increase in the maximum interlock design force for the area near the arc-main cell connection is a prudent design measure (for a 40-deg "Y" connection). Discussions and guidelines for the design of interlock forces based on recent model studies and field observations are available in the literature (Schroeder and Maitland 1979).

Finite Element Models

31. Conventional design procedures are based on concepts which do not explicitly account for the effects of soil-structure interaction. The finite element technique is one approach which has this potential, since it allows one integrated method to predict cell and soil stresses, earth pressures on the cell, and cell and soil deformations.

32. During the past decade, there have been several attempts to model cellular cofferdams by using finite element models. The first finite element models proposed were two-dimensional schemes, namely the plane strain and axisymmetric models. The main short-coming of most early models was that they did not provide for three-dimensional interaction between adjacent cells, nor did they realistically account for the behavior of the sheet pile system, especially the reduced stiffness of the piles in the horizontal plane as compared with the stiffness in the vertical plane. Until recently, most finite element studies treated these stiffnesses the same (Stevens 1980, Clough and Kuppusamy 1985). Additionally, early models did not always consider nonlinear soil behavior and staged construction and loading.

33. Clough and Hansen (1977) and Hansen and Clough (1982) were the first to simulate cofferdam behavior using a vertical slice, plane strain model. The model was used to aid in evaluating the observed performance of the Willow Island Cofferdam. The study was primarily concerned with the deformation response of the cofferdam due to water loadings. Their model was able to consider nonlinear soil behavior, sequential loading patterns, and

complex foundation conditions. Results agreed generally with observed trends and suggested that the vertical slice model could predict cofferdam deformation response with reasonable accuracy. Subsequently, Stevens (1980) independently undertook vertical slice analyses of the Willow Island Cofferdam. He introduced the idea that the lateral stiffness of the model should be less than that in the vertical direction to account for interlock yielding effects.

34. More recently, other finite elements models have been used to model cellular cofferdams. A finite element study of Lock and Dam No. 26 (R) Stage 1 Cofferdam by Clough and Kuppusamy (1985) was conducted to model the response of the cofferdam throughout its entire loading history. This included the initial filling stage, berm placement, dewatering, and flood stage. A combination of three two-dimensional models were used to model the behavior. An axisymmetric model was used to simulate cell filling. Response to cell filling, dewatering, berm placement, and flooding were generated by the vertical slice model. The generalized plane strain model was used to simulate the interaction of the main cell and the arc cell. This was used to study the common wall "Y" connection, a critical section. Each model gave predictions of cell deflections along with the corresponding cell profiles showing the deflected shapes of the cells. The predicted behavior and observed responses compared well. The investigation further evidenced the importance of accounting for the additional flexibility in the horizontal plane of the cofferdam cell due to imperfections in the interlocks. This concept was expressed in terms of a stiffness ratio which related the stiffness of the piles in the vertical plane. The paper showed that two-dimensional models have limitations but, when used in combination, can model cofferdam behavior reasonably well.

35. A later study by Clough et al. (1987) extended the work on the Lock and Dan No. 26 (R) Stage 1 Cofferdam using refined two-dimensional models and a three-dimensional model developed by Mosher (1985). The paper concluded that (a) proper modelling of cofferdam behavior must consider interlock imperfections, and (b) a combination of two-dimensional models can be used to model most, but not all, aspects of cofferdam behavior. A summary of the applicability, advantages, and disadvantages of each of the finite element methods discussed herein is shown in Table 1 along with sketches illustrating each model.

Typical Cofferdam Performance

36. The performance of a cellular cofferdam structure is usually put into a framework whereby the movements that the structure undergoes determine whether or not the cofferdam is performing satisfactorily. The amount of movement that can be tolerated depends upon the purpose of the cofferdam. Permanent cofferdams with architectural finishes are often restricted to movements of less than 1 in. On the other hand, temporary cofferdams are often allowed more than several inches of displacement. It is not uncommon for tall cofferdam cells to undergo more than a foot of horizontal displacement. Cellular cofferdams are yielding, flexible structures that can move up to several feet before a cell rupture occurs (Lacroix, Esrig and Luscher 1970).

37. Generally, cellular cofferdams undergo three critical stages during their design life. These include cell filling, excavation dewatering, and flooding due to high water.

38. Upon filling, the cells bulge out in response to the applied lateral soil and water pressures. Lateral pressures due to the soil are usually highest during filling when the cell fill is unconsolidated. This is especially true if the cell fill does not drain well and is placed hydraulically. Most cofferdam cells bulge out on the order of several inches during the filling operation. The maximum interlock force occurs at the location of maximum bulging which is typically between the dredge line and one-third of the free height of the cell (Schroeder and Maitland 1979).

39. Upon dewatering of the interior of the cofferdam, a net hydrostatic head develops between the exterior and interior wall of the cofferdam. This causes the cofferdam to deflect toward the interior. The amount of deflection during dewatering is usually less than one percent of the free height of the cofferdam (Swatek 1970). The lowering of the phreatic surface in the cell during dewatering sometimes leads to considerable settlement of the cell fill. It may become necessary to add more fill material in order to reestablish the fill grade after dewatering is complete. In general, cofferdams with denser cell fill material will undergo less deflection during dewatering and experience smaller settlements of the cell fill. Subsequent to initial dewatering, cofferdams with good quality fill and good foundations experience very little movement as long as the differential water head remains fairly constant.

40. During high water or flood stage, the water head on the exterior of

the cofferdam increases, and the cofferdam is subjected to a new, higher load than was previously applied. The cofferdam cells respond by rotating toward the interior of the cofferdam until they reach equilibrium under this new load. As the high water from the flood recedes, the cofferdam relaxes slightly, giving rise to a hysteretic type of loading cycle. If the cofferdam develops excessive deflections or is in danger of being overtopped, the inside of the cofferdam can be flooded to neutralize the net hydrostatic water head.

Instrumentation

41. Cofferdam cells have been instrumented in order to evaluate performance and to provide early warning to potential problems. Inclometers installed inside the cells are used to determine movement versus depth. From these, movement profiles and deflected cell shapes can be established. These instruments are expensive to maintain and monitor, and are usually installed in only two or three of the cofferdam cells.

42. Piezometers and observation wells are placed inside the cells and the stabilizing soil berms. These devices allow accurate monitoring of the position of the phreatic surface and the magnitude of uplift pressures. Optical surveys are often used to monitor the movements of cofferdam cells. These surveys are usually set up to monitor movements at the top of all of the cells in an entire cofferdam. On occasion, settlement plates are used to measure fill settlements and strain gages are used to monitor interlock forces.

PART III: COFFERDAMS FOUNDED ON SANDS

43. This part reviews two case histories of cofferdams founded on sands, Lock and Dam No. 26 (R) Cofferdam - Stages 1 and 2, and the Trident Drydock Cofferdam. A general description of each cofferdam and details of construction sequence, site conditions, construction materials, and observed performance data are given for each case.

Lock and Dam 26 (R) Cofferdam - Stages 1 and 2

Background

44. The replacement of the old Lock and Dam 26 located on the Mississippi River near Alton, Illinois, began in 1981 by the US Army Corps of Engineers. Lock and Dam 26 (R) is located 2 miles downstream of the old Lock and Dam 26. Plans for the new structure called for a large, three-stage cellular cofferdam to be built in order to allow construction to proceed in the dry.

45. The three-stage Lock and Dam 26 (R) Cofferdam is one of the largest cellular cofferdams ever to be constructed. All stages of the cofferdam were designed as temporary structures to be removed upon completion of construction. The first stage of the cofferdam was constructed, dewatered, and in full use by the summer of 1982. Since that time, construction inside the first-stage cofferdam has been completed, and this section of the cofferdam has been removed. The second stage was completed by late 1985 and is currently in service. Construction inside the Stage 2 Cofferdam is expected to be finished by 1989. Subsequent to the completion of this work, the third-stage cofferdam will be constructed.

Geometries and dimensions

46. The first stage of the cofferdam was the largest stage and allowed the construction of most of the dam. This stage enclosed an area of about 25 acres and measured approximately 1,500 ft in length, and 800 ft in width. It consisted of 45 main circular cells which were connected by 43 arc cells. Each main cell measured 63 ft in diameter and 60 ft in height above the dredge line. The sheet piles for the cells had an average penetration of about 35 ft into the underlying foundation soils. A layout of the first-stage cofferdam and a schematic of typical cell configurations are shown in Figures 5 and 6, respectively.

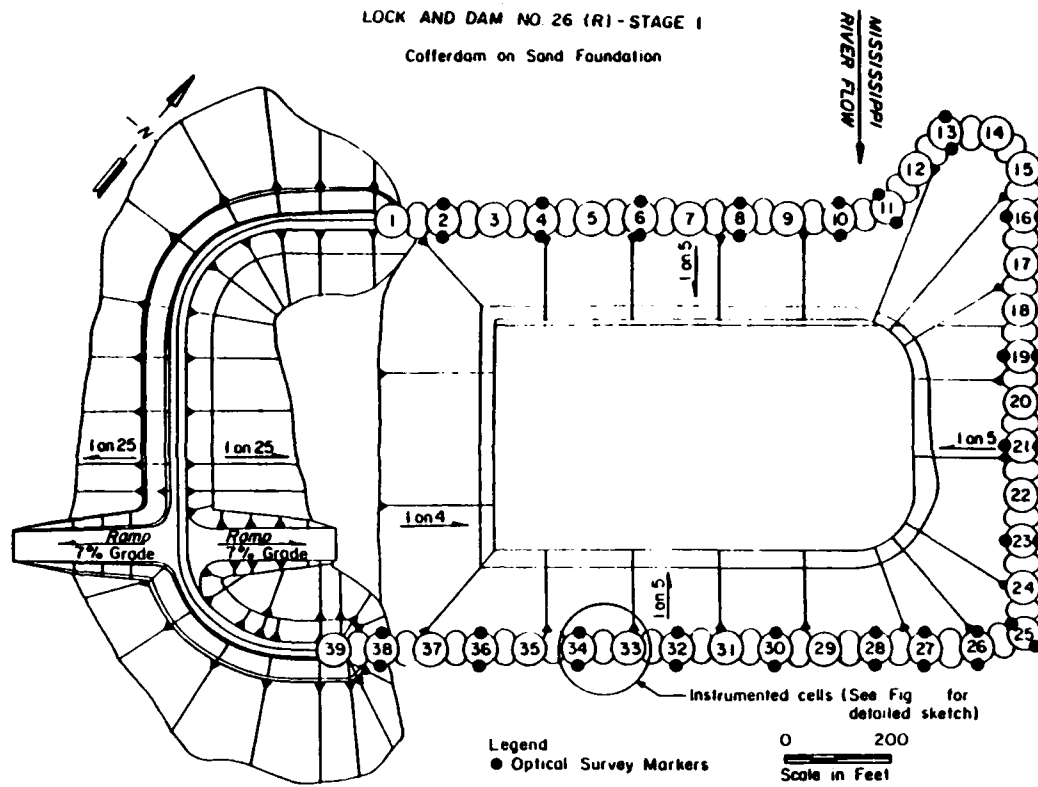


Figure 5. Layout and instrumentation of Stage I Cofferdam

LOCK AND DAM NO. 26 (R)
Cell on Sand Foundation

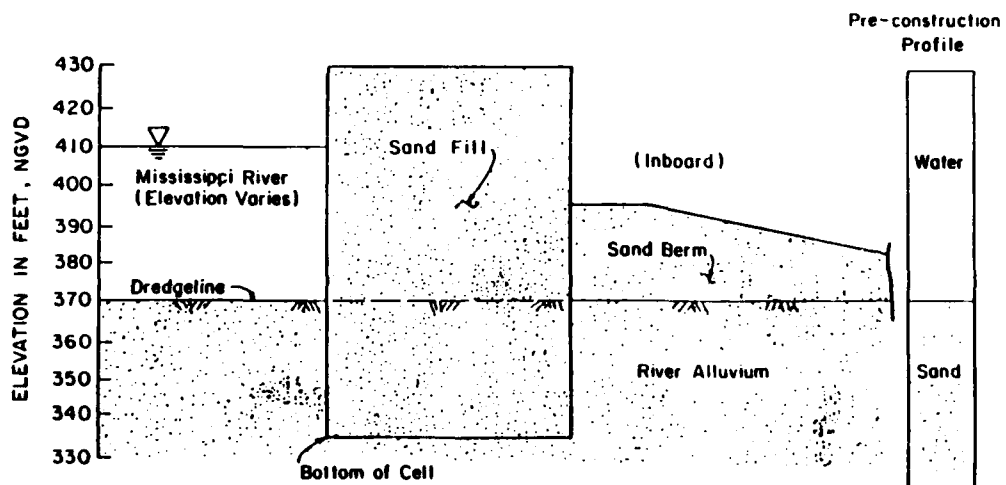


Figure 6. Typical cell schematic of Lock and Dam No. 26 (R)

47. Stage 2 of the cofferdam was built to allow the construction of the 1,200 ft lock and a small section of the dam on either side of the lock. The second-stage cofferdam covers an area approximately 1,900 ft long and 600 ft wide. This stage contains 54 main cells and 52 arc cells. The cells on the Missouri leg of the second-stage cofferdam are 60 ft in height above the dredge line, and the cells on the river leg are close to 80 ft above the dredge line. Cell embedments range from 15 ft on the river side to 35 ft on the Missouri leg. Figure 7 shows the layout of the second-stage cofferdam.

LOCK AND DAM NO. 26 (R)-STAGE 2
Cofferdam on Sand Foundation

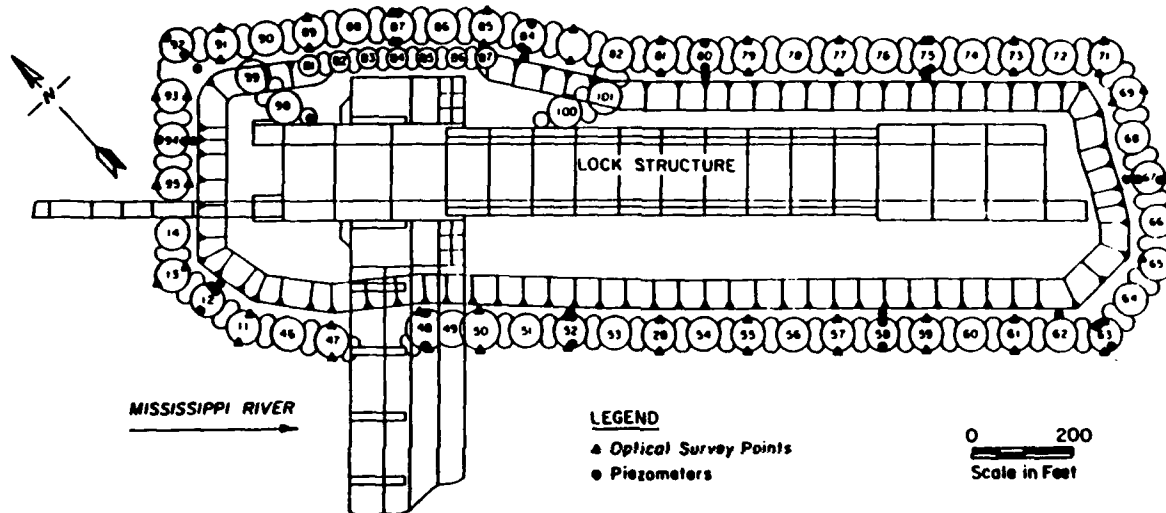


Figure 7. Layout and instrumentation of Stage 2 Cofferdam

48. The third stage of the cofferdam is presently in design and is expected to be under construction by early 1988. This stage of the cofferdam will allow the construction of a second, smaller lock (600 ft long), and the remaining portion of the dam.

Foundation materials and properties

49. The Lock and Dam 26 (R) Cofferdam is founded on 70-ft-thick-alluvial sand deposit underlain by bedrock. The deposit is composed of a series of dense to medium-dense sand layers. Lenses of cobbles and boulders are present in some of the lower layers. For the most part, however, there is little variation among sand layers throughout the deposit. A friction angle of 41 deg was estimated for the foundation sands.

Cell fill materials and properties

50. Riverbed sand, some of which contained gravel, was used for the cell fill. The sand was clean and relatively free-draining. The in-situ

condition of the fill was determined from an extensive laboratory and in situ testing program (Shannon and Wilson 1983; Clough and Goeke 1986). Test results show that cell fills were fairly uniform in density with average relative densities close to 60 percent. A friction angle of 35 deg, a uniformity coefficient of 2.6, and a median grain diameter of 0.5 mm was determined for the fill.

Sheet piles

51. Each main cell consists of 154 steel sheet piles; arc cells are composed of 78 sheet piles. Because higher loads are expected to occur in the common walls between the main cells and the arc cells, high strength PSX-32 sheet piles were used in all common wall construction. US Steel PS-32 sheet piles were used in all other sections of the cells. Weep holes were cut in the sheet piles to allow drainage of the cell fill.

Construction sequence

52. The first operation in the construction sequence was cell filling. The river sand used for the fill was excavated from the riverbed, placed on barges, and allowed to drain. Subsequently, the fill was placed in the cells with a clamshell bucket. Bulldozers were used to level the fill as it reached the tops of the cells. Shortly after cell filling and closure of the cofferdams, sand stability berms were placed against the interior walls. The berms were 25 ft high at most sections of both cofferdams. The deeper river leg of the second-stage cofferdam had berm heights close to 35 ft. Due to space limitations, a small section of the river leg of the Stage 2 Cofferdam was incorporated with a double-row of cofferdam cells in lieu of the sand berms. Dewatering of the cofferdams was achieved by a multistage well-point system. Above-ground pumps which pumped water directly from the pool were used in combination with subsoil well-points. This involved pumping water directly from the pool until subsoil wells could be installed. Each succeeding stage lowered the interior pool elevation below that accomplished by the preceding stage until final dewatering was achieved.

Instrumentation

53. To evaluate the overall performance of the cofferdam, an instrumentation program was instituted by the US Army Corps of Engineers (Shannon and Wilson 1982), (Moore and Kleber 1985). Cells 33 and 34 of the first-stage cofferdam (see Figure 8) were instrumented with earth pressure cells, piezometers, strain gages, inclinometers, and optical survey markers. The Stage 2 cofferdam is instrumented only with piezometers and survey markers. The earth

LOCK AND DAM NO. 26 (R)

Instrumentation Location and Cell Configuration

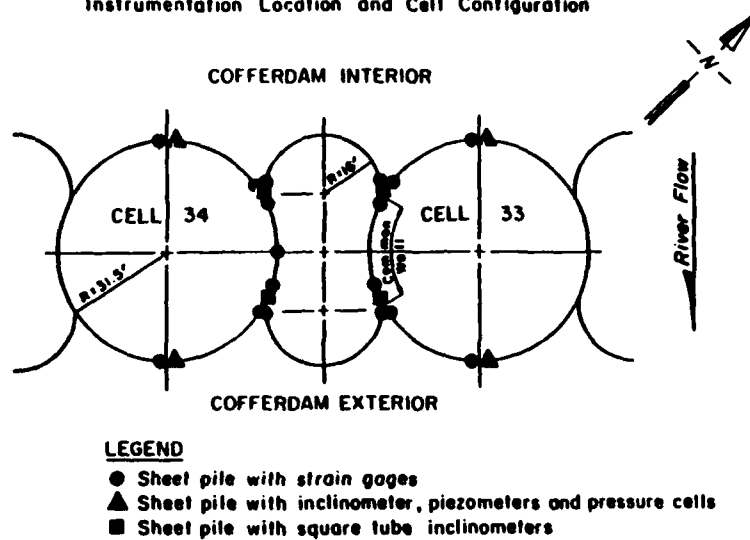


Figure 8. Detail of instrumented section, Lock and Dam No. 26 (R)

pressure cells installed in the two Stage 1 cells did not give credible results and were not considered reliable (Shannon and Wilson 1982). Otherwise, the instrumentation program was relatively successful (Shannon and Wilson 1982; Clough and Kuppusamy 1985). Interpretations of the instrumentation data and an overview of the performance of the Stage 1 Cofferdam have been presented by Kleber (1985).

Observed performance

54. Response to cell filling. This section presents only a brief discussion of the interlock forces and sheet pile movements induced by cell filling. More details of the filling operation and the resulting cofferdam responses are given by Shannon and Wilson (1983).

55. Stage 1 and Stage 2 Cofferdam cells were filled in the same way with the same materials. Upon first filling, the cofferdam cells bulged out in response to the lateral earth pressures induced by the fill material. Average maximum radial deflections determined from inclinometer readings taken after the completion of cell filling were about 4 in. at Cells 33 and 34 of the first-stage cofferdam. There was scatter in the observed movements which is attributed to the difficulty of establishing zero readings on the very flexible sheet pile system prior to cell filling.

56. Interlock forces were estimated from strain gage data. A large amount of variability was present in the strain gage data, but it could be

concluded that the maximum interlock forces occurred during filling. The maximum interlock force was located at approximately one-fourth of the free height above the dredge line as indicated by both inclinometer and strain gage data. Interlock forces measured in the common walls were higher than those measured in the main cells. Figure 9 shows interlock forces measured in both the main cells and the common walls during cell filling. For comparison, the figure illustrates the predictions of five conventional design methods.

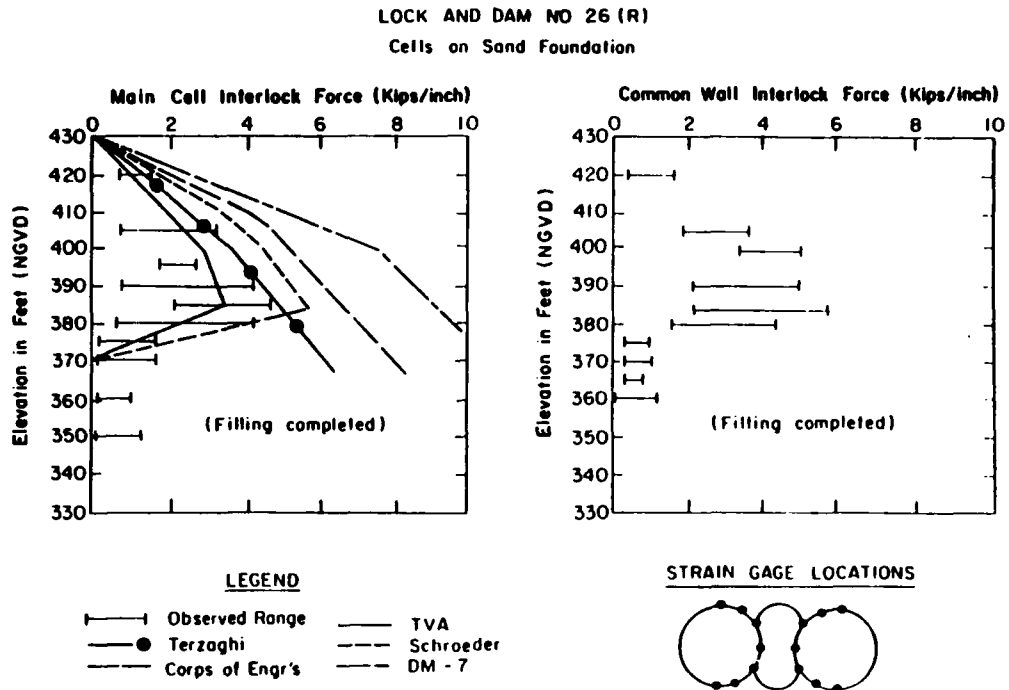


Figure 9. Observed interlock forces and design methods, filling complete

57. Response to berm placement. Sand stability berms were placed inside the cofferdam shortly after the cell filling operation was completed. The berm material consisted of the same dredged river sand as that used for the cell fills. It is estimated that the berms were placed at relative densities close to 55 percent.

58. Upon berm placement, the cells moved approximately 1.0 in. toward the outboard of the cofferdam. Figure 10 shows the movement of Cell 34 during berm placement as determined using inclinometers on the inboard and outboard of the cell. These measurements showed more repeatability than those during filling because the cell has stabilized by the presence of the cell fill. It can be seen that the unsupported portion of the cell (above the dredge line) uniformly translated toward the outboard. Very little deflection occurred

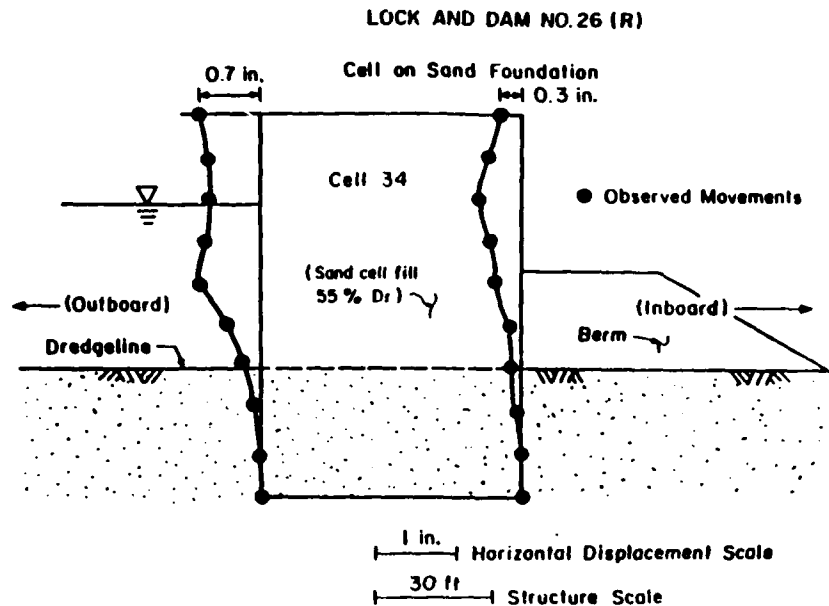


Figure 10. Movement of Cell 34
during berm placement

below the dredge line. Movements of the outboard wall were slightly larger than those observed at the inboard wall. A maximum deflection 0.7 in. was measured at the top of the outboard wall.

59. Strain gage data from the first-stage cofferdam indicated that berm placement caused a reduction in interlock forces. An average (inboard and outboard) reduction of approximately 0.1 kips/in. was observed at elevation 390 ft, 5 ft below the top of the berm.

60. Response to dewatering - Stage 1 Cofferdam. Dewatering of the cofferdam was achieved in several stages with the first one consisting of a water drop 10-15 ft. In this case, the interior pool was lowered by pumping water directly from the pool and expelling it overboard into the river. The cofferdam cells responded to this initial loading by rotating toward the interior. Based on optical surveys of 11 typical cells, approximately 0.5 in. of movement occurred at the tops of both the inboard and outboard walls.

61. In Figure 11, the survey-measured deflection of the top of Cell 8, a typical cell, is plotted against differential head and time. The figure shows differential water head along with the corresponding cell deflections which occurred throughout the early life of the cofferdam. It can be seen that subsequent to the initial pool lowering in February, the differential head remained fairly constant until sub-soil dewatering was begun in late April 1982. Very little additional movement was observed until that time.

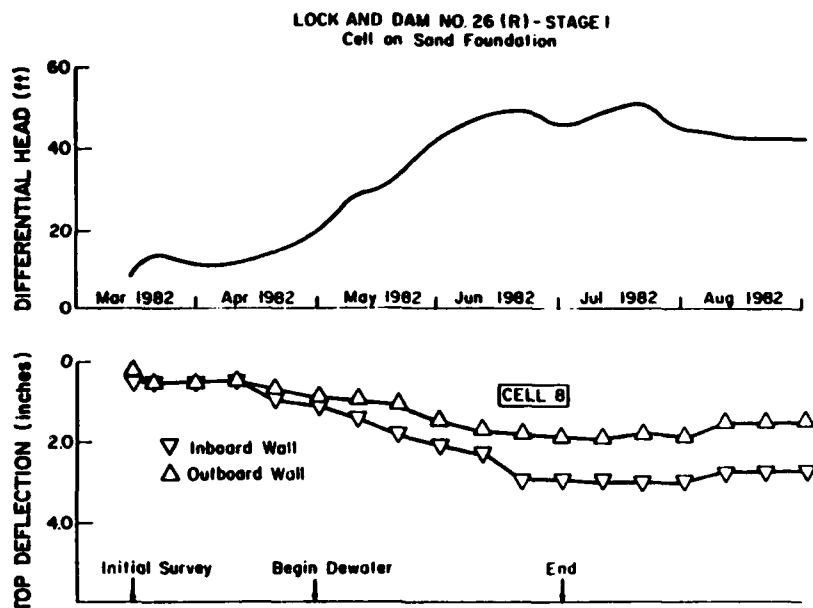


Figure 11. Movements of Cell 8 versus time (optical survey)

62. The majority of the dewatering took place in a period of about 2 months following April and increased the differential head to close to 50 ft by the end of June. As illustrated in Figure 11, the largest increments and fastest rates of movement occurred during dewatering. At the end of dewatering, the deflection of the top of Cell 8 measured approximately 3 in. at the inboard wall and 2 in. at the outboard wall. Optical survey data from 10 other cells indicate that average movements ranged from 1.5 in. at the outboard walls to over 2.0 at the inboard walls. Figure 12 shows a plot of differential water head versus cell deflection for the 11 cells. The average deflections of the inboard and outboard sheets are given along with the upper and lower ranges of deflection. As differential head grows larger, an increase in the following is observed: (a) cell deflection, (b) the difference in the inboard and outboard response, and (c) the range of movements. Subsequent to dewatering, there was almost no increase in cell movement with time. In all cases, the next significant increase in cell movement was observed in December 1982, when the cofferdam was exposed to high water.

63. Figures 13 and 14 show inboard and outboard inclinometer movements due to dewatering for Cells 33 and 34, respectively. The movements as shown are greatly exaggerated with respect to the scale of the structure. Also, the figures show only net lateral movements due to dewatering and do not necessarily represent the true shape of the sheeting. It can be seen that the

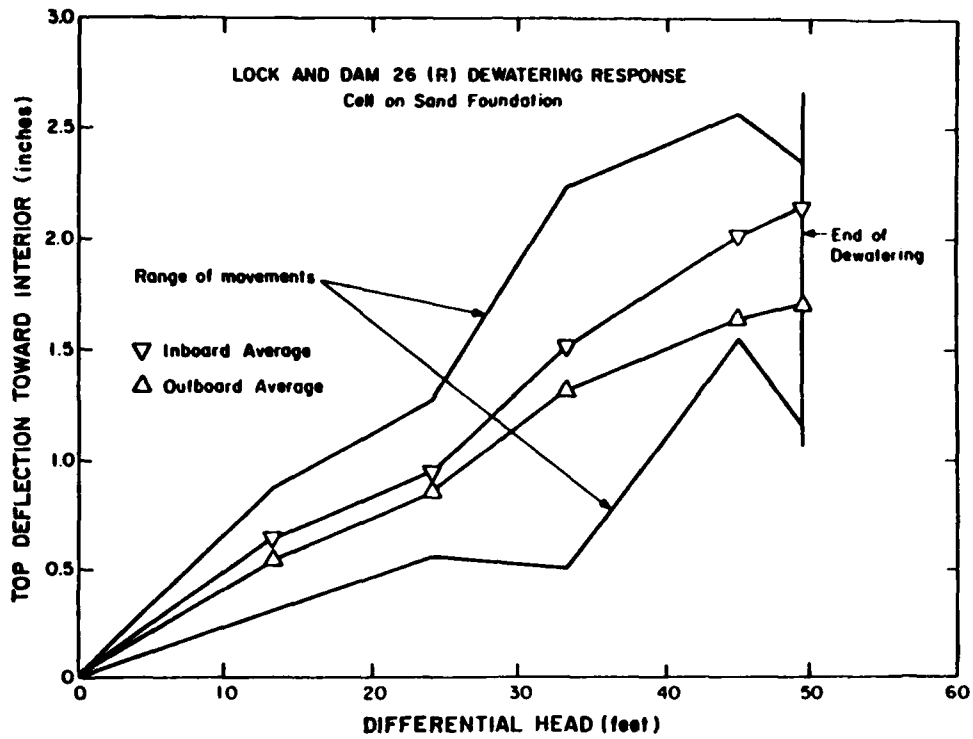


Figure 12. Movements of 11 typical Stage 1 cells during dewatering (optical survey)

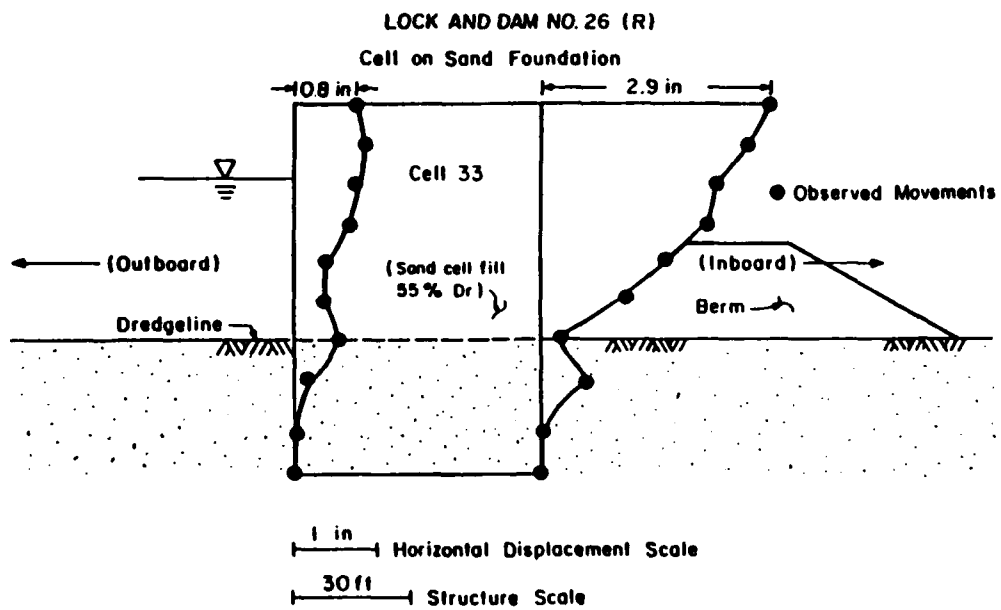


Figure 13. Movement of Cell 33 during dewatering

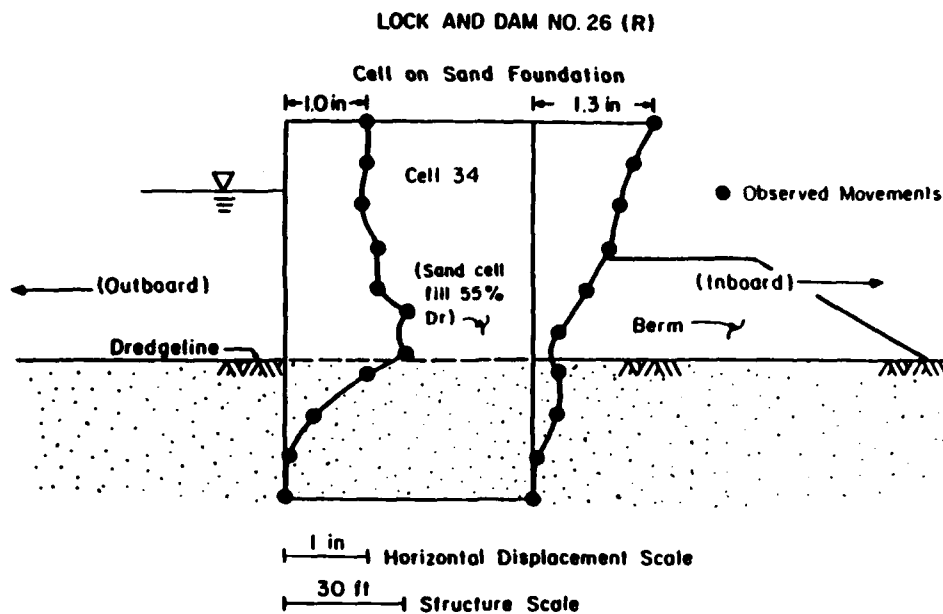


Figure 14. Movement of Cell 34 during dewatering

outboard sheets exhibited slightly smaller movements and somewhat different profiles relative to those of the inboard sheets. This behavior can be understood by examining the manner in which the differential load is applied to the cofferdam during dewatering. Throughout dewatering, the water level on the exterior of the cofferdam remains fairly constant. The differential head is created not by an increase in head on the outboard wall but rather the reduction in head on the inboard wall. The removal of a balancing force (water pressure) on the interior walls of the cells creates the driving force which induces cell movements. This mechanism is strongly suggested in the figures which show the inboard walls inclined sharply toward the interior; whereas, the outboard walls are more nearly vertical (above the dredge line) in profile following dewatering. The consideration of this behavior trend is an important step toward better understanding of cofferdam behavior, especially the interaction of the cell fill.

64. Additionally, Figures 13 and 14 show a small reverse curvature in both the inboard and outboard walls occurring at the dredge line. Below this height, the movements are much less and the slope of the interior wall is closer to vertical. Deflections below the dredge line decrease rapidly as they approach the sheet tips.

65. The movement profiles also give a feel for the contribution of the stability berms toward limiting the deflections. As indicated in the figures, the berms allowed very little bulging to take place near the dredge line.

During dewatering, deflections below the elevation of the berm were less than those in the upper portions of the cells.

66. Response to dewatering - Stage 2 Cofferdam. The dewatering of the Stage 2 Cofferdam began in January of 1986, and was completed by April. As expected, the differential head at the end of dewatering was approximately 65 ft. The cofferdam cells rotated toward the interior in response to this differential water load. With the exception of the river leg, the overall behavior of the second-stage cofferdam was consistent with that of the first stage. It may be remembered that cells on the river leg of the cofferdam have greater heights (80 ft) and shallower embedments (15 ft) than those elsewhere.

67. All movements of the Stage 2 Cofferdam were monitored by optical surveys. Gaps were present in the survey data due to the fact that survey markers were often blocked by construction activity. In some cases, the construction activity induced inconsistent and erratic cell movements, especially subsequent to the initial dewatering period. This made it more difficult to delineate typical cell behavior beyond that point. Where distinguishable, these movements were removed from the data.

68. Figure 15 shows the deflection of Cell 81, a typical Stage 2 cell, plotted against differential head and time. The figure illustrates the response of the cell throughout dewatering and beyond. It can be seen that the deflection of the cell increased dramatically during dewatering with the

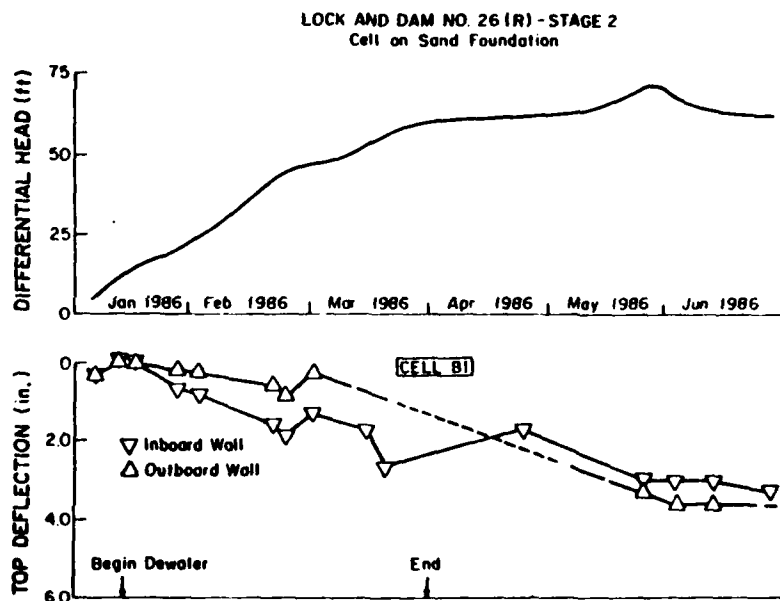


Figure 15. Movements of Cell 81 versus time (optical survey)

inboard wall deflecting more than the outboard wall. At the end of the dewatering, deflections of approximately 2.0 in. and 1.0 in. were observed at the top of the inboard and outboard wall, respectively. Shortly after dewatering, the outboard wall is seen to have experienced the greater movement. This is not completely understood, but may be attributed to construction activities taking place on the top of the cofferdam.

69. Based on survey movements of 16 typical cells the average deflection of the Stage 2 Cofferdam was roughly equal to that of Stage 1. Figure 16 shows the average cell deflections due to dewatering for the 16 cells.

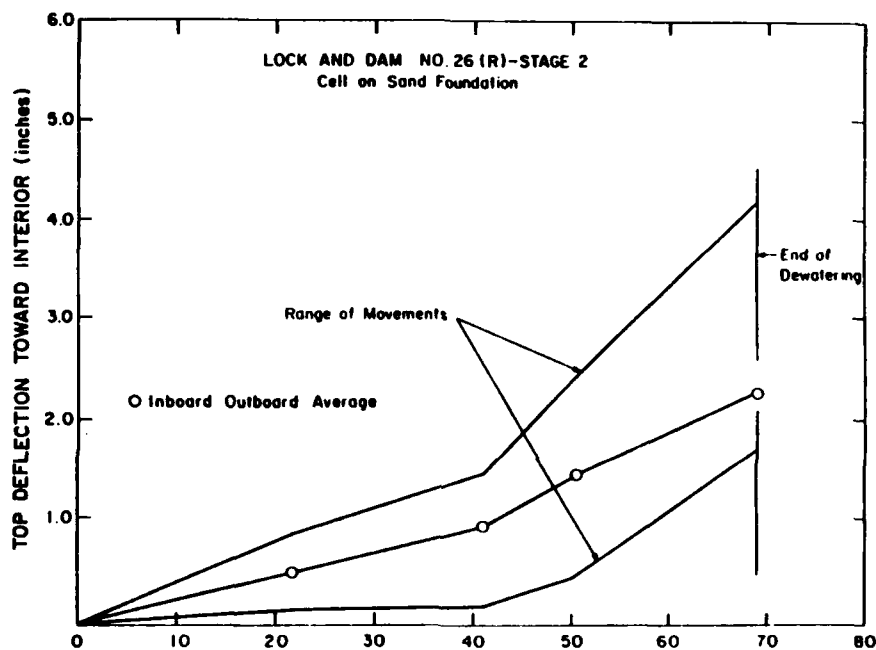


Figure 16. Movements of 16 typical Stage 2 cells during dewatering (optical survey)

Complete, uninterrupted movement data for both walls of the cells were unavailable. Thus, the responses of the inboard and outboard walls were averaged and plotted against differential head. The ranges of movements are provided to indicate the upper and lower movement extremes. It can be seen that average cell deflections and ranges of movement increase with differential head. At the end of dewatering, the average movement at the top of the cells was close to 2.0 in., slightly higher than the Stage 1 average. The higher average movement of the Stage 2 Cofferdam reflects the presence of the river-leg cells. Near the end of dewatering, the upper range of movement is much higher than the average (see Figure 16). This is due to the fact that the cells on the river leg experienced the greatest movements (reflected by

the upper range); but they did not constitute a majority of the total number of cells considered in the average.

70. In all cases, the highest rates and largest increments of movement were observed during dewatering. Very little creep-type movement was observed at any cells subsequent to dewatering. At most cells, the inboard walls deflected more than the outboard walls. As can best be determined from a limited amount of data, the relative wall movements were small and tend to suggest that the cells experienced translations similar to those described for the Stage 1 cofferdam.

71. Response to flooding - Stages 1 and 2. The Stage 1 Cofferdam was exposed to high water on two occasions. The first high water event occurred in December 1982, when the Mississippi River threatened to overtop the cofferdam. As the river elevation approached the top of the cofferdam, it was decided to flood the interior. The cofferdam remained flooded for several days until the high river water subsided. The second flood came during April 1983. In this case, the river elevation again approached the top of the cofferdam, but it was decided not to flood the interior. The floods increased the differential water load on the cofferdam above that which was experienced in dewatering. As a result, the response of the cofferdam during and after the floods was different from that observed during the initial loading (dewatering).

72. Significant cell movements were observed during both flood events. Figure 17 shows a plot of deflection versus differential head. The differential head-deflection curve represents the average behavior of 11 Stage 1 cells throughout dewatering and both flood events. Several points on the curve are labelled to help delineate each load cycle. A table is included in the figure to describe the labels. It can be seen that during the December and April floods, the cells experienced movements first in the inboard direction, followed by movements in the outboard direction once the flood subsided. In both cases, the net movement toward the inboard was larger than the subsequent movement in the outboard direction.

73. As shown in Figure 17, a differential head of about 48 ft was exerted on the cofferdam during normal river stage. During December, the exterior river elevation reached an elevation of 426 ft, 4 ft below the top of the cofferdam, and the differential head at this time was close to 60 ft. In response to the added 12 ft of water head, the cells rotated approximately 1.5 in. toward the inboard side. As the self-initiated flooding was

LOCK AND DAM NO. 26 (R)
Cell on Sand Foundation
(STAGE 1)

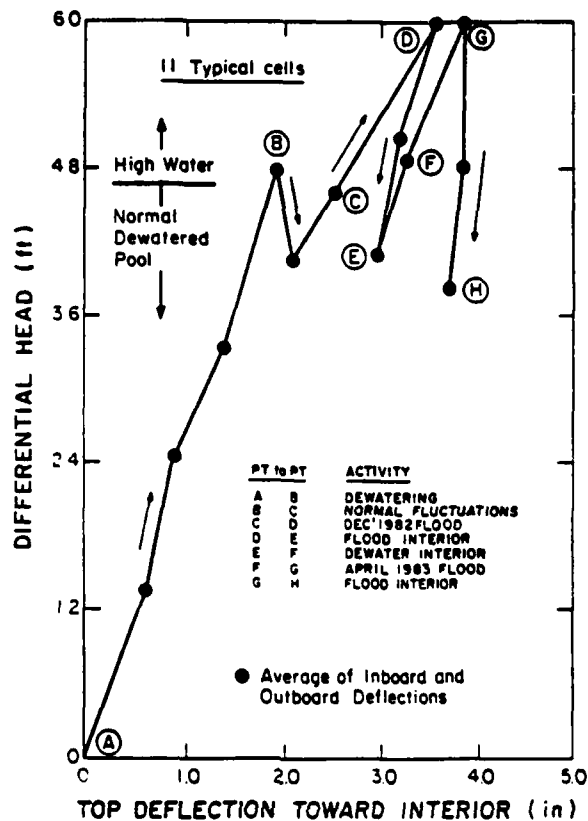


Figure 17. Loading response of 11 typical cells (optical survey)

undertaken, the interior pool was raised to elevation 380 ft, and the differential head was reduced to 46 ft. The cells rebounded approximately 0.5 in. toward the outboard side in response to the load reduction. As the river began to subside, the interior of the cofferdam was dewatered and restored to the normal pool elevation 360 ft. The cells rotated 0.2 in. toward the inboard side of the cofferdam in response to the dewatering. The cofferdam remained essentially at this position for several months until the April 1983 flood event.

74. As the river rose in April, the differential head approached 60 ft once more. The cells again translated toward the inboard. The average movement of the 11 cells was close to 0.5 in. As the flood water receded, the cofferdam cells rebounded very little. Note that the slope of the "unloading" portion of the curve (E to F) is almost flat (zero).

75. This hysteretic type of loading pattern was also observed in the Stage 2 Cofferdam. The Stage 2 Cofferdam was exposed to high water in October

1986. The differential head reached almost 80 ft before the interior of the cofferdam was flooded. For 16 cells examined, the overall behavior of the cofferdam was consistent with that observed at the first-stage cofferdam. As shown in Figure 18, the flood water on the exterior caused the cells to rotate

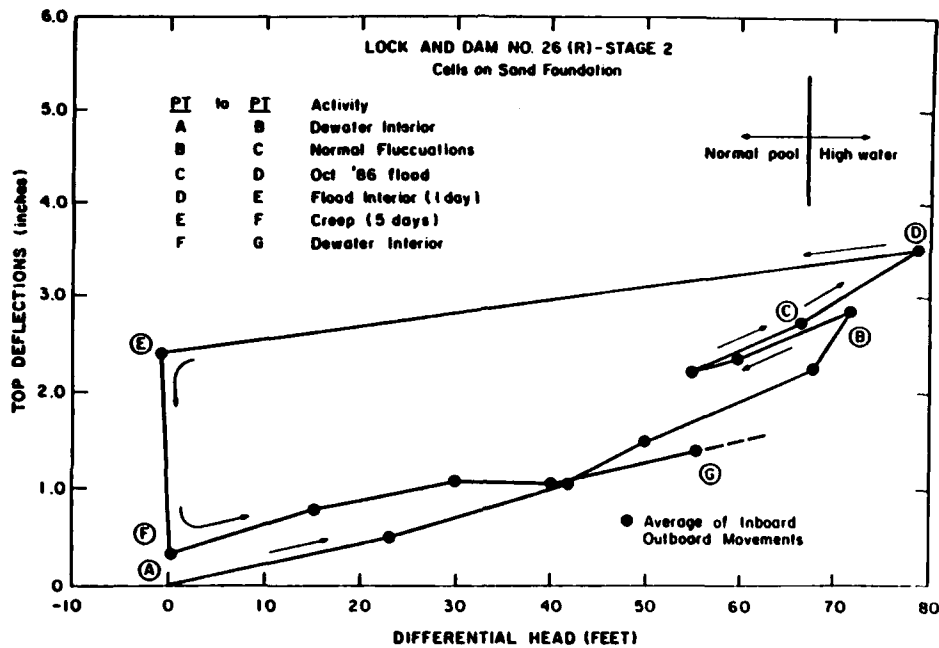


Figure 18. Loading response of 16 cells (optical survey)

approximately 1.4 in. inboard. As the interior was flooded, the differential head dropped to 0 ft, and the cells quickly rebounded 1.0 in. toward the outboard. The cofferdam remained flooded for several days thereafter. During this period, the cells crept slowly toward the outboard of the cofferdam. At the commencement of pool dewatering, the cells were close to their original position prior to the initial January dewatering. This behavior is not unreasonable due to the fact that throughout part of the flood, the interior pool elevation level was actually higher than the outside river elevation.

76. At the Stage 1 and Stage 2 Cofferdams, the loading patterns indicate that the net incremental cell displacements decreased with each successive load of the same magnitude. As the cofferdams came to equilibrium under a load of a given magnitude, their position remained essentially constant until the load was exceeded. Fluctuations in load below this equilibrium load resulted in very small incremental movements.

77. Figure 19 shows the relative wall movements (top of cell) for the 11 Stage 1 cells due to the December and April floods. It can be seen that during flooding, the outboard of the cells moved more than the inboard walls.

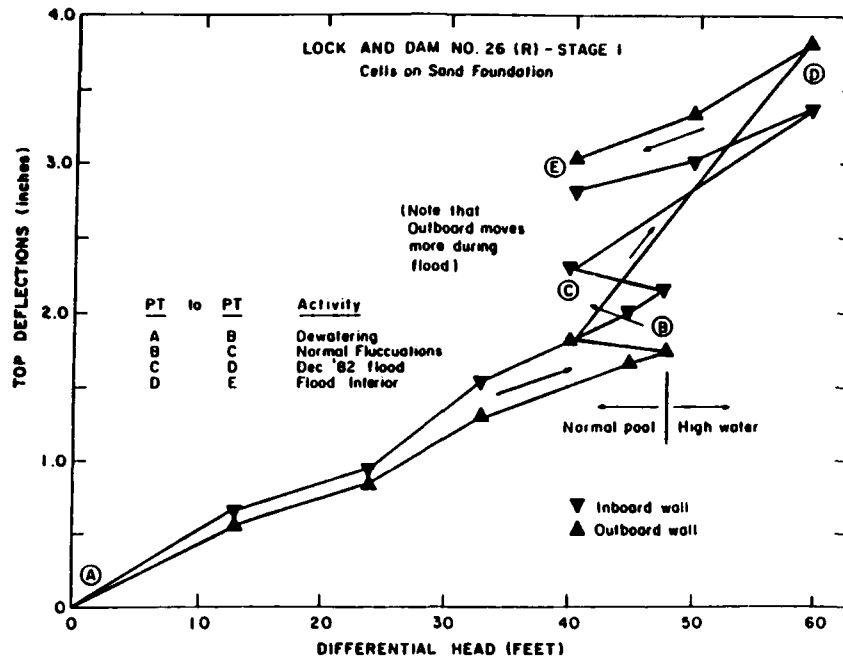


Figure 19. Relative displacements of inboard and outboard walls of 11 cells

This trend is not consistent with that observed during dewatering, where the inboard movement was larger. One explanation for this reversal relates back to the idea of examining the manner in which the differential head is applied. As opposed to dewatering, the additional differential head during a flood is created by an increase in load on the outboard wall of the cofferdam. This tends to accentuate the deflection of the outboard wall. Also, in cases where the interior of the cofferdam is flooded, counteracting water pressure is applied directly to the inboard walls. The water pressure tends to limit the inward movement of the inboard sheets. The behavior of the Stage 2 Cofferdam was slightly different from Stage 1 in that the inboard wall of the Stage 2 Cofferdam exhibited larger movements throughout the entire flood event.

78. Inclinator profiles for the Stage 1 Cofferdam taken during the April 1983 flood by the US Army Corps of Engineers (Shannon and Wilson 1983) indicate that the Cell 34 experienced an approximately rigid-body rotation during the flood event. The profiles show that slightly more movement occurred at the inboard wall of the cell. However, the majority of the cells, as indicated by optical survey, experienced greater movements at the outboard wall. Data for the inboard inclinometer at Cell 33 were anomalous. At the exterior wall, the movement of Cell 33 was roughly equal to that of Cell 34, approximately 0.5 in. at the top. Figure 20 illustrates the inclinometer

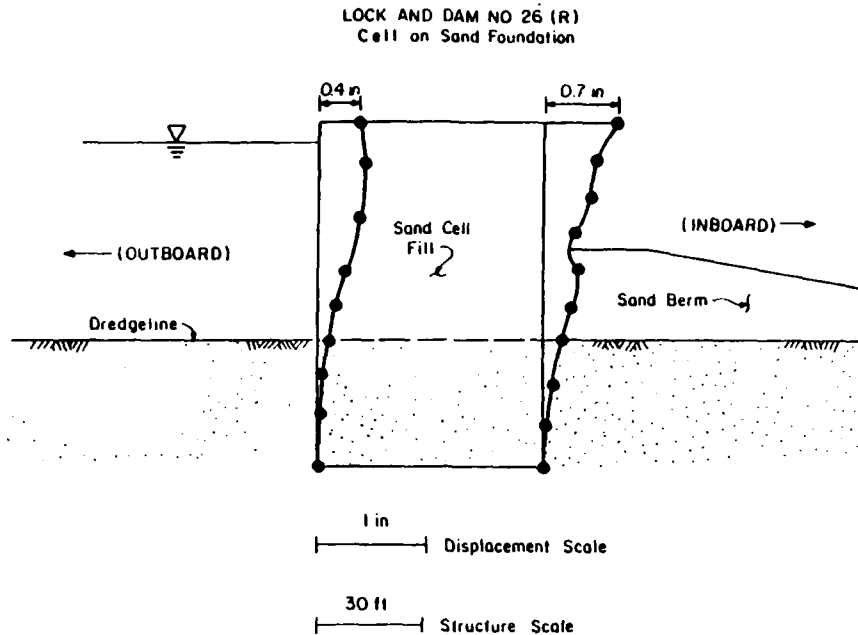


Figure 20. Movement of cell 34
during flood (April 1983)

profile recorded at Cell 34 during the April 1983 flood.

79. Strain gage data from the US Army Corps of Engineers (Shannon and Wilson 1983) indicate that the overall effect of the flood events was to reduce cell interlock forces approximately 1.5 kips/in. As expected, the outboard walls experienced the larger reduction. This is due to the fact that the increased water pressure on the exterior of the cofferdam counteracts the outward pressure of the soil on the inside of the cell, thereby reducing interlock tensions. On the interior walls of the cells, little change in interlock force was observed above the elevation of the interior berm. Below the berm, the interlock forces were reduced as the cells leaned against the berm. In response to the lowered interlock forces at the interior and exterior walls, the interlock forces in the common walls were also reduced. It is interesting to note that during both flood events, Cells 33 and 34 moved in the transverse direction, toward their common connecting arc. One explanation for this is that the inboard and outboard walls tend to flatten due to the flood loadings. As this occurs, the main cells bulge laterally, forming a sort of elliptical-shaped cylinder. The bulging induces lateral pressures on both sides of the common arc cell. As the bulging increases, the pressures increase, and the soil inside the arc becomes more compressible. Thus, the

cells continue to deflect toward the common arc. This mechanism appears to be consistent with the observed changes in the interlock forces.

Trident Drydock Cofferdam

Background

80. The development of the Naval Submarine Base, Bangor, Bremerton, Washington required the construction of new onshore and offshore facilities in an effort to accommodate the Trident class submarine. The submarine base is located on the Hood Canal in the state of Washington. Development plans for the base called for the construction of a new, graving drydock. In order to allow the construction of the drydock to proceed in the dry, it was necessary to install a cellular cofferdam.

81. The cofferdam was designed in part and installed as a permanent structure. Except for one small end section, the cofferdam currently serves as a working platform for the operation of the drydock. Environmental conditions and space constraints posed rigid performance requirements for the cofferdam. The drydock was constructed offshore in deep water. This deep-water location required the cellular cofferdam to retain almost 80 ft of water during extreme high water. Due to space limitations imposed by adjacent pier construction, the cofferdam was constructed and dewatered without the use of internal stability berms. The absence of the berms, coupled with the large differential water load, gave rise to concern for interlock tensions and sliding stability. Prudent design measures were implemented, and the cofferdam was constructed and dewatered without incident. It has been suggested that the Trident Drydock Cofferdam is one of the deepest cellular cofferdams to be successfully dewatered without the use of stability berms (Sorota and Kinner 1981).

Geometries and dimensions

82. The Trident Drydock Cofferdam enclosed an area that measured approximately 774 ft long and 130 ft wide. A site plan showing the layout of the cofferdam is given Figure 21. The cofferdam consisted of 24 main cells and 24 connecting arc cells. The main cells were spaced from 84 ft to 94 ft on center, whatever was necessary to achieve the desired layout of the cofferdam. Each main cell was 76 ft in diameter and stood approximately 80 ft above the dredge line. Generally, cells on the west side of the cofferdam were slightly taller than the other cofferdam cells. Cell embedments ranged

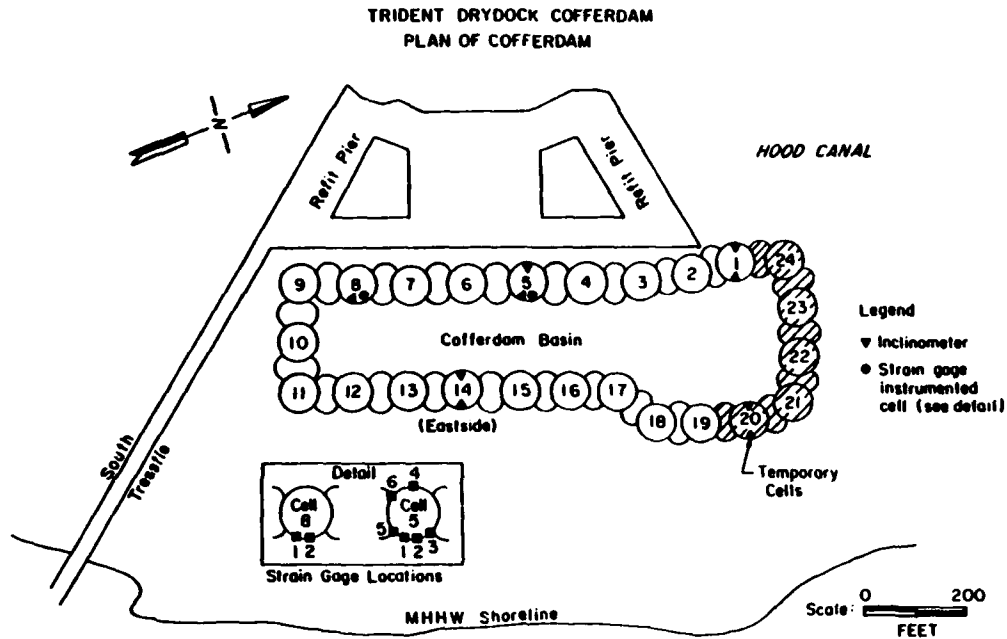


Figure 21. Layout of cofferdam and instrumentation location

from 2 ft to 4 ft. On the average, the cells had about 4 ft of penetration. Figure 22 shows a schematic of a typical cofferdam section.

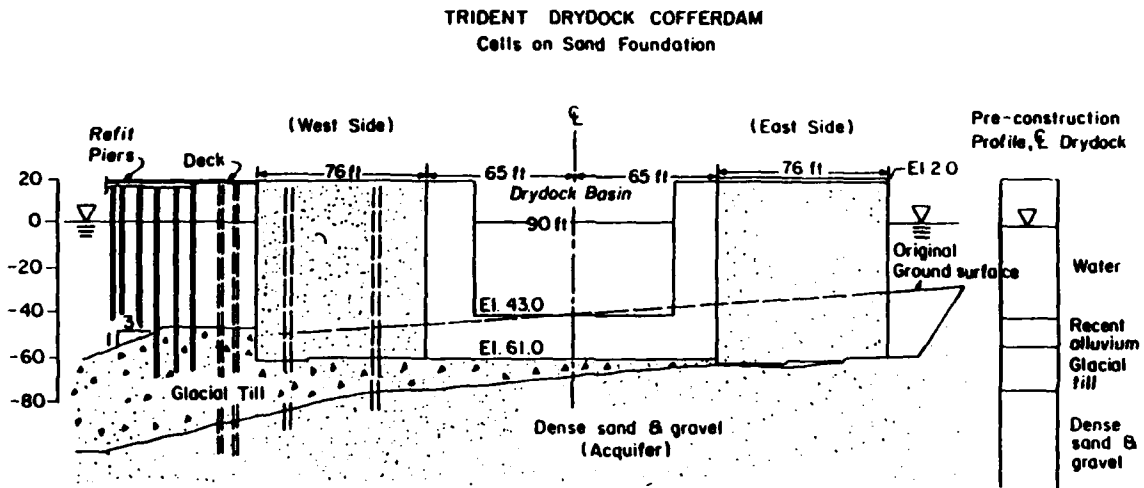


Figure 22. Schematic of typical section

83. As shown in Figure 21, Cells 21 through 24 were located at the entrance (north side) of the drydock basin. These four main cells along with five connecting arc cells were removed shortly after the completion of the drydock. Cells 1 through 20 and their connecting arcs remain as part of a permanent service platform.

Foundation materials and properties

84. The Trident Drydock Cofferdam is founded on a very dense deposit of glacial till underlain by overconsolidated sands and gravels. Due to the dense nature of the till, it was decided that the sheet piles could not be driven more than a few feet into the till without risking pile damage or loss of interlock. Thus, it became necessary to excavate much of the till down close to the final design elevation of the sheet pile tips. As a result, the till is only a few feet thick in most locations and pinches out toward the east side of the cofferdam. The underlying sand and gravel stratum has an estimated thickness of 200 to 250 ft. Penetration resistances measured with a 300-lb hammer falling 30 in. and a split-spoon sampler with a 2.5-in.-inside diam showed blow counts varying from 50 to 200 blows per foot in the till and from 70 to over 400 blows per foot in the sand and gravel. Figure 22 illustrates the arrangement of the foundation soils underlying the cofferdam.

Cell fill materials and properties

85. The cell fill consists of a well-graded, gravelly, coarse to fine sand. The maximum particle size is 2 in. and less than 10 percent of the material passed the No. 200 sieve. The cell fill was densified to a relative density of about 75 percent by deep vibratory compaction. In situ unit weight tests performed subsequent to densification measured an average unit weight of 130 pcf in the cell fill. These unit weight tests were conducted in the upper portions of the cells near the fill surface.

Sheet piles

86. Each main cell consists of 172 sheet piles and four wye sections. The connecting arcs contain 29 to 35 sheet piles as determined by cell location and spacing. All sheet piles are United States Steel PSX-32 sheet piles with a maximum interlock strength of 28 kips/in. The wye connections are 40-deg extruded wye sections. The sheet piles are between 83 and 103 ft in length and were installed with no more than one splice. Weep holes were cut in the sheets to facilitate cell drainage. Figure 23 illustrates the geometry of a representative cell and arc.

Construction sequence

87. Construction at the site began with dredging in the location of the cells down to the bearing stratum. Much of the glacial till overlying the overconsolidated sands and gravels was removed prior to the driving of the sheet piles. Templates were used to drive the sheet piles into the underlying soils. Subsequently, all slough material left over from the dredging

TRIDENT DRYDOCK COFFERDAM
Cell and Arc Geometries

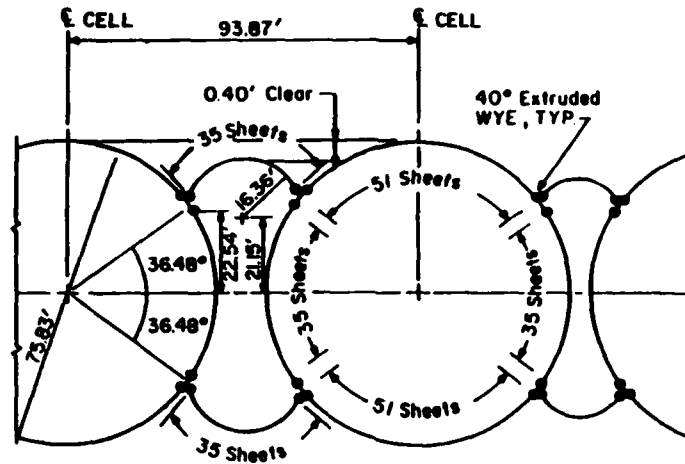


Figure 23. Typical cell and arc

operation was cleared from the cell bottoms prior to cell filling. The cell fill was placed underwater by clamshell bucket and later densified by a vibratory probe. A pressure relief well system was installed prior to the densification to allow the drainage of excess pore pressures. Due to unacceptably high interlock forces created by water pressures inside the cells, it became necessary to dewater the cell fill. The cell fill was dewatered by a series of wells which were installed inside the cells after filling. The cofferdam basin was simultaneously dewatered by a subgrade well system.

Instrumentation

88. Cofferdam performance was monitored by inclinometers, optical survey markers, strain gages, and observation wells. Inclinometers were installed on the inboard and outboard sheets of four main cells and were used to establish deflected cell profiles. Horizontal and vertical movements were monitored by optical survey markers. The markers were placed on the inboard and outboard walls of each cell. Strain gages were placed on several sheet piles in Cells 5 and 8 to measure interlock forces. Observation wells were installed in each main cell and were located adjacent to the inboard walls.

Observed performance

89. Response to filling and compaction. Inclinometers were not installed in the cells until after the cell filling and compaction operations were completed. Thus, the relative movements induced by each operation are not known. However, strain-gages were installed prior to these operations and

indicated cell behavior throughout the early life of the cofferdam. After filling, interlock tensions averaged roughly 5 to 7 kips/in. The subsequent compaction of the fill caused increases in tensions of up to 2 kips/in. For the most part, no significant difference was observed in the interlock tensions in the basin side sheets of Cell 5 as compared with the common wall sheets near the wye connection.

90. Response to dewatering. The initial and most significant differential loadings came on the cofferdam during the dewatering of the interior basin. The cofferdam cells responded to the dewatering by rotating toward the inboard. Subsequent to dewatering, the differential water head was fairly constant, as it varied only with the tide cycle of the Hood Canal. For the most part, the exterior water elevation never reached a level which constituted a flood condition. Hence, no large increments of movement were observed after the dewatering was completed. In all cases, cell movements were small, and the performance of the cofferdam was quite satisfactory..

91. Dewatering of the cofferdam was performed in a systematic manner. It began with an interior pool elevation of +9 ft mean lower low water (MLLW) and ended at elevation -59 ft. Throughout the majority of the dewatering period, the pool was lowered in 10-ft increments at a rate no greater than 5 ft per day. At the end of each 10-ft increment, the cofferdam was checked by visual diver inspection and instrumentation monitoring.

92. The dewatering schedule was interrupted at pool elevation -20 ft to perform a proof test on the cofferdam cells. The -20 ft pool elevation corresponds to an average differential head of 26 ft (considering the tide cycle). This pool elevation was held constant throughout the test period which was completed in 3 weeks. The test was performed on two cells at a time and was designed to check the structural integrity of the cells. During the test, the wells in two adjacent cells were shut off, and the water level inside them was allowed to rise to el 0 ft. The added water pressure acting against the inside of the cells caused the cells to bulge outward, thereby increasing sheet pile interlock tensions. The cells were then closely monitored to ensure that magnitudes of interlock tensions and cell deflections were in keeping with those expected during the final stage of dewatering. Figure 24 shows cell deflection plotted against differential head for Cell 5, a typical cell. As shown, cell deflection grows larger as the differential head increases. Creep movements experienced by the cell during the proof test are clearly delineated. At one point, the deflection-head curve becomes

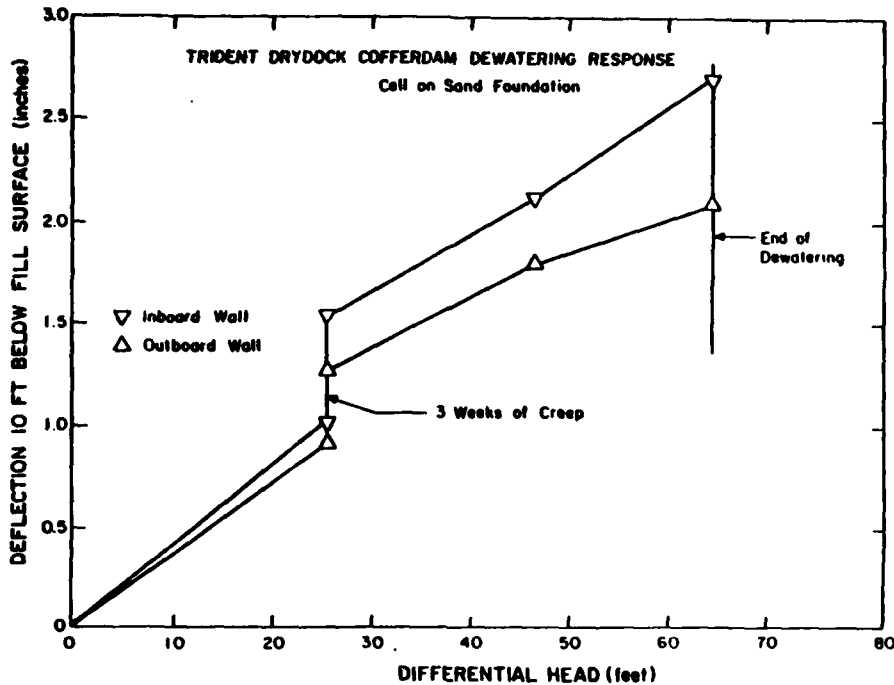


Figure 24. Inclinator movements of Cell 5 during dewatering

vertical, indicating that cell deflection steadily increased although the differential head remained constant. Movement data from seven other cells indicate similar behavior.

93. Subsequent to the proof test, the cofferdam was steadily dewatered until the interior pool elevation reached -59 ft. The differential head increased from 26 ft to approximately 65 ft by the end of dewatering. The cells underwent further deflection toward the cofferdam interior in response to the increased differential head. Figure 25 shows a plot of cell deflection versus differential head for eight cells on the west side of the cofferdam. The plot shows the average inboard wall deflections of the cells and their ranges of movement. The average movement of the cells was close to 3.0 in. at the end of dewatering; whereas, the upper and lower range of deflection was approximately 2.0 in. and 4.0 in., respectively. It can be seen that the slope of the differential head-deflection curve is steeper near the initial part of the curve. This suggests that for equal changes in differential head, the largest increments of movement occurred near the beginning of the dewatering operation. The average deflection of the east side cells was generally equal to or slightly less than that of the west side cells. This is expected since the east side cells have less free height than the west side cells.

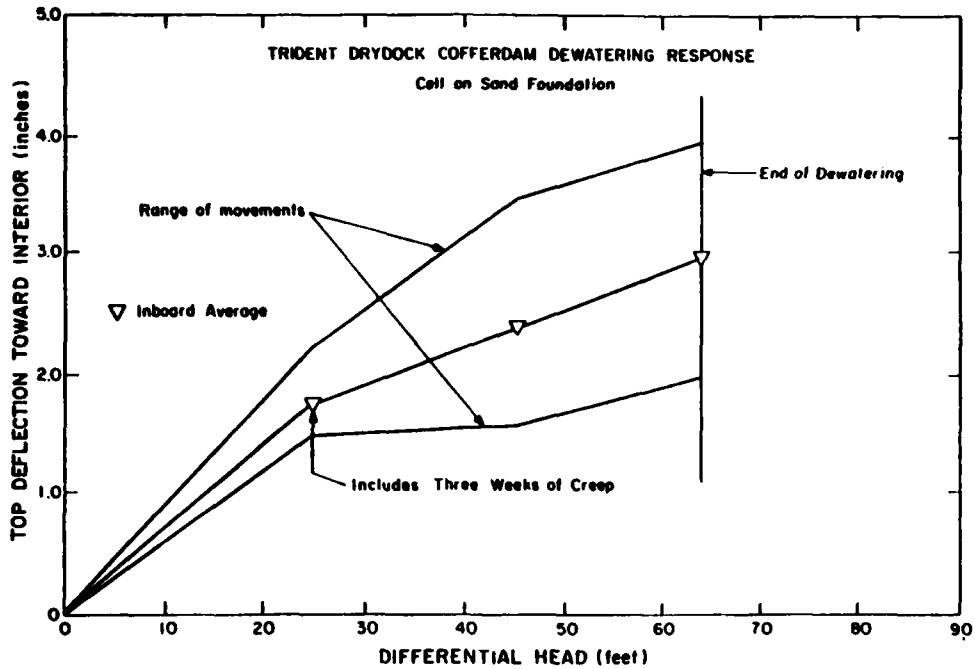


Figure 25. Inboard movements of eight typical cells during dewatering (optical survey)

94. Available data from the literature (Sorota and Kinner 1981) indicate that the largest movements occurred on the inboard walls of the cofferdam. This trend is illustrated in Figure 26 which is based on inclinometer data from Cell 5. The figure shows the movement of the inboard

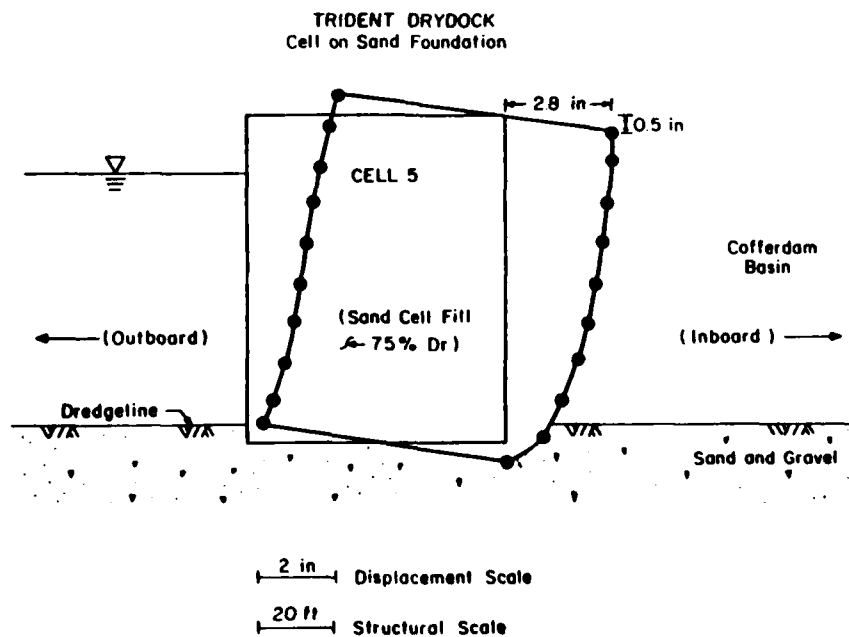


Figure 26. Movement of Cell 5 during dewatering

and outboard walls of the cell throughout dewatering. As shown, the interior wall underwent slightly more bulging than the exterior wall of the cell. The sheets on the loaded side heaved approximately 0.5 in.; whereas, those on the unloaded side plunged 0.5 in. into the foundation soils. This behavior suggests that movement was essentially rigid-body in nature. The high density of the cell fill and foundation, along with the shallow depth of cell embedment, contributed largely to this type of cell rotation.

95. Movements toward the interior continued to occur well after the completion of basin dewatering but at a much slower rate. The decreasing slopes of the deflection-time curves shown in Figure 27 indicate that the

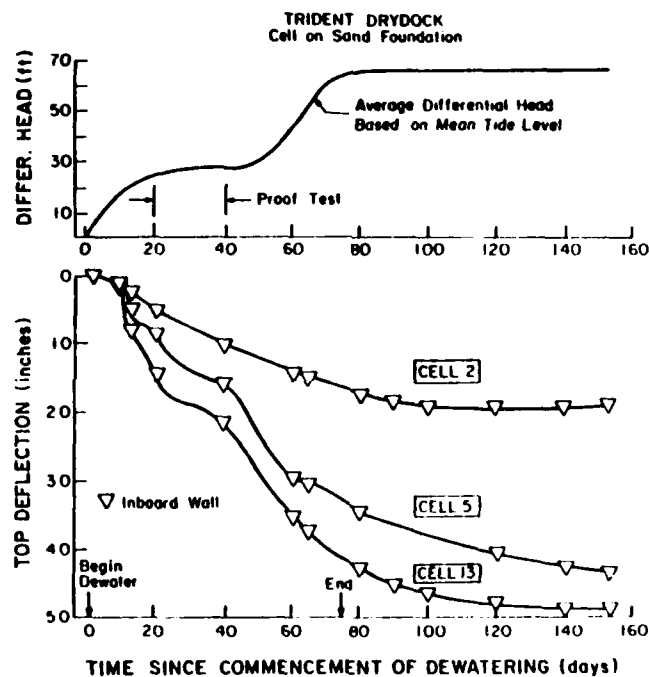


Figure 27. Movement of cells versus time (optical survey)

rates of inward movements continued to decrease with time until all movements ceased several months later. The creep movements were in response to the 65 ft of differential head which remained on the outboard walls throughout drydock construction.

Interlock tensions

96. Throughout basin and cell fill dewatering, the basin-side interlock tensions increased as the outboard tensions decreased. At the outboard sheets, lowering of the water levels decreased the lateral cell pressure

inside the cell. Conversely, at the inboard sheets, the lateral pressures were increased.

97. The proof test caused interlock tensions to increase as much as 2 kips/in. as water pressures inside the cells grew larger. There were differences in this case between the tensions at the wye connections and the basin side sheets. The common wall sheets averaged approximately 20 percent higher tensions than did the basin side sheets (of Cell 5). Maximum tensions in the inboard sheets occurred at 10 ft above the dredge line, while those in the common-wall sheets were located slightly higher. Subsequent to testing, the cells only partially rebounded to their original loads. This is due to the fact that the cell fill displaced outward during the test and prevented the sheets from returning to their original shape.

98. Following dewatering, the removal of a loose fill berm that had accumulated against the interior side of Cell 5 increased the tensions in the inboard sheets of Cell 5 by 1.7 kips/in. This is an important observation which suggests that even loosely-placed soil berms can cause a significant reduction in interlock tensions (Sorota and Kinner 1981). During tide cycles, the tensions changed as much as 1 kip/in., with the highest tensions occurring at low tide.

PART IV: COFFERDAMS FOUNDED ON ROCK

99. This part examines the performance of Willow Island Stage 2 Cofferdam. This cofferdam is of interest since it is founded on rock with little sheet pile penetration. A general description of the background of the cofferdam is presented along with the available instrumentation data. The main objective of this chapter is to introduce the case history and to provide a summary of the overall performance.

Willow Island - Second Stage Cofferdam

Background

100. The Willow Island Second Stage Cofferdam was built to allow the completion of the Willow Island Locks and Dam. The site is located on the Ohio River, 162 miles below Pittsburgh, Pennsylvania, near Willow Island, West Virginia. The project involved the construction of a 1,017-ft-long dam, a main lock 1,200 ft in length, and an auxiliary lock 600 ft long. The dam consisted of eight tainter gates supported by nine reinforced concrete piers. A two-stage cofferdam was constructed to allow pier excavation and other construction to proceed in the dry. The first stage of the cofferdam was used for the construction of five piers of the dam. The Stage 2 cofferdam allowed the construction of the remainder of the dam. The cofferdam was removed subsequent to the completion of the dam in 1975.

Geometries and dimensions

101. The Stage 2 Cofferdam enclosed an area approximately 500 ft in length and 450 ft in width. The cofferdam consisted of 16 circular cells, 5 cloverleaf cells, and 17 connecting arc cells. Figure 28 shows the layout of the cofferdam.

102. Each circular cell measured 65 ft in diameter and stood approximately 55 ft high. The cloverleaf cells were 75 ft in diameter and close to 60 ft tall. All cells were installed with little or no embedment into the underlying foundation. A schematic of a typical Stage 2 cell is illustrated in Figure 29.

Foundation materials and properties

103. The foundation underlying the second-stage cofferdam consists of an alternating strata of sandstone, siltstone, shale, and indurated clay. As shown in Figure 28, a major portion of the cofferdam is founded on a sandstone

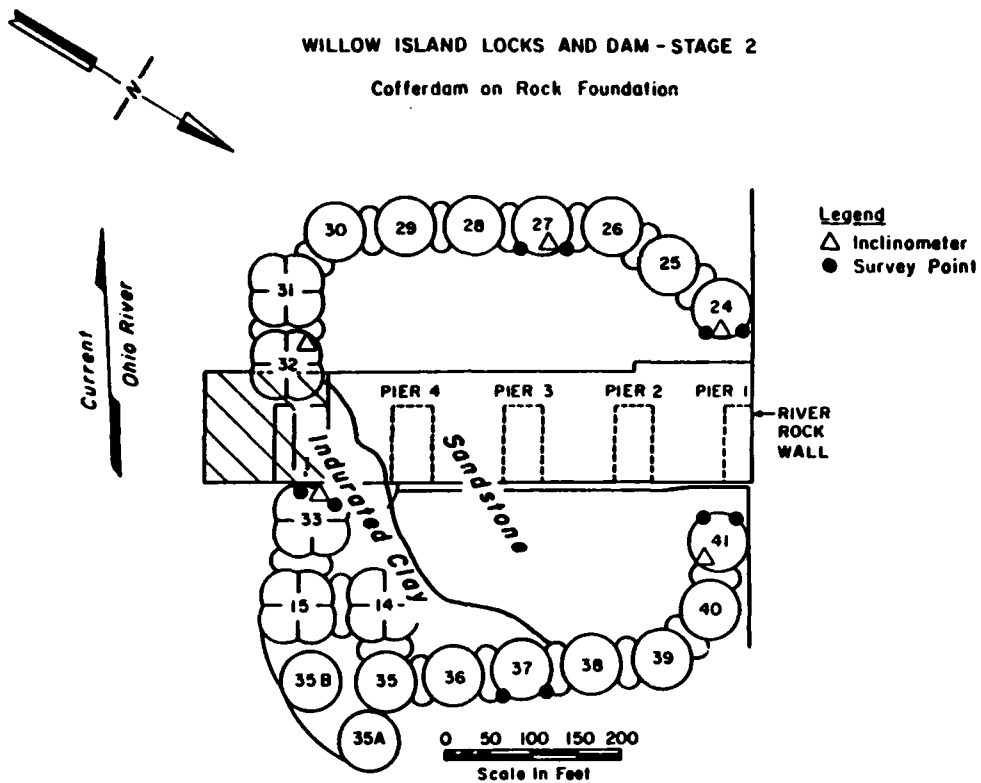


Figure 28. Layout and instrumentation location of Stage 2 Cofferdam

WILLOW ISLAND LOCKS AND DAM
Cell on Rock Foundation

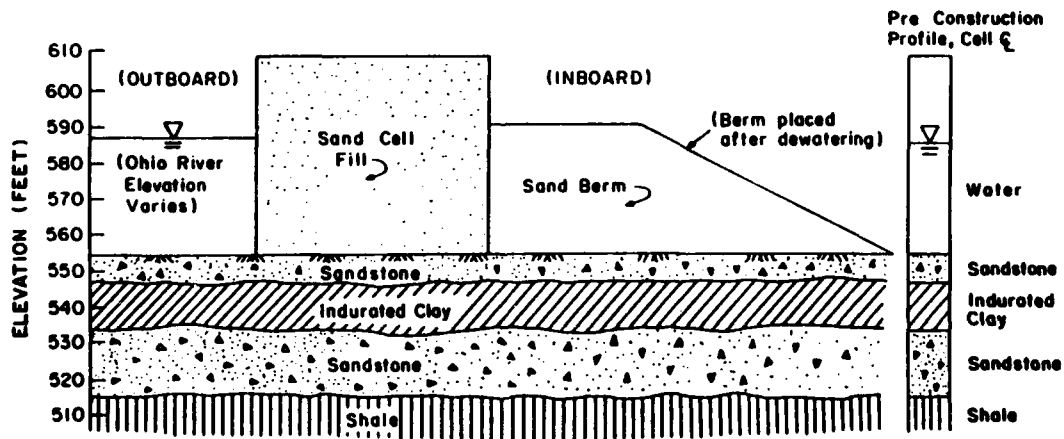


Figure 29. Schematic of typical cell

caprock. A small section of the west end of the cofferdam rests on an indurated clay layer. Cells founded on the sandstone caprock had almost no penetration, while those on the indurated clay had up to 1.5 ft of penetration.

104. The sandstone caprock has an estimated compressive strength of 6,900 psi and a friction angle between 70 and 75 deg. The indurated clay has a cohesive strength close to 5,800 psf and a friction angle of about 40 deg as measured in direct shear materials beneath the Stage 2 cells. Figure 29 shows the typical configuration of foundation.

Cell fill materials and properties

105. The cell fill consisted of free-draining sand and gravel dredged from the river channel. An 18-in. thick layer of stone was placed on top of the fills to provide protection against erosion in the event of overtopping. Based on available data (Hansen and Clough 1982), the cell fill had an estimated friction angle of 30 deg and a cohesive strength of 150 psf. Typical unit weights of the cell fill were close to 110 pcf.

Sheet piles

106. All cells were constructed of MP102 steel sheet piling. Detailed information regarding the number of sheet piles per cell was unavailable. To promote drainage of the fill material, weep holes were cut in the inboard sheet piles of all cells.

Construction sequence

107. The cofferdam cells were constructed using interlocking sheet piles. The cells were filled with sand and gravel material taken from the riverbed. The cofferdam was completed by November 1974. Dewatering of the cofferdam began in January of 1975 and lasted until early February. The interior of the cofferdam was flooded in late February due to high river levels. The second dewatering began on 3 March and was completed by 8 March. Upstream interior berm placement was begun immediately following the second dewatering. Berm placement was interrupted on 21 March when the cofferdam was again flooded due to high water. The final dewatering period lasted from 31 March to 11 April. The upstream berm was completed by 28 April; the downstream berm was finished 2 weeks later.

Instrumentation

108. Prior to dewatering, instrumentation was installed to monitor the overall performance of the cofferdam. Instrumentation located on the inside of selected cofferdam cells included inclinometers, deflectometers, and

pneumatic and phreatic piezometers. Optical survey markers were established on five cells. The upstream and downstream berms were equipped with both pneumatic and phreatic piezometers. As pier construction proceeded, pneumatic piezometers were placed adjacent to pier excavations to monitor pore pressures. The location of the instrumentation is illustrated in Figure 28. The instrumentation as a whole performed well (US Corps of Engineers 1976).

Observed Performance

Response to dewatering

109. The cofferdam was first subjected to differential loading during initial dewatering which began in January 1975. The differential loadings created by dewatering induced cell movements toward the interior of the cofferdam. Based on instrumentation reports (US Corps of Engineers 1976), cell movements were small, and the performance of the cofferdam was generally good.

110. Optical survey data were not available for this study. The movement data presented in the following section primarily consist of inclinometer and deflectometer measurements taken from instrumented cells. Some of the instrumented cells had unusual loading conditions, special geometries (cloverleaves), or foundations that were atypical. The only instrumented circular cells with typical conditions were founded on sandstone caprock.

111. Cells 24 and 27 are circular cells founded on approximately 9 ft of sandstone caprock. These two cells form the basis of the response analyses that follow. The deflection of the cells throughout the early life of the cofferdam is plotted and presented in Figure 30. It is important to note that Cell 24 is tied into the river lock wall and is inhibited from movement in one transverse direction (see Figure 28). Also, the outboard wall is partially shielded from the exterior water load. The quantitative effects of these variables are not known and obscure the ability to delineate typical behavior trends.

112. Figure 30 shows plots of top of cell deflection and differential head versus time for Cells 24 and 27. The deflections given in the figure were measured at the top of the inboard walls by inclinometers. It can be seen that cell deflections increase as the differential head grows larger. Also, it is evident that the largest increments and highest rates of movement occurred during the initial dewatering. Approximately 0.7 in. of movement

WILLOW ISLAND LOCKS AND DAM
Cell on Rock Foundation
(STAGE 2)

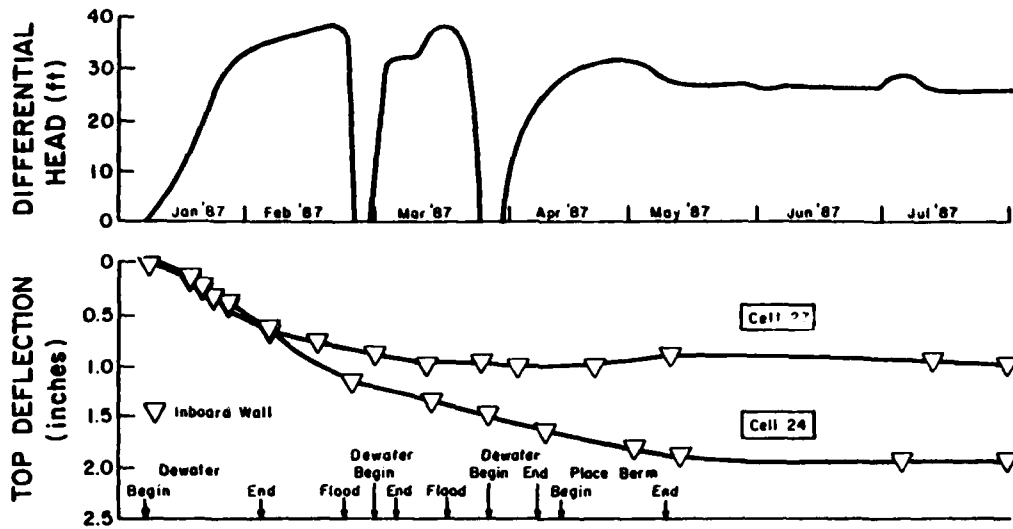


Figure 30. Inclinerometer movements of cells versus time

occurred at the tops of both cells during this period. Figure 31 illustrates the differential head-deflection behavior of both cells during dewatering. After the initial dewatering was completed, the cells continued to move at a slow rate toward the unloaded side of the cofferdam. At the time of the first flood event, the deflection of both cells had increased to almost 1.0 in. The

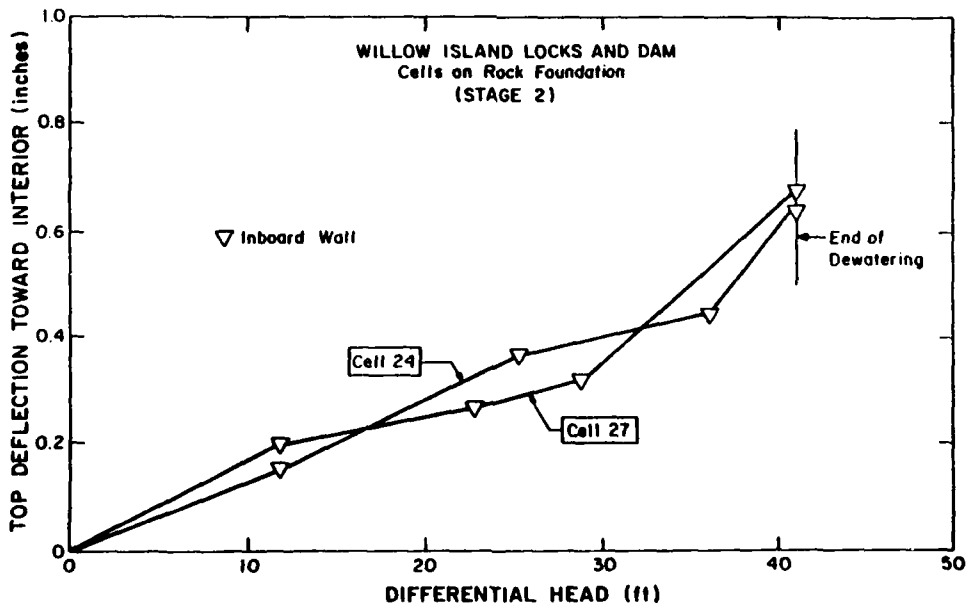


Figure 31. Inclinerometer movements of Cells 24 and 27 during dewatering

response of the cofferdam cells subsequent to this period will be presented later.

113. Inclinometer profiles taken from Cells 24 and 27 indicate that dewatering induced uniform cell translations down to the top of sandstone. Near the sandstone, the cell was strongly distorted and the sheet tips apparently were dragged along the foundation. The inboard wall of each cell leaned a considerable amount toward the interior of the cofferdam. The maximum inboard deflections occurred at the tops of the cells. Deflected profiles of Cells 24 and 27 are given in Figures 32 and 33, respectively. Each profile is greatly exaggerated as compared with the dimensions of the cells. Inclinator profiles from cloverleaf Cell 32 (founded on sandstone) were consistent with this behavior.

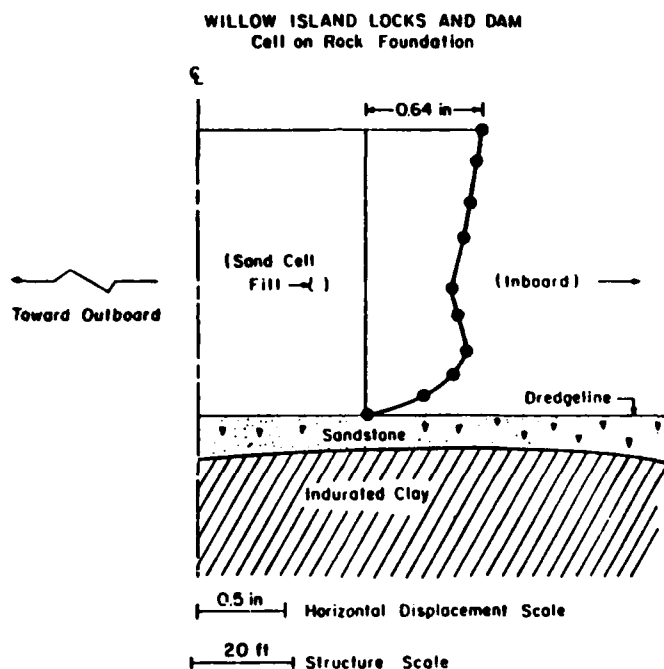


Figure 32. Inboard wall movement of Cell 24 during dewatering

114. Based on inclinometer data from five cells, movements in the underlying sandstone caprock were very small and occurred only in areas where the caprock was thin. No movements were observed in the clay immediately underlying the sandstone, although loss of stability due to sliding on the clay was considered a potential failure mechanism of the cofferdam.

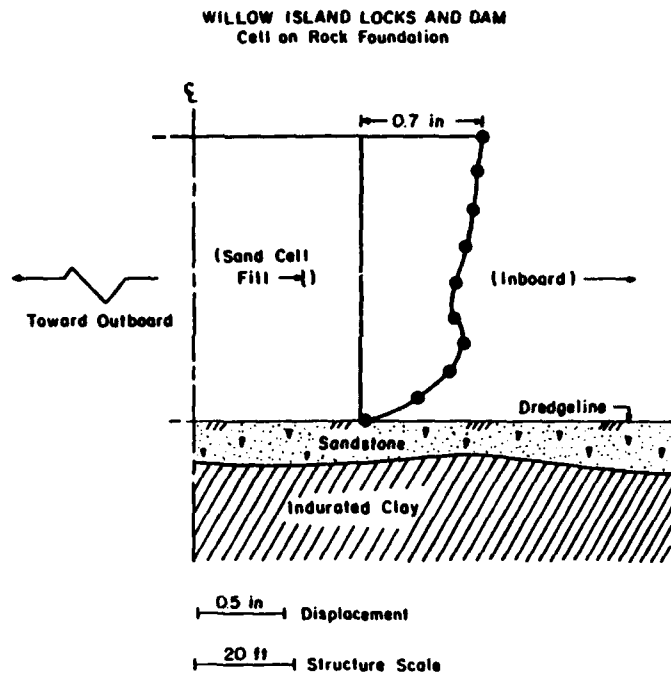


Figure 33. Inboard wall movement of Cell 27 during dewatering

Response to flood

115. Subsequent to initial dewatering, the Willow Island Stage 2 Cofferdam was voluntarily flooded on two separate occasions due to high water in the Ohio River. The cofferdam was dewatered after each flood and restored to normal use. As indicated by plots of differential head versus cell deflections given in Figures 34 and 35, the dewatering responses following each flood event were greatly different from the initial dewatering responses. The curves shown in the figures indicate that the differential head of 35 ft created by the initial dewatering induced the largest incremental movements. As the differential head exceeded 35 ft during high water, the cofferdam was quickly flooded, and the differential head dropped to zero. In response, the cofferdam cells moved in an outboard mode. As the flood water on the exterior of the cofferdam receded, the interior was again dewatered to a differential head of 35 ft. The second dewatering induced very small additional movements toward the inboard side. It can be seen that the slopes of the reload portions of the differential head-deflection curves (corresponding to the second dewatering) are much flatter than the slopes of initial parts of the curves. As shown, similar behavior was observed in subsequent cycles of

WILLOW ISLAND LOCKS AND DAM
Cell on Rock Foundation
(STAGE 2)

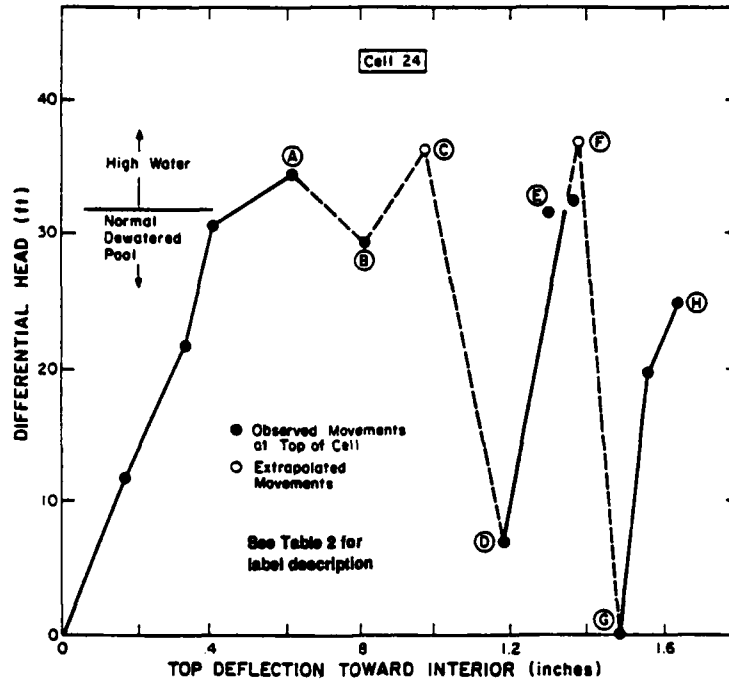


Figure 34. Loading response of Cell 24 (inboard inclinometer)

WILLOW ISLAND LOCKS AND DAM
Cell on Rock Foundation
(STAGE 2)

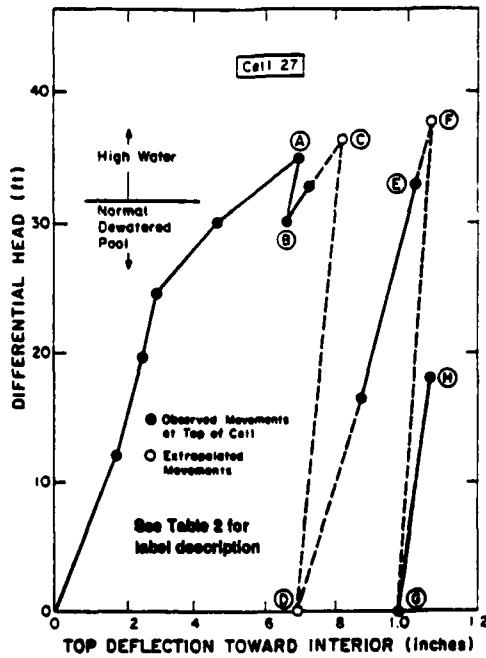


Figure 35. Loading response of Cell 27 (inboard inclinometer)

flooding and dewatering. Such behavior suggests a hysteretic type of loading response.

116. In response to the loadings induced by high water, the shapes of the cells became more pronounced. As illustrated by inclinometer data, the overall deflected shapes of the cells were consistent with those observed during initial dewatering. The location of the maximum cell deflection remained at the top of the cell as the inboard wall leaned further toward the interior. The bulging near the dredge line also increased considerably.

Response of cells on clay

117. As shown earlier in Figure 28, a portion of the cofferdam was founded on indurated clay. For completeness, behavioral differences between cells founded on the indurated clay and cells which rested on the sandstone are noted. Because of a limited amount of performance data, an overall qualitative comparison of cell responses for both types of foundations is not presented.

118. Cells 32 and 33, two cloverleaf cells, are selected for comparison. Cell 32 had a free height of 57 ft, a diameter of 75 ft, and rested partly on sandstone and partly on a concrete spillway. In this case, the sandstone and the concrete are assumed to behave more or less the same. Cell 33 stood 61 ft high, measured 75 ft in diameter, and rested on indurated clay. Cell 33 had between 0.5 and 1.5 ft of embedment into the underlying indurated clay; Cell 32 has no embedment. The figure shows the respective locations of both cells within the cofferdam.

119. As indicated by inclinometer measurements, Cell 33 experienced greater movements during initial dewatering than did Cell 32. Approximately 1.25 in. of displacement took place at the top of Cell 33, while Cell 32 deflected approximately 0.45 in. A significant amount of creep was observed in both cells subsequent to initial dewatering. Cell 32 reached a maximum inboard deflection of 2.04 in. at the top of the cell and 0.15 in. at the dredge line. Inboard deflections at Cell 33 reached a maximum value of 5.76 in. at the top of the cell and 0.68 in. at the dredge line. Berm placement against the inboard walls of the cells immediately decreased the rate of the movements and completely stopped all movements after a short while. For the most part, the magnitude of movements observed at both cells was not greatly different.

120. Each cell exhibited virtually the same type of response to high water. Plots of deflection versus differential head for Cells 32 and 33

delineate a hysteretic loading pattern much like that exhibited by other cells in the cofferdam. At both cells, the net incremental cell displacements decreased with each successive load of the same magnitude.

121. There was a marked difference observed in the deflected shapes of Cells 32 and 33 throughout the 12-month observation period. Figures 36 and 37 show the inboard profiles of the cells after initial dewatering. As shown, Cell 32 experienced a uniform, rigid-body translation across the sandstone/concrete foundation. The tips of the sheet piles were dragged across the foundation as the cell moved toward the interior. The location of the maximum cell deflection was at the bulge which occurred just above the dredge line. Both the top deflection and the bulging near the dredge line increased considerably during dewatering. Minimal cell rotation was observed. The response of Cell 32 was consistent with that of Cells 24 and 27 as discussed previously.

122. Cell 33, on the other hand, experienced a considerable amount of cell rotation in response to the dewatering. Figure 37 shows that the inboard wall leaned considerably into the interior of the cofferdam. The maximum deflection occurred at the top of the cell, while the smallest deflections were observed at the dredge line. Very little bulging was observed in the lower portions of the cell as there was almost a straight-lined variation of displacement from the top of the cell down to the dredge line. The embedded portion of the inboard wall was inclined toward the interior. The top deflection of the cell was close to 1.5 in., while modest deflections of less than 0.06 in. were observed in the sheet piles below the dredge line. A small amount of differential settlement was taking place within the cell before and after the initial dewatering period. The differential settlement of the cell continued for several months but at a decreasing rate.

WILLOW ISLAND LOCKS AND DAM
Cell on Rock Foundation
(STAGE 2)

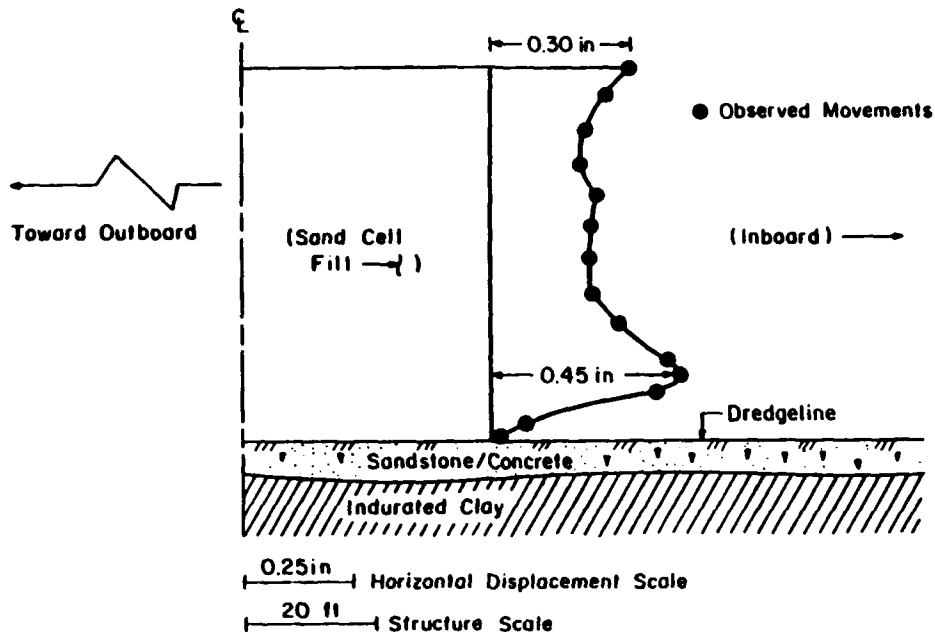


Figure 36. Inboard wall movements of Cell 32 (cloverleaf) during dewatering

WILLOW ISLAND LOCKS AND DAM
Cell on Clay Foundation
(STAGE 2)

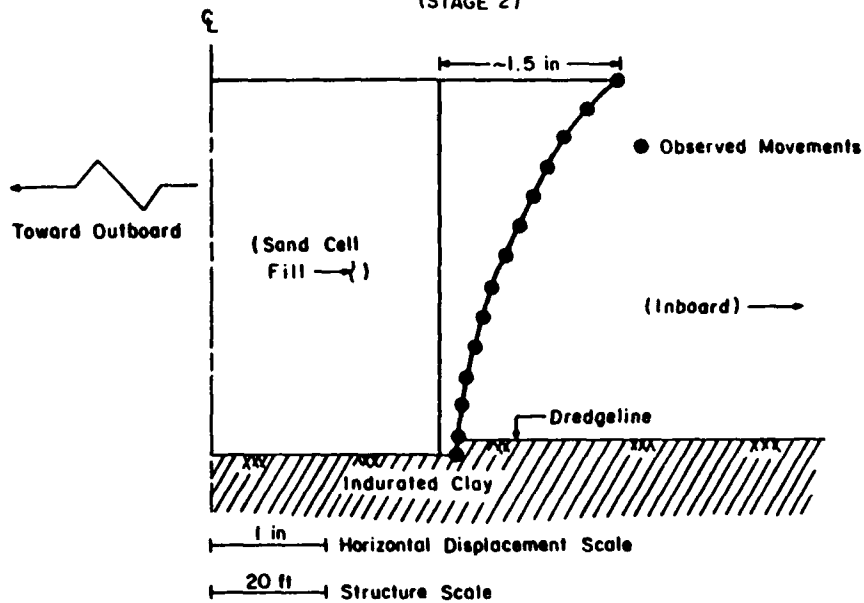


Figure 37. Inboard wall movements of Cell 33 (cloverleaf) during dewatering

PART V: COFFERDAMS WITH UNUSUAL CONDITIONS

123. This part is concerned with cofferdams that have unusual loading conditions, nonuniform cell fill material, or complex foundations. Case studies of the Seagirt Marine Terminal in Baltimore, Maryland, and Williamson CBD Prototype Cells in Williamson, West Virginia are presented. For each case, a general description, details of site conditions and cell construction, and observed performance data are presented. The objective of this part is to offer a general description of each case involved and to present performance data. Part VI (Comparisons of Cofferdam Behavior and General Trends) compares the behavior of the cofferdams discussed in this part with that of typical cofferdams.

Seagirt Marine Terminal Cofferdam

Background

124. The Seagirt Marine Terminal is a proposed new facility for the port of Baltimore, Maryland, designed to provide wharf space for loading and unloading ships and storing goods in transit. The proposed terminal is to be located a few miles southeast of Baltimore. Development plans involve the incorporation of part of an existing cellular cofferdam to serve as the major load bearing element for the terminal structure. A paved storage area is to be located on the inboard side of the cofferdam.

125. The existing cofferdam serves as a retaining structure to hold back dredge slurry material. During cell construction and subsequent slurry placement, as much as 8 ft of movement was observed at some cells. Movements of this magnitude gave rise to uncertainties concerning the suitability of the cofferdam and its ability to perform satisfactorily. This led to studies by Clough and Duncan (1986) who predicted cofferdam responses induced by the proposed new loading conditions using the finite element technique. At the same time, a loading test was conducted in one area of the cofferdam to better estimate cell responses during the proposed new construction.

126. This chapter focuses on three areas of the cofferdam that are typical of the main reaches of the system. Three cells are used to illustrate the behavior--Cells 49, 58 and 66. The loading responses of each cell during initial construction and slurry placement are presented. Results from test loadings at Cell 66 are also given.

Geometries and dimensions

127. The cofferdam is an L-shaped structure, the most of which runs along parallel to the shoreline. The overall length of the structure is approximately 5,000 ft long. The main cells are 62 ft in diameter and spaced 75 ft on centers. Cell height varies from cell to cell, but is generally greater on the inboard (loaded) side of the cofferdam. Figures 38, 39, and 40 show schematics of Cells 49, 58 and 66 after initial construction. The outboard walls of all three cells were approximately 36 ft in height above the dredge line. Cell heights on the inboard side of the cofferdam were 51 ft for Cells 49 and 58, and 41 ft for Cell 66. The tops of all the cells were at elevation +10 ft (MLLW). As shown, embedments on the inboard ranged from 12 ft at Cell 49 to more than 30 ft at Cell 66. Outboard embedments were close to 35 ft for all three cells.

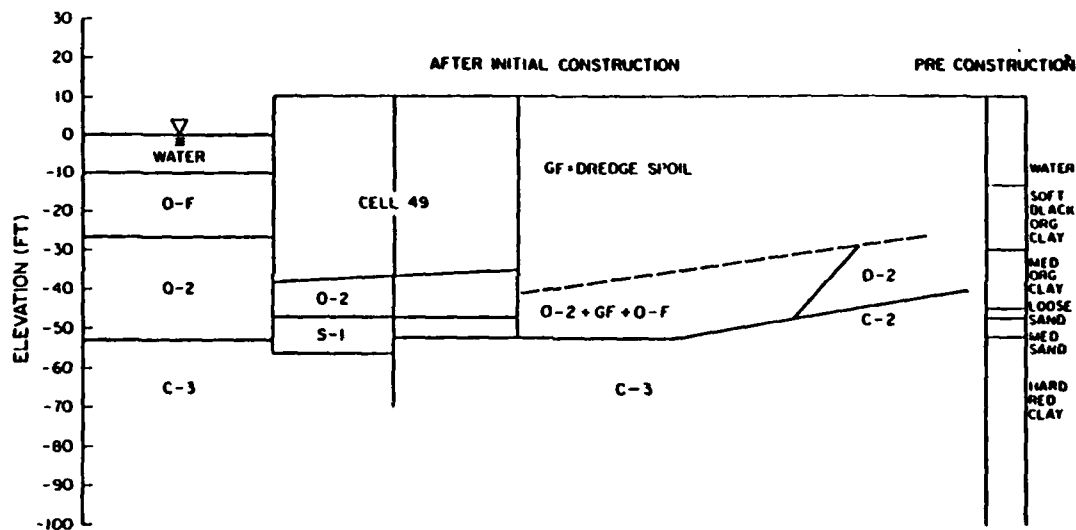


Figure 38. Soil profile after initial construction, Cell 49

Foundation, berm, and backfill materials and properties

128. Figures 38, 39, and 40 show the soil conditions at each cell. The foundation soils vary in type and thickness from place to place in the cofferdam.

129. Cell 49 is founded on a layer of hard, fissured clay with slickensides (called C-3 in Figure 38). Measured, undrained shear strengths of the clay varied from 1,250 to 2,500 psf. Blow counts taken in the material were consistently over 70 blows per foot. The clay had an average natural water content of 22 percent.

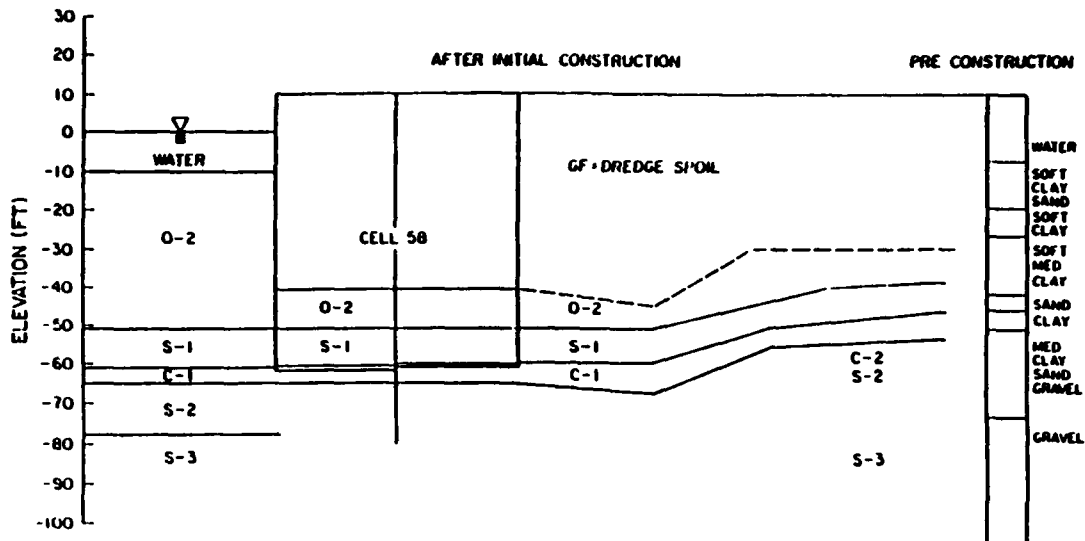


Figure 39. Profile after initial construction, Cell 58

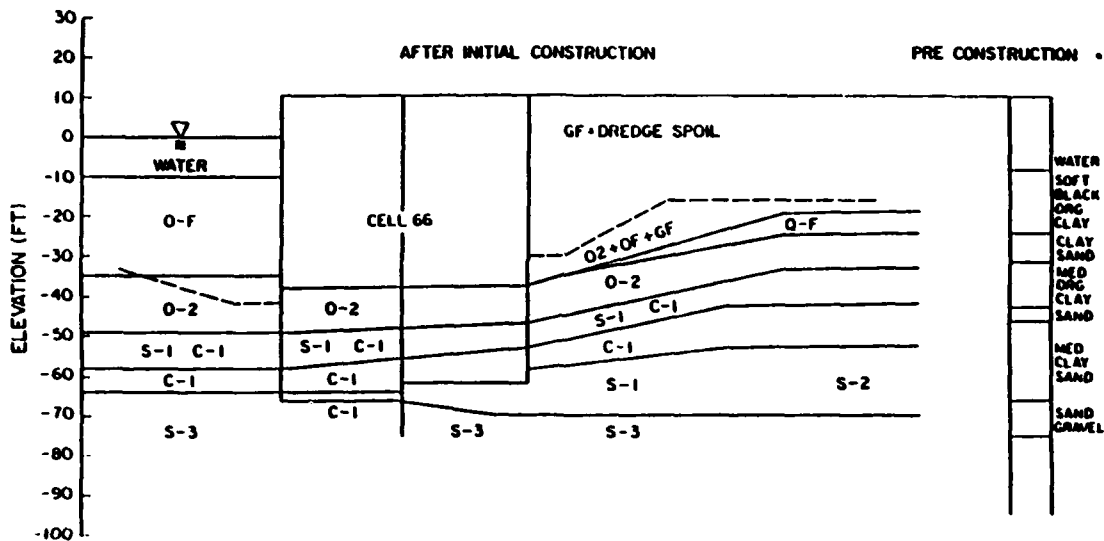


Figure 40. Profile after initial construction, Cell 66

130. Cell 58 is immediately underlain by a dense to very dense sand layer (called S-3 in Figure 39). Blow counts in the sand were greater than 100 blows per foot, and it had an estimated friction angle of 40 deg. The sand layer is underlain by a thin layer of stiff clay (C-1) with cohesive strengths ranging from 1,200 to 2,000 psf. Blow counts in the clay ranged from 20 to 60 blows per foot.

131. As shown in Figure 40, Cell 66 is founded on alternating layers of stiff clay (C-1) and medium sand (S-3). The sand and clay are the same as those found at Cell 58.

132. The slurry material placed behind the cofferdam consisted mainly

of sand and silt. The material has an estimated drained friction angle of 30 deg and a submerged unit weight of 50 pcf. Upon placement, the material is thought to have behaved more as a dense slurry with an estimated equivalent fluid pressure of ~70 pcf.

133. Stability berms were placed on the outboard side of the cofferdam shortly after slurry placement. The berms were typically 15 ft to 20 ft thick and primarily composed of sand and silt, but contained a small amount of gravel. A friction angle of 32 deg has been estimated for the berm material.

Cell fill

134. The lower portions inside the cofferdam cells were composed of in situ soils inasmuch as the inside of the cells was not excavated of these soils prior to cell filling. Importantly, the top layer of the in situ soils consists of a weak, organic clay (0-2).

135. The upper portion of the cell fills consists primarily of sand. Sand fill was placed directly on top of the 0-2 clay layer. As shown in the figures above, the sand makes up approximately three-fourths of the cell fill in Cells 49, 58 and 66. Standard Penetration Tests in the sand fill, which contained some gravel, yielded blow counts ranging from 13 to 25 blows per foot. It was estimated that the fill had a friction angle of 35 deg and a buoyant unit weight of 62 pcf.

136. Underlying the sand fill in all three cells is a 10- to 15-ft thick layer of weak, organic silty clay. The material has a cohesive strength which ranges from 100 to 1,200 psf. Blow counts in the clay layer varied from 0 to 2 blows per foot, and plastic limits ranged from 30 to 45 percent with liquid limits from 65 to 115 percent. Natural water contents of the clay varied from 45 to 85 percent and were consistently half-way between the liquid and plastic limits. The soils underlying the organic clay layer are considered foundation soils.

Instrumentation

137. Explicit information concerning the early instrumentation at the cofferdam was not available. However, it is reported that monitoring of both vertical and horizontal movements of the cells was performed and began after some movements had already taken place (Clough and Duncan 1986). Slope indicators were used to record movements of Cell 66 during test loadings conducted at the cell.

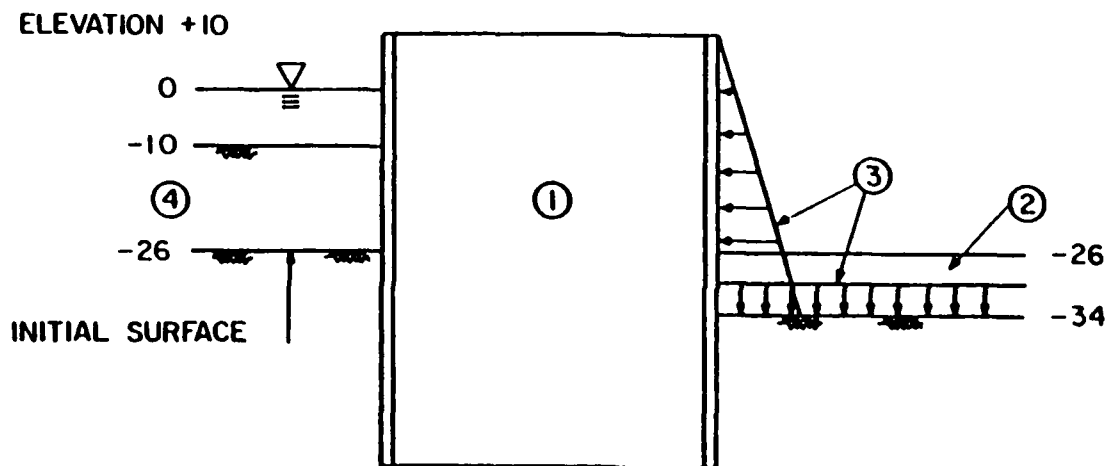
Sheet piles

138. Each main cell is composed of 152 web-shaped sheet piles and 4 wye

sections. The arc cells consists of 46 sheet piles, excluding the common walls. The wye connectors were 30-deg riveted sections made of PS-32 sheet piles. All other piles were PS-28 sheet piles.

Construction sequence

139. Construction began with sheet pile installation and cell filling. Subsequently, a large excavation was made on the inboard side of the cofferdam in preparation for the slurry backfill. The excavation extended down to approximately el -34 ft. (MLLW). Almost 50 ft of slurry backfill material was then placed in the excavated area which extended from the top of the cofferdam at el +10 down to the dredge line at elevation -34 ft. Excessive movements observed at some cells after slurry placement prompted the installation of soil berms on the outboard side of the cofferdam. Figure 41 illustrates the sequence of events discussed herein.



- ① INSTALL AND FILL CELL
- ② EXCAVATE 0-2 LAYER TO ELEV -34 INBOARD
- ③ FILL INBOARD (LINEARLY VARYING HORIZONTAL PRESSURE AND VERTICAL PRESSURE)
- ④ FILL OUTBOARD TO ELEV -10

Figure 41. Construction of cells

Response to initial construction--Cells 49, 58 and 66

140. The initial construction operation consisted of sheet pile installation, cell filling, excavation and slurry placement on the inboard and berm placement on the outboard. Each of these operations induced some amount of cell movement. Observation of cofferdam movements began sometime between cell filling and slurry placement; movements were monitored for 5 years thereafter. At the time the observations were begun, some movements had

already taken place. Thus, the actual movements that preceded slurry placement are not well known.

141. Placement of the slurry backfill was the primary load-inducing component of the operation. Observations of cell movements during the initial construction period indicate that the largest increments and fastest rates of movement took place during slurry placement.

142. The slurry backfill material was placed hydraulically below water against the inboard wall of the cofferdam. At the end of placement, the slurry backfill was even with the top of the cofferdam as it extended from the top of the cells down to the dredge line. In other words, as shown in Figures 38, 39, and 40, the loaded portion of the inboard wall of the cofferdam included the entire free height, which varied from 41 ft at Cell 66 to 51 ft at Cells 49 and 58.

143. As stated earlier, the slurry had an assumed equivalent fluid pressure of 70 pcf upon placement (Clough and Duncan 1986). To minimize lateral pressures on the cofferdam, the finer portions of the slurry backfill were placed further away from the inboard wall. As time passed, the slurry began to consolidate and behave as a fully frictional material. Lateral pressures on the cofferdam were thereby reduced to the frictional component of the slurry. Horizontal displacements of the cofferdam in the loaded direction probably reduced the lateral pressures to the active state. Thus, subsequent to slurry placement, the lateral load on the cofferdam decreased with time from its original magnitude to some lesser amount. To get a better feel for the magnitude of forces involved, the induced slurry loadings are calculated using conventional earth pressure theory and then converted into equivalent water heads. For instance, a 50-ft head of slurry with an equivalent fluid pressure of 70 pcf would produce a lateral force of close to 87.5 kips. This corresponds to an equivalent water head of approximately 53 ft. Such a conversion facilitates comparisons with other cofferdams and provides a framework whereby the reader is better able to judge the cofferdam's performance.

144. Figure 42 shows the deflection of Cell 66 plotted against time, for the initial construction period. During backfilling, which began in July of 1981, approximately 41 ft of slurry was placed against the cell. Assuming an equivalent fluid pressure of 70 pcf, and induced lateral load of approximately 59 kips/ft is calculated. This corresponds to an equivalent water head of about 43 ft. The cell responded by rotating toward the outboard

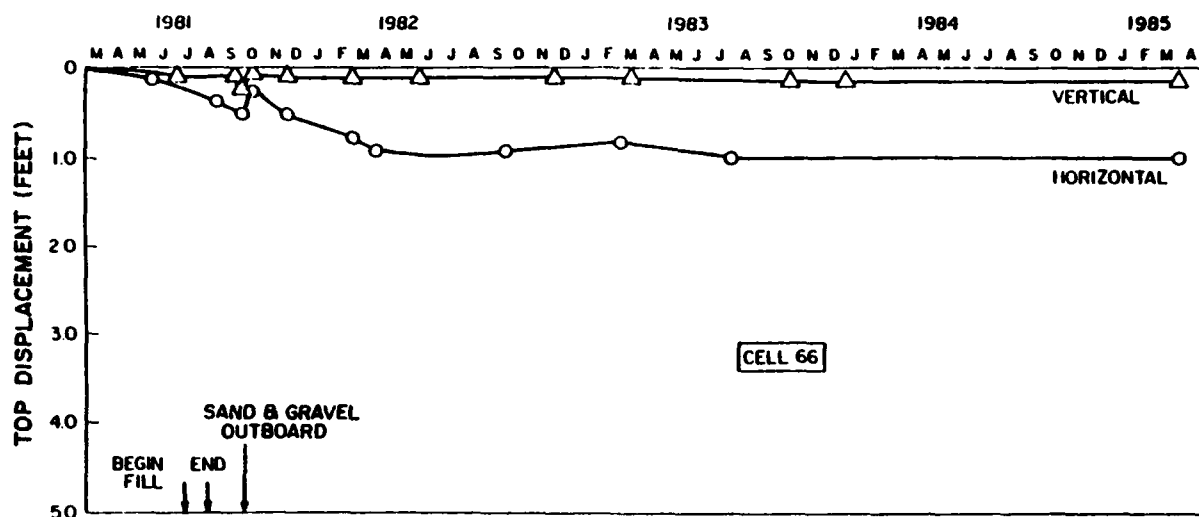


Figure 42. Measured displacements of Cell 66 toward outboard (inclinometer)

with approximately 0.20 ft of horizontal movement. In late September 1981, a 24-ft stability berm consisting of mostly sand with some gravel was placed on the outboard of the cofferdam. The soil type of the berm material was similar to that of the slurry backfill material. Placement of the berm slowed the rate of vertical movement and initially reversed the horizontal movement of the cell for a short time. However, horizontal displacements toward the outboard resumed and continued to occur at a slow rate. The reversed movements are not completely understood, but support the idea that the magnitude of the lateral forces induced by the berm decreased with time. One way in which this behavior can be explained relates back to the idea of consolidation of the sand and gravel materials. Since the berm material was placed in the same manner as the slurry backfill, it is estimated that it too had an equivalent fluid pressure of 70 pcf upon placement. At this time, the horizontal forces induced by the 24-ft soil berm on the outboard were comparable with those induced by the slurry backfill which now behaved as a fully frictional material in an active state. In response to the reduction of net load on the inboard, the cofferdam began to move toward the inboard side. As time passed and deflections toward the inboard continued, the berm material consolidated to a fully frictional material and was reduced to the active state. The forces induced by the slurry material apparently once again began to dominate. In response, the cofferdam reversed its inboard movement and began to deflect toward the outboard. As illustrated in the figure, the

movements toward the outboard continued at a steady rate until March 1982. Approximately 1 month later, all cell movements ceased. At this time, over 1.0 ft of cumulative horizontal displacement had taken place. It can be seen that a considerable portion of the cumulative movements at Cell 66 resulted from creep movements that occurred subsequent to slurry backfilling. These creep movements are primarily attributed to the weakness and compressibility of the soft clay (0-2) which was left in the cell. To make clearer the behavior described above, a plot of differential head versus deflection and time is provided in Figure 43. The differential head-deflection curve shown

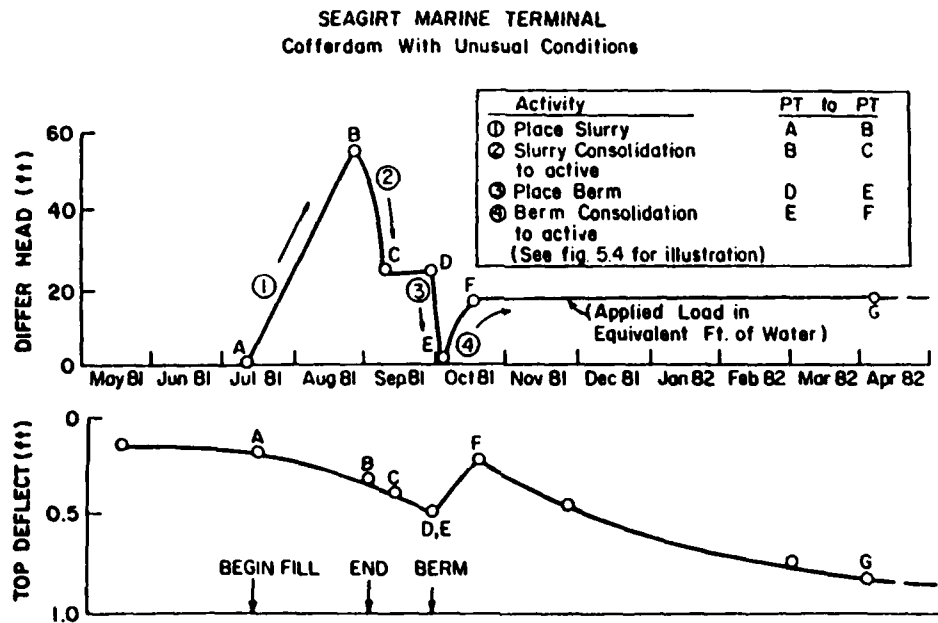


Figure 43. Movement of Cell 66 during initial construction (inclinometer)

in the figure represents the response of Cell 66 during slurry backfill placement, backfill consolidation, berm placement on the outboard, and berm consolidation. Prominent points on the curve are labelled. The figure is provided with a table which fully describes the activity from one point on the curve to the next.

145. Similar behavior was observed in Cells 49 and 58 throughout the early life of the cofferdam, as illustrated in Figures 44 and 45. The figures show the deflection of each cell plotted against time. The deflections given in the figures are based on inclinometer movements recorded at the cells. It can be seen that the deflections of Cells 49 and 58 are considerably larger than those which occurred at Cell 66. During slurry placement, Cells 58 and 49 were both loaded with an equivalent water head of 53 ft. Cell 49

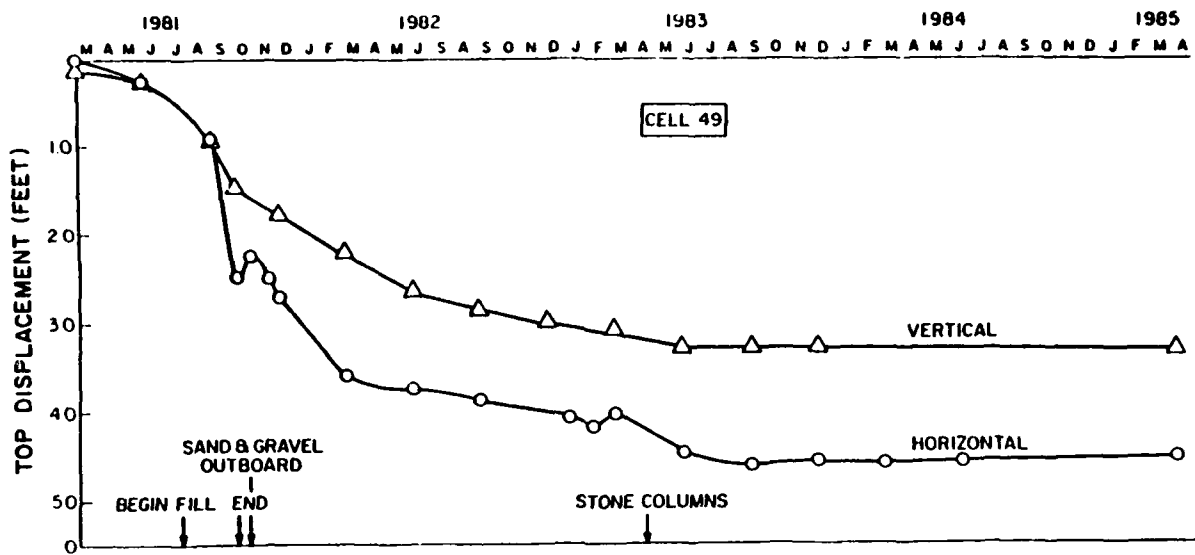


Figure 44. Measured displacements of Cell 49 toward outboard (inclinometer)

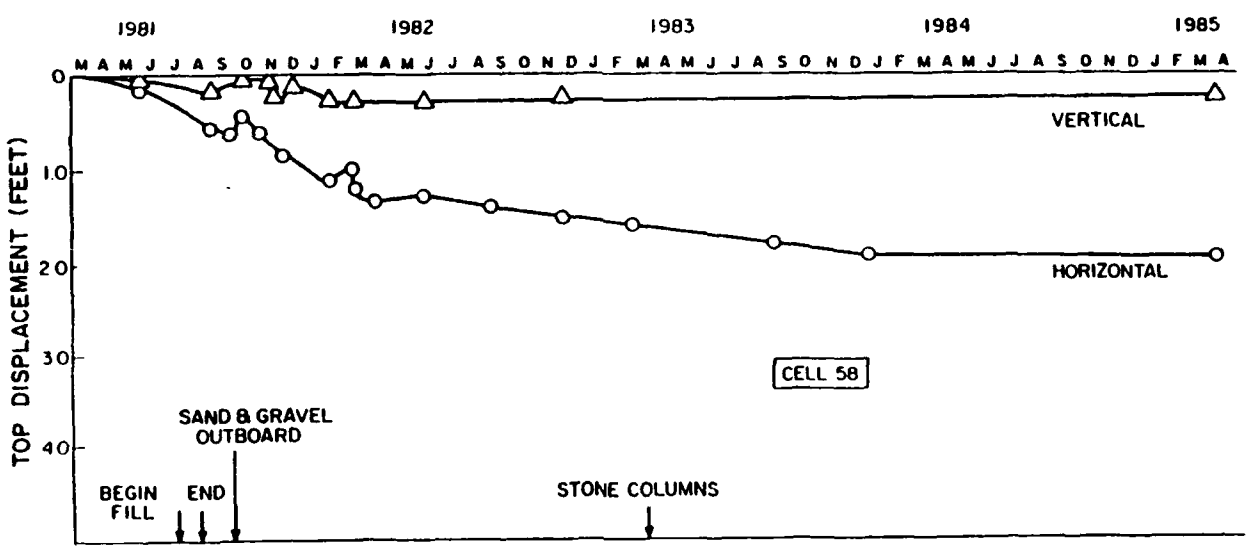


Figure 45. Measured displacements of Cell 58 toward outboard (inclinometer)

experienced horizontal movements of close to 2.0 ft during slurry placement, while Cell 58 underwent approximately 0.22 ft of horizontal displacement. Cell 49 experienced a vertical deflection of approximately 0.9 ft; less than 0.3 ft of vertical movement was observed at Cell 58. Creep movements increased the cumulative horizontal displacements of Cells 49 and Cell 58 to approximately 4.5 and 1.3 ft, respectively, by the end of the observation period in 1985.

146. The construction techniques used and the loading induced on the cofferdam throughout initial construction were similar at all sections of the cofferdam. The differences in the magnitude of the movements resulted primarily from the differences in the soil conditions at each cell. Field observations and finite element analyses (Clough and Duncan 1986) indicate that most of the cell movements were associated with the strength and compressibility of two clay layers (C-3 and O-2). The soft clay (O-2), which was left inside the cells in all three cases, contributed to cell movements primarily through shear deformations. Excessive shear deformations in the layer prompted large horizontal displacements and cell distortions, especially in the lower portions of the cells. Where large vertical cell displacements occurred in the cofferdam, this is mainly attributed to the C-3 layer. Field observations of Cell 49 indicate that C-3 material did not provide adequate skin friction to support the sheet piles, and thus allowed a plunging failure of the pile tips. Cell 49 rotated toward the outboard, simultaneously undergoing large vertical and horizontal displacements. Cells 58 and 66, which were founded in dense sand and stiff clay, experienced mostly horizontal translations and very little vertical movements. Inclinator profiles of the cells during the initial construction period were not available.

Response to test loading--Cell 66

147. In June 1985, a load test was conducted at Cell 66 to model proposed new construction. The test consisted of two stages and was designed to induce loadings on the cell comparable to those expected during the new construction. The first stage of the test consisted of a dredging operation which lowered the outboard dredge line to el -42 ft. The dredging basically removed the O-2 and O-F layers (see Figure 40) on the outboard of the cell. During the second stage, a 1,000-psf surcharge fill was placed atop the slurry backfill on the inboard of the cofferdam. The additional loadings produced considerable cell displacements which were closely monitored by inclinometers. The induced deflections were modest as compared with those caused by initial construction. A plot of cell deflection versus applied load and the sequence of events for the test is given in Figure 46.

148. In essence, the excavation of the O-2 and O-F material removed a restraining force on the outboard of the cell. Effectively, this is synonymous to an increase in differential load of the same magnitude. It should be remembered that at the time the dredging was begun. Cell 66 had already deflected more than 1.0 ft toward the outboard. The lateral pressures induced

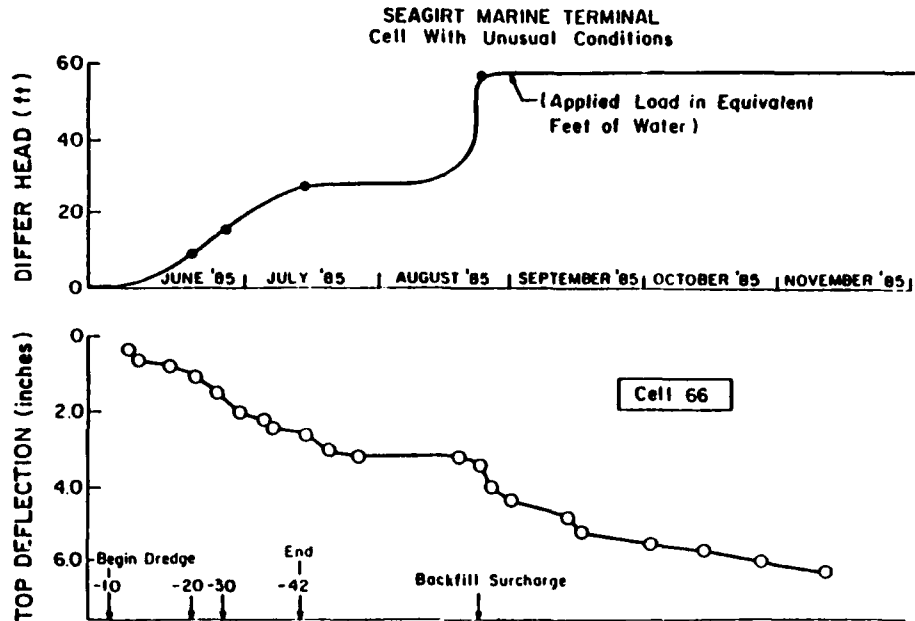


Figure 46. Movement at top of Cell 66 during test loading (inclinometer)

by the 0-2 and 0-F soil layers were presumably somewhere between the at-rest and passive state. Based on engineering judgment and limited soil data, a lateral earth pressure coefficient of 1.0 was chosen to estimate the outboard soil pressures. Thus, it was estimated that the soil removal took away approximately 14 kips of restraint from the outboard. This corresponds to an increase of differential load equal to approximately 21 ft of water. In response to the load increase, Cell 66 translated approximately 3.0 in. toward the outboard, as indicated by inclinometer measurements.

149. The second phase of the operation, application of the fill surcharge, increased the lateral load on the cell by an amount corresponding to approximately 30 ft of equivalent water head. At this point, the net lateral load induced by the test was equal to over 50 ft of water. The load induced by the fill surcharge resulted in a movement of 2 in. toward the outboard, as measured at the top of the cell.

150. Inclinometer profiles recorded during the loading test indicate that the most of the movement was associated with shear distortions of the 0-2 materials inside the cell. As Figure 47 shows, the upper portion of the cell, which was filled with sand, experienced an almost rigid-body translation in response to the added loads. The lower portion of the cell, filled with the weak 0-2 material, underwent distortions giving rise to large horizontal displacements of the cell.

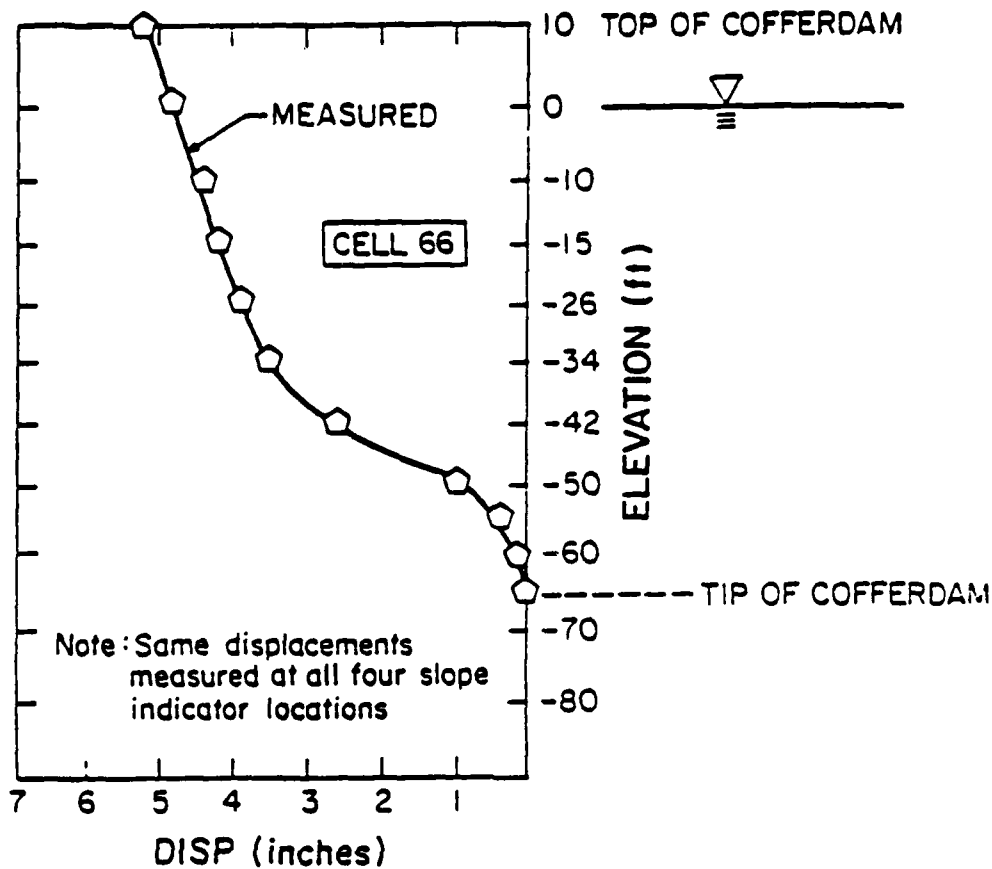


Figure 47. Inclinometer movement of Cell 66 during test loading

Williamson CBD Prototype Cells

Background

151. The Williamson (CBD) Sheet-pile Cell Floodwall is a proposed new structure for the town of Williamson, West Virginia. The floodwall is to provide local flood protection along Tug Fork in Williamson. This case is interesting and unusual in that it is necessary to leave varying portions of natural riverbank clays within the cells as opposed to the conventional practice of backfilling with cohesionless materials. For this reason, it is particularly important to have a good feel for the amount of movement that will occur in the floodwall.

152. Two prototype cells were constructed, instrumented, and monitored to help determine the feasibility of the floodwall concept. In addition, a finite element analysis of the floodwall was performed (Peters, Leavell, and Holmes 1987). The analysis was primarily concerned with determining whether

continued cycles of flooding would induce increasing net cell movements toward the river. A discussion of the performance of the two prototype cells during filling and a synopsis of the finite element study are presented.

Geometries and dimensions

153. The proposed floodwall is a linear structure made up of circular sheet-pile cells that run along Tug Fork. The two prototype cells are approximately 53 ft in diameter and have a center-to-center spacing of about 71 ft. The cells are joined by wye connectors to a common arc cell.

154. The cells were installed into the side of the riverbank. Due to the natural slope of the riverbank, the landward side of the cells have less free height than the river face of the cells. The sheets on the landward side of the cells were driven flush to the existing ground surface. The riverside sheets are longer and extend 15 ft above the top of the landside sheet piles. The tops of the sheet piles vary linearly from el 675 ft on the river side to el 661 ft on the land side. The average free height of the riverside sheets is about 35 ft. The landward side of the cells has no unsupported height and an embedment of just over 50 ft. The depth of embedment on the river side varies between 30 and 35 ft. Figure 48 shows a typical section of the two prototype cells. The plan of the cells, as shown in Figure 49, illustrates the geometries of the two-cell system.

Foundation and cell fill--materials and properties

155. The soil profile at the site consists of a 10-ft partially saturated clay layer underlain by a 45- to 50-ft layer of medium clay. Both clay layers are underlain by a layer of sand and gravel of more than 20 ft in thickness. The sheet pile tips were driven down to this sand and gravel layer.

156. The major portions of the cell fill consisted of the natural riverbank clay material which was left in the cells. As shown in Figure 48, the upper portions of the cells were excavated of the clayey riverbank soils. The excavation removed more of the clay material on the river side of the cells than on the landward side. The excavated material was replaced by a sand and gravel fill that extended from el 640 ft up to el 661 ft. Above el 661 ft, the cell was filled with a more fine-grained cap material. Between these two materials is a 2-ft layer of drainage material and filter cloth. A friction angle of 36 deg has been estimated for the sand and gravel fill.

157. The underlying clay material left in the cells is a medium clay

WILLIAMSON CBD PROTOTYPE CELLS
Cell With Unusual Conditions

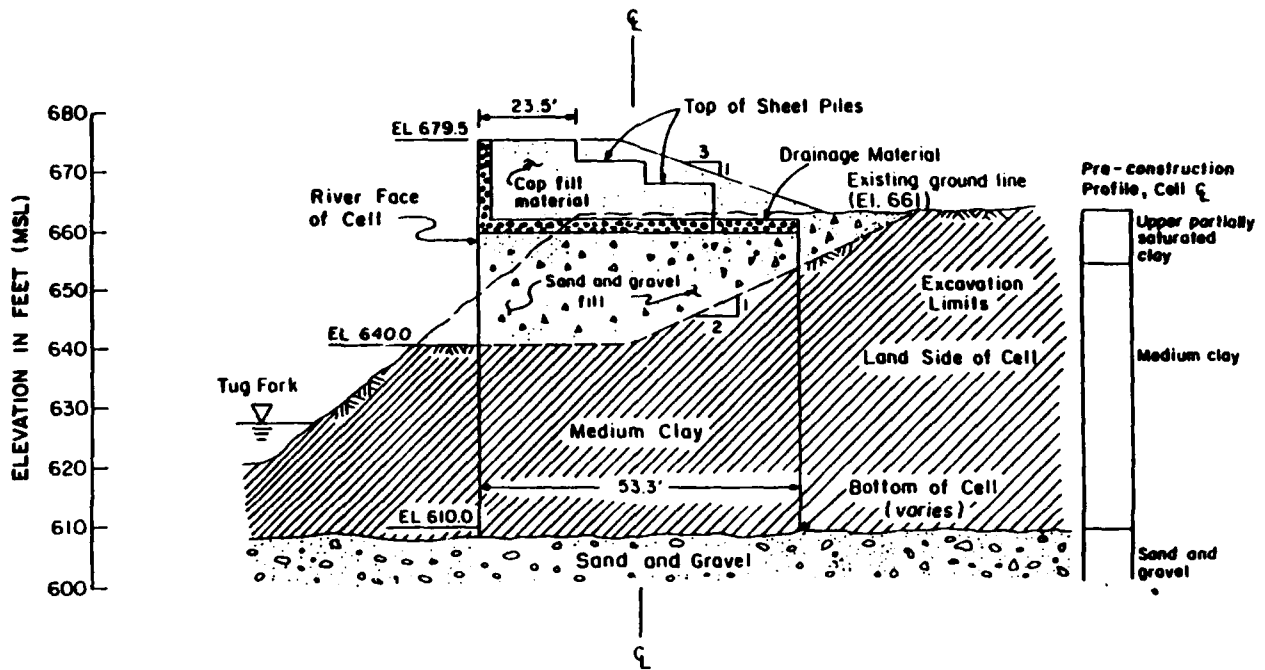


Figure 48. Typical cell section

WILLIAMSON CBD PROTOTYPE CELLS
Plan of Cells and Instrumentation Location

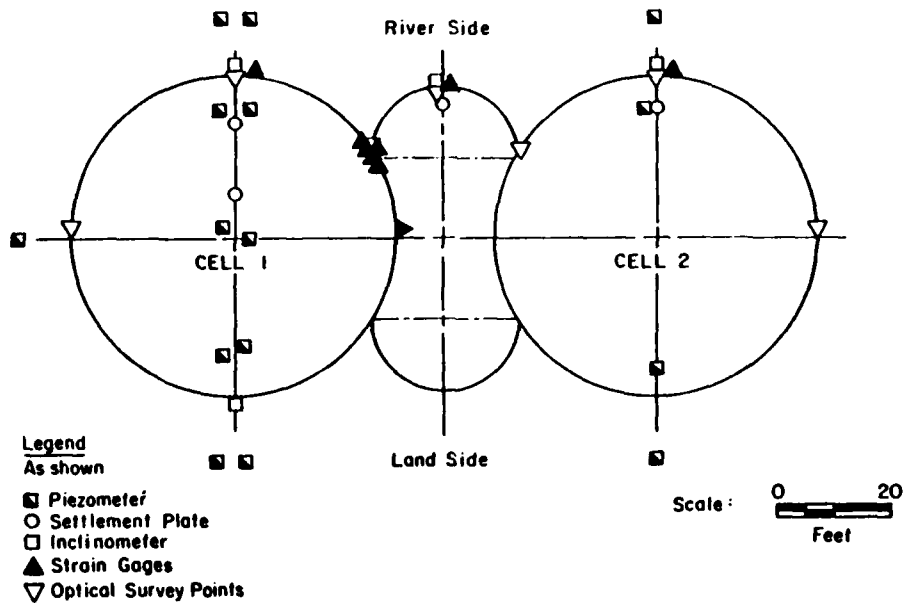


Figure 49. Geometries and instrumentation, Cells 1 and 2

varying from 30 ft to 40 ft in thickness inside the cells. The clay has an estimated undrained cohesive strength of about 0.6 tsf. Consolidation tests in the clay show the coefficient of consolidation to vary from 0.02 to 0.03 sq cm/sec. A more complete list of soil parameters for all of the materials is available in the Task 1 report from Peters and Leavell (1985).

Instrumentation

158. The two prototype cells were instrumented with strain gages, inclinometers, optical survey markers, and piezometers. Settlement plates were installed in the cell fills to monitor vertical movements of the underlying natural clay material left in the cells. Temperature sensors along with vibration and noise monitors were also included in the instrumentation program. The vibration and noise monitoring were primarily associated with the driving of the sheet piles. The location of the instrumentation is shown in Figure 49.

159. Instrumentation measurements were made at various stages throughout the construction of the cells and beyond. It was originally intended to begin instrumentation monitoring immediately after the sheet piles were driven, before any of the fill was placed. However, due to construction problems, the readings were begun after some of the fill had already been placed. Because of this, the initial value or zero point for the instrumentation is questionable. Since the completion of the filling operation, the instrumentation was read at approximately monthly intervals. Specific details of the instrumentation program and a summary of its performance is given in Dodson-Lindblom Associates, Inc. (1986).

Construction sequence

160. The construction of the cells began with the excavation of the clay material down to the desired elevation. Next, the sheet piles were driven to form the cells. The granular cell fill was then placed on top of the underlying clay soil in lifts of 8 ft, 9 ft, and 13 ft, successfully. The final elevation of the top of the fill surface was 674.5 ft.

Observed performance

161. The performance of the cofferdam as based on the instrumentation monitoring has been difficult to assess due to questionable initial readings. Secondly, construction activity, especially pile driving, made it difficult to delineate typical cell behavior. However, general conclusions could be drawn from the instrumentation data as outlined by Peters, Leavell, and Holmes (1987) and Dodson-Lindblom Associates, Inc. (1986).

162. It is important to keep in mind that for the most part, the cells at this site are not exposed to a significant differential load. The primary loading that will be induced on the system is the flooding of Tug Fork. At the time of this report, the cofferdam prototype cells had not been exposed to high water. Thus, no relationship between differential water load and observed cell deflection can be established. The cells did, however, experience horizontal movements during the filling operation. Inclinator measurements indicate that the riverside sheet piles moved as much as 0.4 ft toward the river in response to the placement of the granular fill. A small amount of horizontal movement occurred after filling. This is attributed to the adjustment of the cell fill due to the consolidation in the clay. Figure 50 illustrates the deflection of Cell 1 during filling.

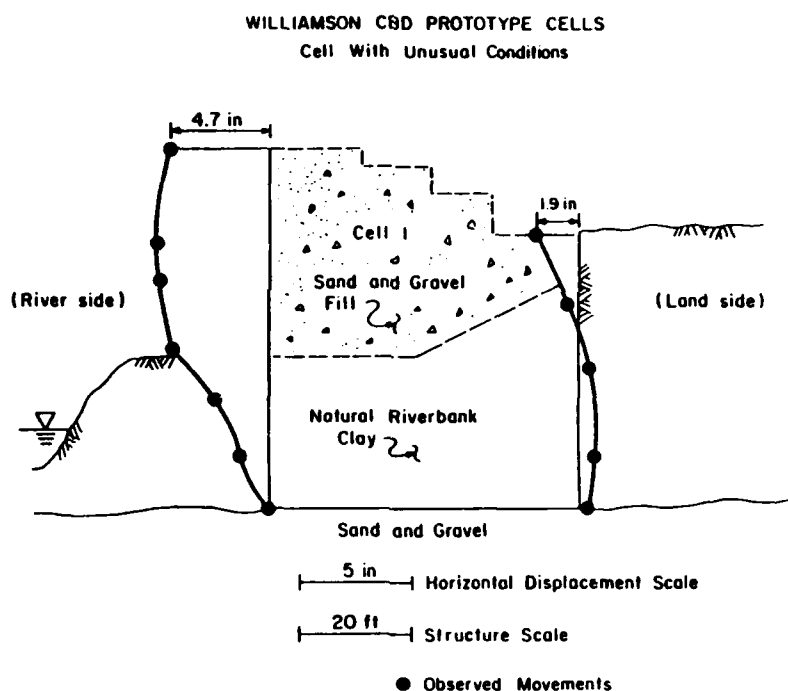


Figure 50. Movements of cell during filling

163. Measured settlements of the cell fill ranged from 0.16 ft in Cell 1 to 0.65 ft in Cell 2. A detailed comparison of construction activity and settlements suggests that pile driving caused settlements of up to 0.4 ft in Cell 2. The settlements caused by pile driving appear to have been immediate; whereas, the settlements caused by fill placement took several days to occur. Considering this effect, the net settlements due to the cohesionless fill placement are an estimated 0.11 ft at Cell 1 and 0.24 ft at Cell 2.

164. The finite element analysis performed by Peters, Leavell, and

Holmes (1987) showed good agreement between predicted results and observed field behavior during cell construction. Subsequently, the system was analyzed to predict the response of the cells to flooding. The analyses show the displacements caused by flooding to vary from about 2.5 to 4.0 in. This is roughly the same amount of movement that occurred during cell construction. This is expected in that the differential load applied to the cells during flood stage is comparable with that induced by the filling operation.

165. It was found that the rebound of the cells toward the river after the flood is larger than the initial movement of the cells toward the landward direction during flooding. Hence, a net displacement of the cells toward the river is expected to result from each cycle of flooding. This trend was investigated by performing the finite element analysis with four cycles of flooding and unloading. The study found that net cell displacements toward the river decrease with each successive increment of flood load. Also, the analyses show that the secondary loading responses in the landward direction are less than the primary response. This behavior has also been suggested by Kleber (1985).

PART VI: COMPARISONS OF COFFERDAM BEHAVIOR
AND GENERAL TRENDS

166. The purpose of this chapter is to contrast the behavior of the five case histories in an attempt to establish common trends and guides that can be used to judge cofferdam behavior for future cofferdams. Particular emphasis is placed on the issue of deformations of the cells since this aspect of cofferdam response is least understood of cofferdam design parameters. Key parameters and performance indicators are provided for the case histories in Table 3.

Deformations of the Top of the Cells--Initial Loading

167. Because of the pattern of cell deformation in all of the case histories included in this study, the top of the cells typically showed the largest lateral displacement of any location on the cells. In Table 3, the data for top of cell movements range from less than 1 in. to more than 5 in. The levels of movements sustained by the cells are significant, but given the large size of the cells, they are indicative of stable behavior.

168. In earlier parts, it was shown that a relationship existed between the top of cell deflection and the differential head applied to the cell. To allow for these relationships to be compared, it is useful to normalize the behavior. One simple means for normalizing the response is to divide the cell movement and the differential water head by the free cell height, as shown in Figure 51. In this way, all of the relationships are reduced to a common format which is independent of differences in cell height.

169. In Figure 52, the average normalized response plot is given for four of the case histories which are loaded by differential water heads. Those case histories where the differential loading is produced by slurry (Seagirt) and soil (Williamson) are not included in this plot in order to isolate case histories with only water loading. As was the case for cell deformations, the normalized plot shows a linear relationship in the early phases. In the later phases of loading, most of the response curves show more rapid increases of movements. This aspect of the behavior is attributed to an increase of moment arm about the cell base as the exterior water rises higher and higher on the cell. The larger moment arm is generated because the loading after initial dewatering is usually due to flooding, and the increment

COMPARISONS AND GENERAL TRENDS

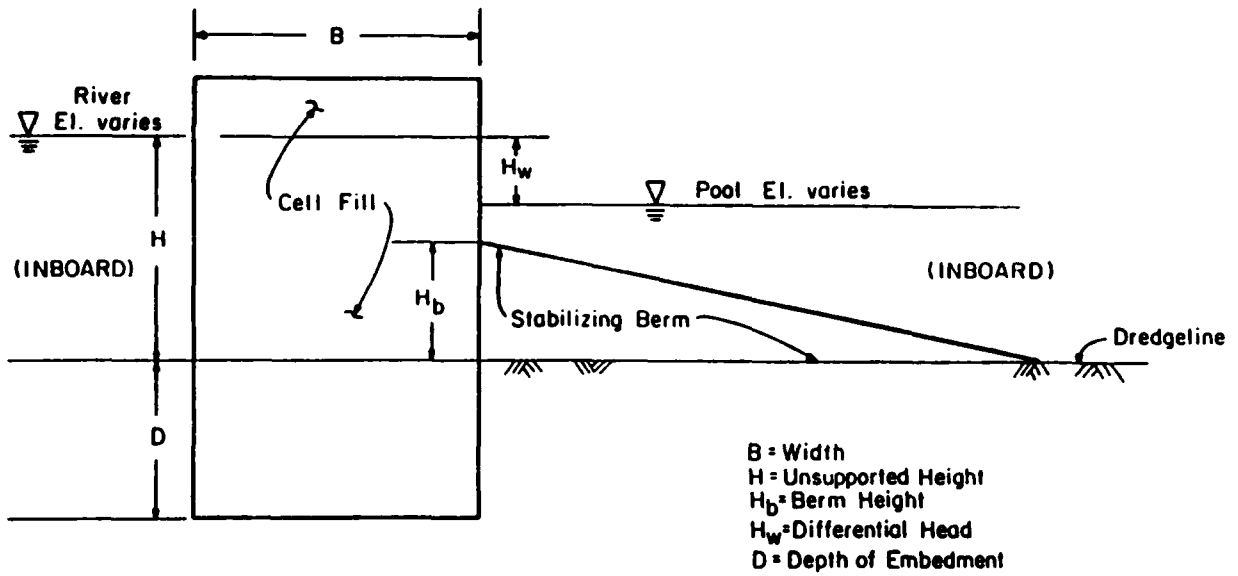


Figure 51. Convention used in comparisons

COMPARISONS AND GENERAL TRENDS

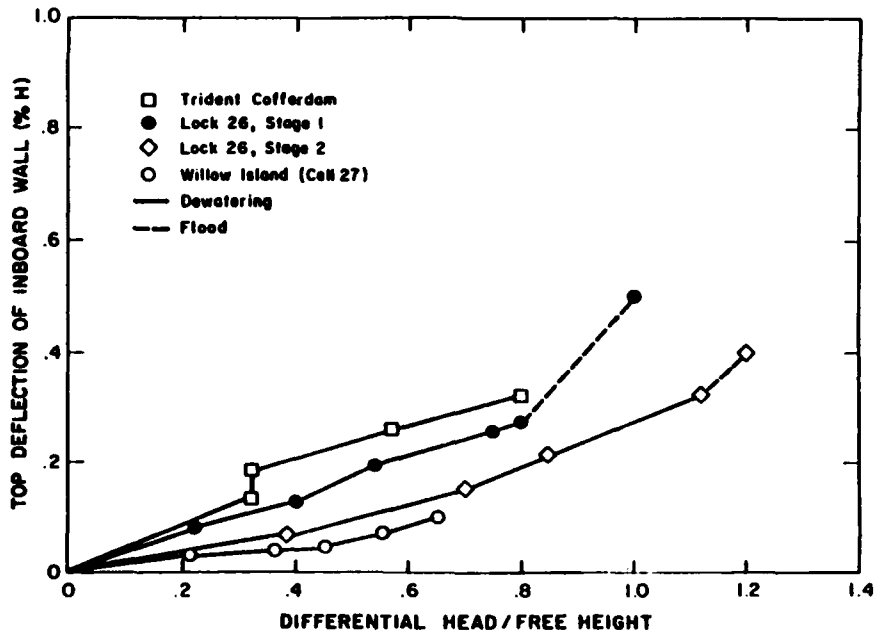


Figure 52. Composite plot of normalized response to differential loading

of loading in this case has a resultant that occurs higher on the cell than in the initial dewatering.

170. The plots of normalized movements versus normalized differential heads show that while the trends of the response curves from the different cofferdams are similar, the actual magnitudes of the normalized movements are somewhat different. For example, at the loading ratio of 0.7, the dimensionless lateral cell movements range from a low of 0.1 percent for the Willow Island case to a high of 0.28 percent for the Trident Cofferdam. In one sense, the differences in dimensionless lateral cell movements are not large, and this is important in using the information for estimating movements for future cofferdams. However, the differences that do exist can be related to factors which are important to cell behavior. The keys to the relative behavior appear to be:

- Presence or absence of stabilizing berms.
- Cell width to height ratio.
- Type of foundation material.
- Quality of cell fill.

171. For reference, Table 5 compares the cofferdams loaded by water heads in terms of the key parameters. Examining Table 5, it may be seen that the Willow Island Cofferdam exhibits positive factors in favor of reducing its deformation relative to the other cofferdams in three of the categories. Notably, it has the largest width to height ratio, a stabilizing berm, and a stiff rock foundation. On the other hand, the Trident Cofferdam has only one of the factors in favor of reducing its deformations relative to the others, in that its cell fill was compacted and hence was in a denser condition than for the others. Otherwise, the Trident Cofferdam did not have a stabilizing berm, its width to height ratio was small, and it was founded not on rock but on sand. The two cofferdams for Lock and Dam 26 (R) have conditions that fall in between those of the Trident and the Willow Island Cofferdams.

172. Of the Stage 1 and 2 Cofferdams for Lock and Dam 26 (R), Stage 1 had the more favorable conditions in that its width to height ratio was larger than that for Stage 2. However, as indicated by the response curves in Figure 52, the Stage 1 Cofferdam experienced more normalized deflection than did the Stage 2 Cofferdam. Intuitively, it would be expected that this trend would be reversed since the Stage 2 Cofferdam has a smaller aspect ratio. One explanation for the higher position of the Stage 1 curve relates back to the method of comparison used thus far in presenting the load-deflection behavior

of all the cases. The response curves shown in Figure 52 relate cofferdam movement to applied differential head. This type of comparison can be misleading in some cases when differential head alone is used as the loading parameter, because neither the position of the applied resultant force nor the location of the phreatic surface inside the cell is taken into consideration. Two identical cofferdams exposed to the same differential head are not necessarily exposed to the same overturning moment. For equal changes in differential head during dewatering, a change in outside water elevation will have an accentuated effect upon the overturning moments as compared with interior pool fluctuations. Also, as the position of the phreatic surface increases, more of the cell fill becomes submerged and the overturning resistance of the cell is decreased.

173. Considering this information, while on the one hand the differential head at Lock and Dam Stage 1 and 2 was about equal, on the other hand the resultant exterior water force was in a higher position at the Stage 1 cofferdam through the Stage 2 Cofferdam throughout dewatering. In Figure 53, the movements of Lock and Dam 26 (R) Stages 1 and 2 and those for the Trident Cofferdam are shown plotted against the overturning moment calculated for the water loadings on the cells. As is apparent, the movements follow a consistent pattern, increasing as the moments increase. Also, for the same

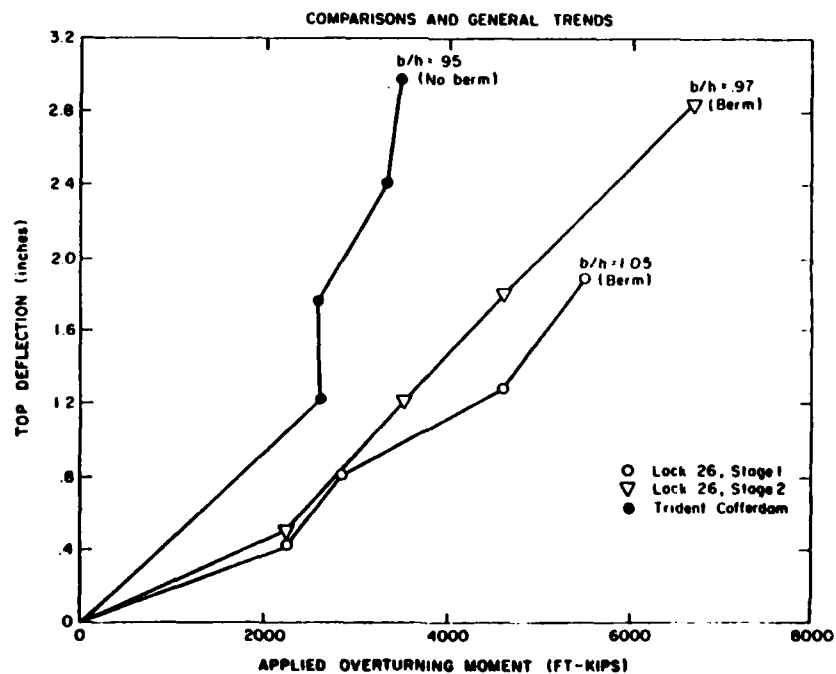


Figure 53. Deflections versus overturning moments during dewatering

overturning moment, the Stage 1 cells experienced slightly less deflection than did the Stage 2 cells. The response curve from the Trident case is higher than both of the curves from the Lock and Dam 26 (R) cells as expected because it has a higher moment exerted on it. This supports the notion that the moment of the loading does have an impact on the behavior when differential head alone is used to define loading intensity.

174. Considering all of the key factors, one would rank the conditions from best to worst in order of the cofferdams as: Willow Island, Lock and Dam 26 (R), and Trident. Recalling the relative positions of the nondimensionalized movement curves in Figure 52, it can be seen that the smaller movements are directly associated with the better conditions for the cofferdams, with the movements increasing in order from Willow Island to Lock and Dam 26 (R) to Trident.

175. In addition to the key factors identified in Table 5, it is worthy of mention that at the Trident Cofferdam, a special proof loading was applied and held for a period of 21 days. This loading induced a creep effect that was identified in Part III. The direct influence of the loading on the nondimensionalized response curves in Figure 52 is seen in the form of the increase in deflections with no increase in load ratio at the load ratio level of about 0.3. The creep effect also served to increase the Trident Cofferdam movement relative to the others.

176. At this point, it is useful to consider the special cases represented by the Seagirt Cofferdam and the Williamson Prototype Cells. Of these, the Seagirt Cofferdam is best suited for a comparison with the cofferdams since it had the largest lateral loading and was a continuous cofferdam as opposed to the isolated cells of the Williamson case. In Figure 54, the nondimensionalized movements of the top of Cell 66 of the Seagirt Cofferdam are plotted against the loading ratio, and for comparison, those from the other case histories previously discussed are also included. It may be remembered that Cell 66 was founded on sandy soils. A layer of organic clay remained in the cell under the sand fill placed to complete the cofferdam. As noted earlier, the loading for the Seagirt Cofferdam was induced by a slurry, and this was converted to an equivalent water head to calculate the load ratio.

178. Not unexpectedly, the response for Cell 66 of the Seagirt Cofferdam is much larger than that for the other cases. Its nondimensionalized movements are about three times those of the Trident Cofferdam. Relative to

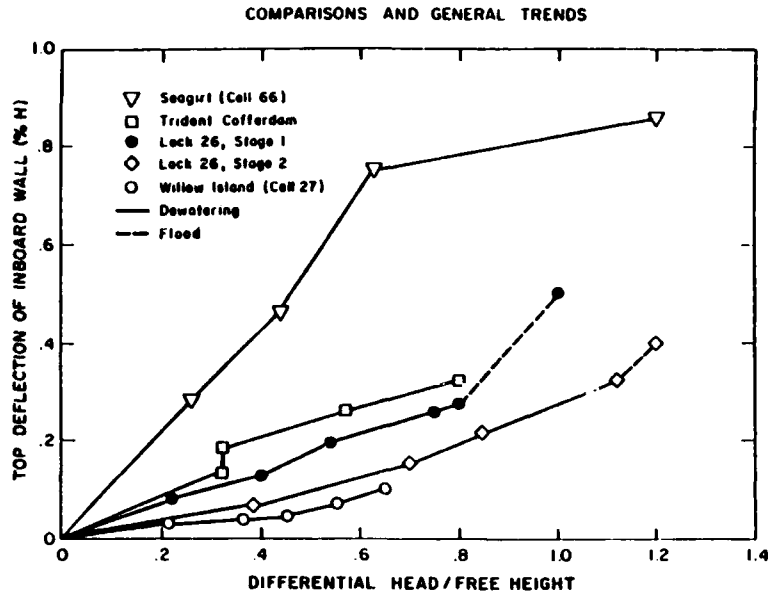


Figure 54. Composite plot of normalized response to differential loading

the key factors used to compare the characteristics of the other cofferdams, the Seagirt case suffers particularly in two areas. First, its fill contains a soft organic clay layer as opposed to the uniform sands in the other cofferdams. Second, during the initial and most severe loading period, there was no stabilizing berm in place to assist in controlling movements.

Deformations of the Tops of the Cells--Repeated Loading

179. One of the more important aspects of cofferdam behavior is the response under repeated loading. First, knowledge of this is significant relative to development of proper modeling techniques for finite element codes for analysis of cofferdams. Second, it is critical to the general idea of predicting deformations of cofferdams in that we need to know if the deformations tend to cumulate or stabilize. Three of the cases in this study were subjected to repeated loading--Lock and Dam 26 (R), Stages 1 and 2, and Willow Island. Figures 17, 18, 33, and 34 presented the response of the cofferdams in these cases under the loadings of several high water events.

180. Examination of the repeated loading effects from the mentioned figures leads to the following conclusions:

- a. The application of a loading to the cofferdam higher than that felt previously leads to a response that is a continuation of that under the primary loading. The form of the response is

largely as if any stress history before the new higher loading is forgotten.

- b. The cofferdam exhibits a stiffer response to unloading than primary loading. As a result, there is a permanent set if the cofferdam should be completely unloaded.
- c. During reloading the cofferdam response is also stiffer than during primary loading until such time as the previous maximum loading is reached.

The general pattern of behavior indicated in these conclusions is consistent with that observed in other types of soil-structure interaction problems. The indications are that the deformations under repeated loading increase, but not in a manner as if the loading continually followed the primary loading behavior. Because the response of the cofferdam is considerably stiffer on reloading and unloading than in the case of primary loading, the deformations under repeated loading cumulate slowly.

Time-Dependent Movements in the Cofferdams

177. Time-dependent movements may occur in cofferdams during or after loading; however, they are only obvious if they occur under sustained loading since the movement of the cells can only be explained through a time-dependent effect. Time-dependent movements in soil-structure interaction problems are typically related to consolidation in saturated cohesive soils, or creep in any type of soil. Creep effects are the largest when the soil is weak, or the loading is such that the loading mobilizes enough shear stress in the soil to exceed some limit beyond which the soil continues to deform under no increase in loading.

- a. Time-dependent movements in the case histories were most apparent in the Seagirt and Trident Cofferdams. Because of the unusual foundation conditions at the Williamson Prototype Cells, it would be expected that time-dependent movements will also occur there, but the data available for this study only covered the initial response of the cells.
- b. The time-dependent movements in the Seagirt Cofferdam were large, and can be attributed primarily to the presence of the cohesive soils left in the cells and those in the foundation. Because the soils in the cells themselves were very soft, it seems likely that they were the largest source of the time-dependent behavior. Whether the movements were due to consolidation or creep cannot be determined.
- c. The time-dependent movements in the Trident Cofferdam were delineated, as noted previously during the proof loading. These can only be attributed to creep inasmuch as the cell

fill and foundation were sands. That creep movements would occur in this case but not in the other water cofferdams is thought to be due to the fact that the Trident Cofferdam did not have a stabilizing berm, it has the highest loading of the case histories, and it has the smallest width to height ratio. If this hypothesis is true, then it suggests that the Trident Cofferdam conditions are such as to some degree to push the limits of loading of cofferdams. Further studies of this issue would appear to be warranted.

Lateral Movements of the Inboard and Outboard Sheet Piles

181. The issue of lateral movements of the sheet piles in the cofferdams relates to both the magnitude and form of the behavior. In terms of the former, it is notable that, during initial dewatering, the inboard side of the cofferdam cells moved more than the outboard side of the cells in all cases considered. This behavioral trend can only be confirmed for the situation where the differential loading is induced by dewatering since there is not adequate information for other forms of loading to draw conclusions. The larger movements of the inboard sheet piles are attributed in Part 3 to the way in which the differential head is applied to the cofferdam, and the resultant change in soil unit weight inside the cofferdam. During dewatering, the phreatic surface drops to the bottom of the cofferdam on the inboard side, but it remains at its original level on the outboard side. As a result, the soil on the inboard side of the cofferdam fill, which is largely now above the water table, goes to the total unit weight condition. On the outboard side, most of the soil remains submerged, and its unit weight relative to that on the inboard side is about half as large. Additional support for this argument is derived from the fact that the situation is reversed during some instances after the water inside the cofferdam is raised in anticipation of flooding, and the riverside water falls before the inside of the cofferdam is dewatered. Where this occurred, the outboard side of the cells deflected more than the inboard side.

182. The issue of the deflected shape of the sheet piles is addressed in Figure 25, where the measured profiles from the inclinometers on the inboard side of the cofferdam are normalized in terms of the cofferdam free height and maximum deflection. The deflected shapes represent only the effects occurring during differential loading. Any deformations due to filling are factored out. In all cases, the maximum movement occurred at the

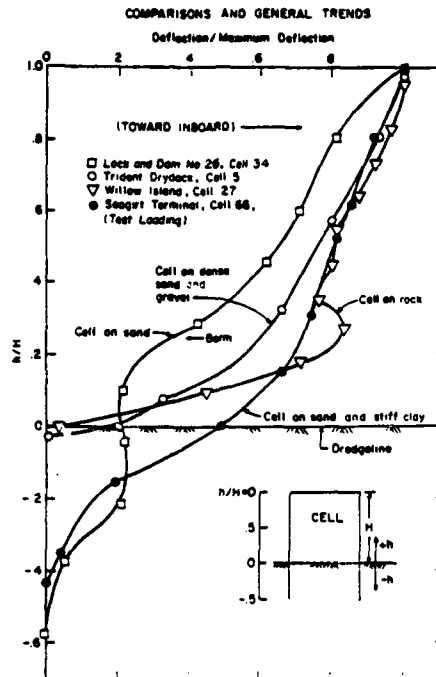


Figure 55. Normalized cell profiles after dewatering

top of the cell. Whether this is due only to the exterior differential loading or local influences of construction activities such as traffic on the cells or positioning of loading cranes is not known. Finite element analyses by Singh and Clough (1988) suggest that there has to be an influence of the latter factor to explain the outward bending of the topmost part of the cells.

183. The shape of the lower portion of the cofferdams is influenced by the type of foundation and embedment of the cells. Both at the Willow Island and Trident Cofferdam, there was a very small penetration of the cell into the underlying foundation. Near the dredge line, the cell profiles in these cases show curvature towards zero cell deflection at the toe of the sheet piles. It is important to note that this may not actually be zero deflection since the toe of the sheet pile also coincides with the toe of the inclinometer casing. Given that an inclinometer measures movement relative to the toe of the casing, there is no way to know if the toe is moving. In any case, there is a sharp curvature of the sheet piles in the two cases where there was little penetration, with the shapes suggesting that the cells to some degree could be translating over the foundation.

184. For both the Seagirt and Lock and Dam 26 (R) cases, there was considerable embedment of the sheet piles in the foundation. For these cases, the deflection profile suggests that the cell is roughly tilted about some

point along the embedded length. There is a noticeable difference in the profile for the Seagirt (Cell 66 test loading) and Lock and Dam 26 (R) cases just above the dredge line, where the Seagirt sheet piles show more bulging outwards. The smaller deflection of the sheet piles for the Lock and Dam 26 (R) cases is attributed to the stabilizing effect of the berm used on the dewatered side of the cofferdam in this instance but not present in the Seagirt cofferdam.

Interlock Tensions

185. The only cases with sufficient information available for the comparison of interlock tension are the Trident Cofferdam and the Lock and Dam 26 (R) Cofferdam. In examining both cases, it can be seen that the primary increases in interlock tensions were associated with filling. In the case of the Trident Cofferdam, compaction of the fill further increased interlock tensions by up to 20 percent. The placement of a soil berm at the Lock and Dam 26 (R) Cofferdam caused a reduction in interlock forces of about 10 percent of the maximum interlock forces observed during filling. On the other hand, the removal of a loose soil berm at the Trident Cofferdam caused an increase of close to 20 percent in interlock tensions. In this case, the soil berm was in place for dewatering and was removed shortly after. Removal of the berm transferred the soil stresses taken by the fill to the interlocks. Cofferdam dewatering at the Lock and Dam 26 (R) site caused an average reduction of close to 30 percent of the maximum interlock force. As expected, less reduction was observed above the top of the berm surface. Instrumentation at the Trident Cofferdam shows a slight increase in tensions as a result of cofferdam dewatering. This is perhaps due to the fact that the Trident Cofferdam was dewatered without the use of soil berms. As suggested by the performance of both cofferdams, it seems reasonable to expect that when soil berms were used, all phases of construction subsequent to cell filling (except fill compaction) will cause either negligible changes in interlock tensions or slight reductions in interlock tensions.

186. The location of the maximum interlock forces at both cofferdams was in the common wall between the main cell and the arc cell. At the Lock and Dam 26 (R), the interlock tensions at the common wall were close to 30 percent higher than the main cell interlock force as compared with 20 percent higher common wall force at the Trident site. The higher tensions found in

the common walls is consistent with the predictions made by conventional design theories.

187. The height of the maximum interlock force at the Lock and Dam 26 (R) site occurred at 15 ft above the dredge line. This corresponds to the conventional design location of $H/4$. The Trident Cofferdam experienced its maximum interlock forces at about 10 ft above the dredge line, which corresponds to $H/8$. The increased cell height and shallow embedment for the Trident case probably caused the maximum interlock tensions to occur closer to the dredge line.

PART VII: SUMMARY AND CONCLUSIONS

188. This investigation consists of the study of the behavior of five large cellular cofferdams under the influence of differential loading. The cofferdams in many cases were instrumented with a number of devices to measure interlock forces or cell deformations, although in one instance only survey data for movements of the top of the cells were available. The primary intent of this study was to document cell deformations and trends of behavior that can be used to test finite element program prediction and to help establish benchmarks for procedures for predicting cofferdam deflections.

189. The cofferdams in the study have differing types of foundations, cell fills, dimensions, and loadings. Three of the case histories are similar in that the loading on the cofferdam is generated by water, inasmuch as the cofferdams are used to allow excavation in the dry within a body of water. In the other two, the loadings were produced by either soil or a soil-slurry. These two cases were also unique in that the soils inside of the cell above the mudline were not completely excavated, leaving a soft layer of soil which was not free-draining beneath the sandy fill used to occupy the remainder of the cell area.

190. While there were many common trends of behavior in the cofferdam, the differing conditions also led to differences in response. The largest effects are observed between those cofferdams with unconventional fills and those with conventional free-draining sand fills. However, even where only seemingly modest differences existed, this was reflected in behavioral differences. The conclusions which can be drawn from the material assembled in this study are as follows:

- a. A clear correlation exists between the movement of the top of the cofferdam cells and the amount of differential load applied to them. With increasing loads, there are increased movements.
- b. The nature of the correlation of movement to load depends upon many factors, including cell height to width ratio, foundation material, cell fill material, presence of a stability berm, and whether the loading is monotonic or cycled.
- c. Cell movements tend to decrease with increases in cell width to height ratio, stiffness of cell fill or foundation, and presence of a stability berm.
- d. The presence of weak, compressible soils in the cell fill, or highly stressed conditions on a sand fill leads to movements

of a time-dependent nature under sustained loading of the cofferdam.

- e. No significant time-dependent movements were observed for cofferdams with conservative designs and where the foundation was composed of rock or dense sands.
- f. Under fully dewatered conditions, conservatively designed cofferdams founded on sands or rocks exhibit maximum lateral movements at the top of the cofferdam, and the movements are in the range of 0.1 to 0.3 percent of the free cell height toward the dewatered area. Under flood loadings, the same cofferdams have lateral movements on the order of 0.3 to 0.6 percent of the free cell height.
- g. After a flood loading, the cells relax from their peak displaced positions, but during the process of reducing the load, the cell response is stiffer than that which followed in reaching the peak position. This leads to a permanent set in the cells after removal of the flood load, in that they never return to their original position before flooding.
- h. If flooding loadings occur for several cycles, a form of hysteretic response is observed in the cofferdam deformation pattern. Displacements cumulate during second and third cycles of flood loading, but at a decreased magnitude than in the first cycle of flooding.
- i. During dewatering, the inboard side of the cofferdam will move slightly more than the outboard side due to the greater increase of soil pressure which develops on the inboard as the water level drops toward the inboard within the cell with dewatering.
- j. Interlock tensions are generally the greatest at the end of filling of the cofferdam.
- k. Interlock tensions are the largest in the common wall between the arc and main cells. For the two cases where this was observed, the common wall interlock tensions were on the order of 20 to 30 percent higher than those in the main cell.

BIBLIOGRAPHY

- Barker, R., Lewis, C., Oliver, W., and Mould, K. 1985 (May). "Sheetpile Interlock Connection Testing Program," Report No. VPI/CE-ST-85-10, Virginia Polytechnic Institute and State University, Blacksburg, VA.
- Clough, G. W., and Hansen, L. A. 1977. "A Finite Element Study of the Behavior of the Willow Island Cofferdam," Technical Report No. CE-218, Stanford University, Stanford, CA.
- Clough, G. W., and Kuppusamy, T. 1985 (Apr). "Finite Element Analysis of Lock and Dam 26 Cofferdam," Journal of the Geotechnical Engineering Division, American Society of Civil Engineers, Vol 111, No. 4, pp 521-544.
- Clough, G. W., and Duncan, J. M. 1986 (Apr). "Finite Element Analysis of Cofferdam Movements During Construction of the Seagirt Terminal, Baltimore," STV/Lyon Associates, Baltimore, MD.
- Clough, G. W., and Goeke, P. M. 1986. "In-Situ Testing for Lock and Dam 26 Cellular Cofferdam," Proceedings, Use of In-Situ Tests in Geotechnical Engineering, American Society of Civil Engineers Specialty Conference, Geotechnical Special Publication No. 6, pp 131-145.
- Clough, G. W., Mosher, R., Singh, Y. P. and Kuppusamy, T. 1987 (Jun). "Two and Three Dimensional Finite Element Analyses of Cellular Cofferdams," Soil-Structure Interaction Conference, Paris, France.
- Cummings, E. M. 1957 (Sep). "Cellular Cofferdams and Docks," Journal of the Waterways and Harbors Division, American Society of Civil Engineers, Vol 83, No. WW3, Proceedings Paper 1366, pp 13-45.
- Dismuke, T. D. 1975. "Stress Analysis of Sheet Piling in Cellular Structures," Proceedings, Conference on Design and Installation of Pile Foundations and Cellular Structures, Fang, H. Y. and Dismuke, T. D. (eds.), Envo Publishing Co., Lehigh Valley, PA, pp 339-365.
- Dodson-Lindblom Associates, Inc. 1986 (Oct). "Instrumentation," Interim Report Task 3.1, Williamson CBD Prototype Cells, Williamson, WV, US Army Engineer District, Huntington, Huntington, WV.
- Esrig, M. I. 1970 (Nov). "Stability of Cellular Cofferdams Against Vertical Shear," Journal of the Soil Mechanics and Foundations Divisions, American Society of Civil Engineers, Vol 96, No. SM6, pp 1853-1862.
- Hansen, J. B. 1953. "Earth Pressure Calculations," The Danish Technical Press, The Institute of Danish Civil Engineers, Copenhagen.
- Hansen, L. A., and Clough, G. W. 1982. "Finite Element Analyses of Cofferdam Behavior," Proceedings, 4th International Conference on Numerical Methods in Geomechanics, Edmonton, Alberta, Canada, Vol 2, pp 899-906.
- Kleber, K. B. 1985. "A Review of the Lock and Dam No. 26 (Replacement) First Stage Cofferdam," Special Project and Report submitted to the Faculty of Virginia Polytechnic Institute and State University, in partial fulfillment of the requirements for the degree of Master of Engineering, Blacksburg, VA.
- Krynine, D. P. 1945. "Stability and Stiffness of Cellular Cofferdams," by K. Terzaghi, Transactions, American Society of Civil Engineers, Vol 110, Paper No. 2253, pp 1175-1178.

- Lacroix, Y., Esrig, M. I., and Luscher, U. 1970. "Design, Construction and Performance of Cellular Cofferdams, Lateral Stresses in the Ground and Earth Retaining Structures," American Society of Civil Engineers, pp 271-328.
- Maitland, J. K., and Schroeder, W. L. 1979 (Jul). "Model Study of Circular Sheetpile Cells," Journal of the Geotechnical Engineering Division, American Society of Civil Engineers, Vol 105, No. GT7, pp 805-820.
- Matlock, H., and Reese, L. 1969. "Moment and Deflection Coefficients for Long Piles," Handbook of Ocean and Underwater Engineering, J. J. Myers, C. H. Holm, and R. F. McAllister, eds., McGraw-Hill, Inc., New York.
- Moore, B. H., and Kleber, B. K. 1985. "Multiple Integrated Instrumentation Programs Lock and Dam No. 26, Mississippi River," Proceedings, Congress on Large Dams, pp 621-641.
- Mosher, R. 1985. "Three Dimensional Finite Element Analysis of Cellular Cofferdams," Thesis submitted in partial fulfillment of the requirements for the degree of Doctor of Philosophy to the Faculty of Virginia Polytechnic Institute and State University at Blacksburg, VA.
- Ovesen, N. K. 1962. "Cellular Cofferdams: Calculation Methods and Model Tests," Bulletin No. 14, The Danish Geotechnical Institute, Copenhagen, Denmark.
- Peters, J. F., and Leavell, D. A. 1985 (Jul). "Appendix X: Finite Element Analysis of Williamson CBD Sheetpile Cell Floodwall," Task 1, US Army Engineer District, Huntington, Huntington, WV.
- Peters, J. F., Leavell, D. A., and Holmes, T. L. 1987 (Feb). "Finite Element Analysis of Williamson CBD Sheetpile Cell Floodwall," Prototype Cell Analysis, Task II, US Army Engineer District, Huntington, Huntington, WV.
- Schroeder, W. L., and Maitland, J. K. 1979. "Cellular Bulkheads and Cofferdams," Journal of the Geotechnical Engineering Division, American Society of Civil Engineers, Vol 105, No. GT7, pp 823-837.
- Schroeder, W. L., Marker, D. K., and Khuayjarernpanishk, T. 1977 (Mar). "Performance of a Cellular Wharf," Journal, Geotechnical Engineering Division, American Society of Civil Engineers, Vol 103, No. GT3, Paper No. 12790, pp 153-168.
- Shannon and Wilson, Inc. 1982 (Sep). "Analysis of Instrumentation Data," Interim Report Task 3.1, Lock and Dam No. 26 (Replacement), Mississippi River, US Army Engineer District, St. Louis, St. Louis, MO.
- Shannon and Wilson, Inc. 1982 (Sep). "Finite Element Models," Final Report Tasks 3.2, 3.3, and 3.4, Lock and Dam No. 26 (Replacement), US Army Engineer District, St. Louis, St. Louis, MO.
- Shannon and Wilson, Inc. 1983. "Summary Report, Instrumentation Data Analyses and Finite Element Studies for First Stage Cofferdam, Lock and Dam 26 (Replacement)," US Army Engineer District, St. Louis, St. Louis, MO.
- Singh, Y. P., and Clough, G. W. 1988. "Finite Element Analyses of Cellular Cofferdams," Technical Report prepared under Contract No. DACW39-86-K-0007, US Army Engineer Waterways Experiment Station, Vicksburg, MS.
- Sorota, F., and Kinner, E. B. 1981 (Dec). "Cellular Cofferdam for Trident Drydock: Design," Journal of the Geotechnical Engineering Division, American Society of Civil Engineers, Vol 107, No. GT-12, pp 1643-1655 and pp 1657-1676.

Sorota, M. D., Kinner, E. B., and Haley, M. X. 1981 (Dec). "Cellular Cofferdam for Trident Drydock: Performance," Journal, Geotechnical Engineering Division, American Society of Civil Engineers, Vol 107, No. GT12, Paper No. 16733, pp. 1657-1676.

Stevens, R. F. 1980. "Study of the Behavior of a Cellular Cofferdam," Thesis presented in partial fulfillment of the requirements for the degree of Doctor of Philosophy to Duke University, Durham, NC.

Swatek, E. P. 1967 (Aug). "Cellular Cofferdams Design and Practice," Journal of the Waterways and Harbors Division, American Society of Civil Engineers, Vol 93, No. WW3, Proceedings Paper 5398, pp 109-132.

Swatek, E. P. 1970. "Summary-Cellular Structure Design and Installation," Proceedings, Conference on Design and Installation of Pile Foundations and Cellular Structures, H. Y. Fang and T. D. Dismuke, eds., Envo Publishing Co., Lehigh Valley, PA, pp 413-423.

Tennessee Valley Authority. 1957 (Dec). "Steel Sheet Piling Cellular Cofferdams on Rock," TVA Technical Monograph No. 75, Vol 1, pp. 61-62, 66-67, and 69.

Terzaghi, K. 1945. "Stability and Stiffness of Cellular Cofferdams," Transactions, American Society of Civil Engineers, Vol 110, Paper No. 2253, pp 1083-1202.

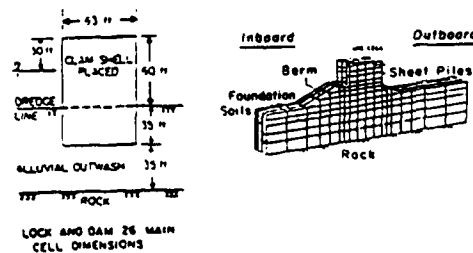
US Army Corps of Engineers. 1976 (Nov). "Review of Instrumentation Program for the Second Stage Cofferdam, Willow Island Locks and Dam, Ohio River," US Army Engineer District, Huntington, Huntington, WV.

Winterkorn, H. F., and Fang, H. Foundation Engineering Handbook, Van Nostrand Reinhold Co., New York, pp 445-480.

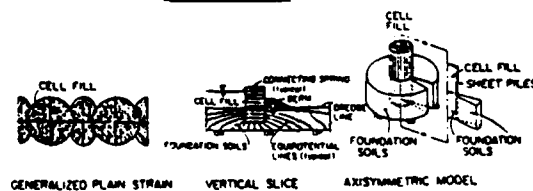
Table 1
Two-Dimensional Finite Element Models

Model (1)	Purpose (2)	Advantages (3)	Disadvantages (4)
Axisymmetric	Provide data on effects filling isolated cell	<ul style="list-style-type: none"> • Simple to perform • Accounts for effects cell embedment • Provides data on location of maximum deflection and interlock tension upon filling 	<ul style="list-style-type: none"> • Does not consider effects of stage other than filling • No cell interaction
Vertical slice	Provide data on loading stages other than filling	<ul style="list-style-type: none"> • Can consider effects of all stages of loading • Provides data on history of behavior from filling to flood stages 	<ul style="list-style-type: none"> • Time consuming to perform if loading is complex • Does not consider 3-D loading effects
Generalized plane strain	Provide data on interaction between cells during filling	<ul style="list-style-type: none"> • Simple to perform • Accounts for interaction of cells • Provides data on common wall and connection behavior 	<ul style="list-style-type: none"> • Does not consider influence of dredgeline support • Considers only effects of cell filling

Three-Dimensional Finite Element Model



Two-Dimensional Model



Background .

Table 2

Description of Loading History, Willow Island

<u>PT to PT</u>	<u>Activity</u>	<u>Time</u>
O A	Initial dewater (High River)	Jan 7-Feb 3
A B	Normal pool	Feb 4-Feb 19
B C	High water	-Feb 21
C D	Flood cofferdam	Feb 24
D E	Dewater	Mar 3-Mar 8
E F	High water	-Mar 18
F G	Flood cofferdam	Mar 21
G H	Dewater	Mar 31-Apr 11

Table 3

Key Aspects of Cofferdam Behavior

Cofferdam	Comparison of Cofferdams: Design				Sheet Piles	Cell Fill	Foundation	Berms
	Height (H) ft	Diameter (B) ft	B/H	Embedded ft				
Lock and Dam 26 Stage 1	60	63	1.05	35	PS-32, PSX-32, 40 wye	Sand, 55% Dr, placed by clamshell. Good.	Sand, medium to dense. Good.	Sand, 25 ft high. In place for dewatering.
Lock and Dam 26 Stage 2	60-80	63	0.90*	15-35	PS-32, PSX-32, 40 wye	Sand, 55% Dr, placed by clamshell. Good.	Sand, medium to dense. Good.	Sand, 25 ft to 35 ft high. In place for dewatering.
Trident drydock	80	76	0.95	2-4	PSX-32 40 wye	Sand, densi- fied to 75% Dr, by vibratory probe. Excellent.	Dense sand and gravel till. Excellent.	None used.
Willow Island	55	65	1.18	0.5-1.5	M ¹⁰²	Sand and Gravel. Good.	Sandstone, hard clay. Excellent.	Sand, 30 ft. Placed after dewatering.
Seagirt terminal	36	62	1.72	20-30	PS-28 PS-32 30 wye	Silty sand, placed on top of 10 ft clay layer. Poor.	Sand and soft to stiff clay. Fair.	Silty sand. Placed after initial loading. 10- to 25 ft high.
Williamson CBD prototype cells	35	53	1.51	30-35	--	Sand and gravel, placed on top of medium clay. Poor.	Sand and gravel. Good.	None used.

* Average.

Table 4

Key Aspects of Cofferdam Behavior

Cofferdam	Fmc* (K/in.)	Fcw* (K/in.)	Height of Fmc, ft	Maximum Differential Load	Average Deflection		Comments
					Maximum Differential Load	Maximum Differential Load	
Lock and Dam 26 Stage 1	4 (1.3 Ka)	5.8	H/4	60-ft water- head	3.8 in. (0.5% H)		Good performance. Negligible creep.
Lock and Dam 26 Stage 2	NA	NA	NA	80-ft water- head	3.5 in.** (0.4% H)		Good performance. Negligible creep.
Trident drydock	8 (2.1 Ka)	8	H/8	80-ft water- head	3.0 in. (0.3% H)		Very good performance. Some creep during dewatering.
Willow Island	NA	NA	NA	40-ft water- head	NA		Very good performance. Little creep.
Seagirt terminal	NA	NA	NA	60-ft equiv- alent waterhead	Several feet		Clay in cell caused large movements. Much creep. Poor performance.
Williamson CBD prototype cells	--	--	--	--	--		Clay in cell caused large fill settlements.

* Fmc, Fcw = Max. interlock force after filling: main cell, common wall, respectively; NA = not available.

** As of December 1986.

Table 5

Comparison of Cofferdams Loaded by Differential Waterheads
in Terms of Key Parameters

<u>Cofferdam</u>	<u>Berm?</u>	<u>Width/Height</u>	<u>Foundation</u>	<u>Fill</u>
Trident	No	0.95	Dense sand and gravel till	Dense sand
Willow Island	Yes	1.18	Rock	Medium sand
Lock and Dam 26 (R) Stage 1	Yes	1.05	Dense sand	Medium sand
Lock and Dam 26 (R) Stage 2	Yes	0.95	Dense sand	Medium sand